UNIVERSIDAD AUTÓNOMA DE MADRID

FACULTAD DE CIENCIAS

DEPARTAMENTO DE BIOLOGÍA MOLECULAR

Modeling Aurora B function and regulation

TESIS DOCTORAL

Gonzalo Fernández-Miranda Pérez

MADRID, 2009

Centro Nacional de Investigaciones Oncológicas

Ignacio Pérez de Castro Insúa, Investigador del Grupo de División Celular y Cáncer del Centro Nacional de Investigaciones Oncológicas (CNIO)

y

Marcos Malumbres Martínez, Jefe del Grupo de División Celular y Cáncer del Centro Nacional de Investigaciones Oncológicas (CNIO)

Certifican: que **Gonzalo Fernández-Miranda Pérez** ha realizado bajo su dirección el trabajo de Tesis Doctoral titulado:

Modeling Aurora B function and regulation

Revisado el presente trabajo, consideran que reúne todos los méritos necesarios para su presentación y defensa con el fin de optar al grado de Doctor por la Universidad Autónoma de Madrid.

Ignacio Pérez de Castro

Marcos Malumbres

Abbreviations

3-MC: **3-M**ethyl**c**holanthrene

Ad-CRE: **Ad**enoviruses expressing **CRE** recombinase

Ad-GFP: **Ad**enoviruses expressing **GFP**

BAC: **B**acterial **A**rtificial **C**hromosomes

BrdU: **Br**omo**d**eoxi**u**ridine

BSA: **B**ovine **S**erum **A**lbumin

cDNA: **C**ommplementary **DNA**

CMV: **C**yto**m**egalo**v**irus promoter

CNIO: **C**entro **N**acional de **I**nvestigaciones **O**ncológicas

DMBA: 7,12-**d**i**m**ethyl**b**enz[α]**a**nthracene

DMEM: **D**ulbecco's **M**odified **E**agle's **M**edium

DMSO: **D**i**m**ethyl **s**ulf**o**xide

EDTA: **E**thylene**d**iamine**t**etraacetic **A**cid

ES cells: **E**mbryonic **S**tem **C**ells

EV: **E**mpty **V**ector

FBS: **F**etal **B**ovine **S**erum

GAPDH: **G**lycer**a**ldehyde-3-**p**hosphate **de**h**y**drogenase

GFP: **G**reen **F**luorescence **P**rotein

H&E: **H**aematoxylin and **E**osin

HR: **H**omologous **R**ecombinantion

IF: **I**mmuno**f**luorescence

IHQ: **I**mmuno**hi**stochemistry

KDa: **K**ilo**Da**lton

KO: Animals or cells derived from a gene **k**nock-**o**ut strain

KI: Animals or cells derived from a gene **k**nock-**i**n strain

LacZ: beta-galactosidase

MEFs: **M**ouse **E**mbryonic **Fi**broblasts

MMTV: **M**ouse **m**ammary **t**umour **v**irus promoter

NEO: **Neo**micine

PBS: **P**hosphate **B**uffered **S**aline

PCR: **P**olymerase **C**hain **R**eaction

PFA: **P**ara**f**orm**a**ldehyde

qRT-PCR: **q**uantitative **R**everse **T**ranscriptase **P**olymerase **C**hain **R**eaction

rtTA: **r**everse **t**etracycline **T**rans**a**ctivator

SDS: **S**odium **D**odecyl **S**ulphate

shRNA: **s**hort **h**airpin **RNA**

siRNA: **s**mall **i**nterference **RNA**

Tet: **Tet**racycline

TetO: **Tet**racycline **O**perator elements

Tet-P: **Tet**racycline-responsive minimal **p**romoter

Tg: **T**rans**g**enic mice

TK: **T**hymidine **K**inase

TPA: 12-O-**t**etradecanoyl**p**horbol-13-**a**cetate

tTA: **t**etracycline **T**rans**a**ctivator

UAM: **U**niversidad **A**utónoma de **M**adrid

UTR: **Un**translated **r**egion

WB: **W**estern-**B**lot

WT: **W**ild **T**ype

X-GAL: 5-bromo-4-chloro-3-indolyl-b-D-**gal**actopyranoside

SUMMARY 1

RESUMEN 3

INTRODUCTION 5

1. THE MAMMALIAN CELL DIVISION CYCLE 5

2. CELL CYCLE CHECKPOINTS 6

2.1 INTERPHASE AND THE RESTRICTION POINT 6

2.2 DNA DAMAGE CHECKPOINTS 7

2.3 THE SPINDLE ASSEMBLY CHECKPOINT 8

3. CONTROL OF MITOSIS AND CYTOKINESIS BY POST-TRANSLATIONAL MODIFICATIONS 8

3.1 UBIQUITINATION AND SUMOYLATION 9

3.1.1 Ubiquitination 9

3.1.2 SUMOylation 10

3.2 PHOSPHORYLATION 11

4. THE AURORA FAMILY OF PROTEIN KINASES 13

4.1 AURORA KINASES FUNCTION AND LOCALIZATION 13

4.1.1 Aurora A: centrosomes and spindles 13

4.1.2 Aurora B: the catalytic member of the chromosomal passenger complex 14

4.1.3 Aurora C: only a male meiotic kinase? 15

4.2 REGULATION OF AURORA KINASES 15

4.2.1 Aurora A is regulated by Tpx2 16

4.2.2 Aurora B is regulated in a CPC-dependent manner 17

4.2.3 Aurora C, the unknown member of the family 18

4.3 MOUSE MODELS OF AURORA KINASES 18

4.4 AURORA KINASES AND CANCER 19

AIM OF THE WORK 21

MATERIALS & METHODS 23

1. GENETICALLY MODIFIED MOUSE MODELS 23

1.1 ANIMAL HOUSING 23
1.2 GENERATION OF MOUSE MODELS 23
1.2.1 Construction of targeting vectors 23
1.2.2 Generation of quimeras 24
1.2.3 Generation of Aurora B conditional, knock-in and null alleles 24
1.3 MOUSE CROSSES 25
1.4 MOUSE GENOTYPING 25
1.5 TREATMENTS IN LIVE ANIMALS 26
1.5.1 Wound healing 26
1.5.2 Hepatectomy 26
1.5.2 Tumor induction 26
2. HISTOLOGICAL AND IMMUNOHISTOCHEMICAL ANALYSIS 27
3. EMBRYOS 27
3.1 EMBRYO CULTURE AND EXTRACTION 27
3.2 EMBRYO MICROINJECTION 29
4. CELL CULTURE 29
4.1 MEFS CULTURE, EXTRACTION AND INFECTION 29
4.2. HUMAN AND MOUSE CELL LINES 30
5. BIOCHEMICAL PROCEDURES 30
5.1 RNA EXTRACTION AND REAL-TIME-PCR 30
5.2 DNA CLONING 31
5.4 IMMUNOFLUORESCENCE 31
5.4 X-GAL DETECTION IN EMBRYOS AND CELLS 31
5.5 PROTEIN EXTRACTION AND ANALYSIS 31
5.6 IMMUNOPRECIPITATION AND IN VITRO KINASE ASSAYS 32

RESULTS 33

1. SUMO REGULATION OF AURORA B 33
1.1 AURORA B IS MODIFIED BY SUMO 33
1.1.1 Identification of a putative SUMOylation motif conserved in Aurora B 33
1.1.2 Aurora B mouse protein is SUMOylated at K207 residue 34
1.2. ECTOPIC EXPRESSION OF A SUMO-DEAD AURORA B PROTEIN INDUCES CELLULAR DEFECTS 35

1.2.1 Lack of Aurora B SUMOylation at K207R induces polyploidy and nuclear defects 35
1.2.2 Lack of Aurora B SUMOylation compromises cell viability 36
1.3. AURORA B IS REGULATED BY SUMO 37
1.3.1 SUMOylation of Aurora B is important for correct mitotic progression and completion of cytokinesys 38
1.3.2 SUMO regulates Aurora B and Incenp centromeric localization 40
1.3.3 SUMOylation affects Aurora B function without reducing its kinase activity 41
1.3.4 An abnormal SUMOylation of Aurora B affects its oncogenic properties 42
2. DEVELOPMENT OF MOUSE MODELS 44
2.1 GENERATION OF A CONDITIONAL KNOCK OUT MOUSE MODEL 44
2.2 GENERATION OF A β-GALACTOSIDASE KNOCK-IN MOUSE MODEL 44
2.3 GENERATION OF A TETRACYCLINE-INDUCIBLE MOUSE MODEL 47
3. PARTIAL *IN VIVO* INACTIVATION OF AURORA B 50
3.1 LACK OF ONE ALLELE OF AURORA B DOES NOT RESULT IN MAJOR ALTERATIONS DURING MOUSE DEVELOPMENT 50
3.1.1 Aurora B heterozygous MEFs proliferate well in culture 50
3.1.2 Aurora B heterozygous mice are fertile although few of them develop hypospermia 50
3.2 LACK OF ONE ALLELE OF AURORA B RESULTS IN IMPAIRED PROLIFERATION AND SLIGHT PROTECTION AGAINST TUMOUR INDUCTION 51
3.2.1 Impaired in vivo proliferation in Aurkb(+/–) mice 52
3.2.2 Slight protection against tumour induction in Aurkb(+/–) mice 52
3.3 LACK OF ONE ALLELE FOR AURORA B INCREASES SUSCEPTIBILITY TO SPONTANEOUS TUMOUR DEVELOPMENT IN AGED MICE 54
4. LETHALITY AND COMPLEMENTATION BY AURORA C 55
4.1 GENETIC ABLATION OF AURORA B DOES NOT DISTURB EARLY EMBRYONIC DIVISIONS 55
4.1.1 Aurora B-deficient embryos progress normally to a blastocyst stage 55
4.1.2 Aurora B is expressed during first cell divisions 55
4.1.3 Histone H3 is properly phosphorylated and Incenp is correctly localized in early embryos lacking Aurora B 57
4.1.4 Aurora B-null blastocysts display normal size and cell number 58
4.2. GENETIC ABLATION OF AURORA B RESULTS IN MITOTIC ABERRATIONS AND LETHALITY AFTER IMPLANTATION 58

4.2.1 Histological examination of abnormal implanted Aurora B-null embryos 59
4.2.2 DNA damage and activation of the p53 pathway leads to apoptosis in implanted embryos lacking Aurora B 59
4.2.3 Aurora B-deficient cells arrest at prometaphase/metaphase with an active SAC 60
4.2.4 Embryos fully degenerate at E9.5 in the absence of Aurora B 60
4.3 GENETIC ABLATION OF AURORA B RESULTS IN ABNORMAL ADVANCED BLASTOCYSTS 61
4.3.1 Aurora B-null advanced blastocysts display an aberrant ICM surrounded with abnormal TGC 61
4.3.2 Lack of Aurora B prevents proper chromosome segregation in ES cells 62
4.3.3 Aurora B-deficient ES cells arrest at prometaphase with a functional SAC and mislocalization of the CPC 63
4.4. AURORA C COMPENSATES FOR AURORA B FUNCTION DURING EARLY EMBRYONIC DEVELOPMENT 65
4.4.1 Aurora C is highly expressed in early embryos 65
4.4.2 Inhibition of Aurora B/C results in a severe arrest in early embryos 66
4.4.3 Aurora C plays a crucial role in driving proper mitosis in early cell divisions 68
5. ESSENTIAL FUNCTIONS OF AURORA B IN G1/S PROGRESSION AND MITOSIS 68
5.1 AURORA B DEPLETION IN MEFS PROVOKES A DELAY IN THE ENTRY INTO S-PHASE 70
5.2 AURORA B DEFICIENCY INTERFERE WITH G1-S PROGRESSION IN VIVO AFTER PARTIAL HEPATECTOMY 71
5.3 AURORA B MAY REGULATE G1-S TRANSITION BY MODULATION OF THE MTOR PATHWAY OR P21 LEVELS 72
5.3.1 In Aurora B-depleted MEFs 72
5.3.2 In Aurkb(+/–) livers after hepatectomy 72
5.4 DEPLETION OF AURORA B IN MEFS RESULTS IN MULTIPLE NUCLEI, MICRONUCLEI AND APOPTOSIS 74
5.5 AURORA B-DEFICIENT MEFS ACCUMULATE IN PROPHASE / PROMETAPHASE WITH MISALIGNED CHROMOSOMES AND SPINDLE ABERRATIONS 76
5.6 DEPLETION OF AURORA B IN MEFS LEADS TO ACCUMULATION OF γ-TUBULIN ASTERS AND/OR SUPERNUMERARY MTOCS 77
5.7 AURORA B-DEFICIENT MEFS SHOW A WEAK MITOTIC CHECKPOINT THAT RESULTS DEFECTIVE AFTER SPINDLE PARTITION 77

DISCUSSION 81

1. REGULATION OF AURORA B BY SUMOYLATION 81
2. NEW MODELS FOR STUDYING AURORA B FUNCTION AND THERAPEUTIC VALUE IN VIVO 84
3. AURORA B AND AURORA C DURING EARLY EMBRYONIC CELL DIVISIONS 88
4. AURORA B IS A REGULATOR OF SPINDLE DYNAMICS AND SPINDLE POLE INTEGRITY.....89
5. AURORA B ROLE IN G1-S TRANSITION 91
6. CONCLUDING REMARKS 91

CONCLUSIONS 93

CONCLUSIONES..... 95

REFERENCES..... 97

APPENDIX 107

Summary

Aurora kinases are critical regulators of the cell cycle and their inhibition may have beneficial effects in cancer therapy. Aurora B interacts with Survivin, Borealin and Incenp to form the Chromosomal Passenger Complex (CPC), which is involved in the regulation of microtubule-kinetochore attachments and cytokinesis. In this work, we have characterized a new regulatory mechanism of Aurora B based on posttranslational modification by SUMO peptides. SUMOylation of Aurora B regulates its localization at kinetochores and may also modulate its activity during mitosis. In addition, we have generated and characterized the first loss-of-function models for Aurora B function in mammals. Using these models we have observed that Aurora C, but not Aurora B, is required for cell division in early zygotes. Whereas genetic disruption of the CPC proteins (Incenp, Survivin or Borealin) results in early embryonic lethality at the morula stage, Aurora B-null embryos get implanted and die at post-implantation stages due to mitotic defects. This is due to the critical function of Aurora C during these embryonic cycles. Acute deletion of Aurora B in somatic cells that do not express Aurora C results in delayed G1/S progression from quiescence in vitro and in vivo, suggesting ubiquitous mitotic-independent functions of this kinase. Aurora B-null cells display chromosomal misalignment in the absence of Mad2 at the kinetochores. In addition, lack of Aurora B results in the formation of multiple γ-tubulin-positive microtubule organizing centers (MTOC) and aberrant astral microtubule nucleation. Thus, complete genetic ablation of Aurora B suggests a critical role for this protein in preventing supernumerary MTOCs and modulating microtubule dynamics during mitosis.

Resumen

La familia de quinasas Aurora son reguladores cruciales del ciclo celular y su inhibición parece tener efectos terapéuticos en cáncer. Aurora B forma parte del complejo pasajero de los cromosomas (CPC) formado por las proteínas Survivina, Borealina e Incenp, el cual regula importantes funciones durante la fase de mitosis tales como las interacciones entre los microtúbulos y los cinetocoros y el proceso de citocinesis. En este trabajo hemos caracterizado un nuevo mecanismo de regulación de Aurora B basado en la modificación post-traduccional a través de los péptidos de SUMO. La SUMOilación de Aurora B regula su localización en el centrómero de los cromosomas y parece que también es capaz de modular su actividad durante mitosis. Además, hemos generado y caracterizado los primeros modelos animales de pérdida de función de Aurora B en mamíferos. Gracias a estos modelos hemos observado que Aurora C, pero no Aurora B, es necesaria para la división celular en embriones tempranos. Mientras que la pérdida de función de las proteínas del CPC (Incenp, Survivina o Borealina) produce letalidad embrionaria en el estadio de mórula; los embriones que carecen de Aurora B son capaces de desarrollarse hasta implantarse en el útero materno momento en el cual mueren debido a defectos mitóticos. Este inesperado resultado es consecuencia de la función compensatoria que ejerce Aurora C durante los primeros ciclos embrionarios. Por otro lado, la eliminación aguda de Aurora B en células somáticas que no expresan Aurora C, produce un retraso en la progresión G1/S del ciclo celular, tanto *in vivo* como *in vitro*, en aquellas células que estaban en un estado de quiescencia anterior, lo cual sugiere que Aurora B tiene funciones ubicuas independientes de las ya descritas en mitosis. Además, hemos observado que las células que carecen de Aurora B presentan problemas a la hora de alinear los cromosomas durante mitosis y que estos problemas aparecen cuando el regulador Mad2 está ausente en los cinetocoros. Por último, la ausencia de Aurora B da lugar a la formación de múltiples centros organizadores de microtúbulos y produce defectos en la nucleación de los microtúbulos del aster. De esta manera, la eliminación genética de Aurora B sugiere que esta proteína es esencial para prevenir la aparición de múltiples centros organizadores de microtúbulos, y que además modula la dinámica de los microtúbulos durante mitosis.

Introduction

1. The mammalian cell division cycle

Ever since Rudolf Virchow (1821–1902) proclaimed his famous "*Omnis Cellula e cellula*" ('All cells are derived from cells'), the challenge has been to understand how cells divide and how they faithfully transmit genetic information from one cell generation to the next. A basic eukaryotic cell cycle consists of four phases (Figure 1). Basically, a cell replicates its genetic material during S phase (DNA synthesis) and segregates this material into two daughter cells during M phase (mitosis) with the posterior division of the cytoplasm (cytokinesis). The preparation stage for S phase, in which the cell grows, is called G1 (gap 1); while the period between S phase and M phase, in which the cell prepares for cell division, is called G2 (gap 2). In mammals, the majority of the adult cells are in a quiescent phase named G0, and only in the presence of specific mitogenic stimuli or signals cells decide to progress through the cell cycle (Figure 1). The G1, S, and G2 phases are also known as interphase since no dramatic morphological changes are observed in these phases.

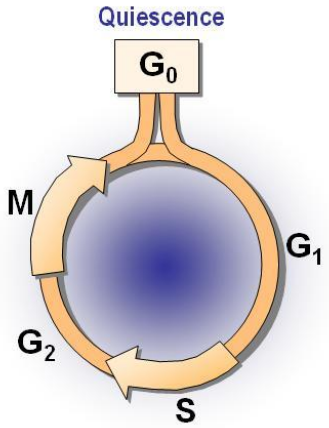

Figure 1. Cell cycle phases. Quiescent cells are in G0. Cells that decide to cycle enter into G1 to prepare DNA synthesis that occurs in S phase. Once the genome is duplicated, cells prepare to divide during G2. Finally, chromosome segregation and cell division takes place in M phase.

Mitosis is the process of nuclear division in which the previously duplicated genome is structurally reorganized into compact chromosomes, each made up of two identical sister chromatids that are equally segregated into two daughter cells. The result of the mitotic process is that each daughter cell inherits one complete set of chromosomes, apart from one centrosome (the

main microtubule- organizing centre of animal cells) and the appropriate complements of the cytoplasm and organelles. Mitosis is divided into five different phases: prophase, prometaphase, metaphase, anaphase and telophase (Figure 2a). During prophase, interphase chromatin condenses into well-defined chromosomes and previously duplicated centrosomes migrate apart, thereby defining the poles of the future spindle apparatus. Prometaphase abruptly starts when the nuclear envelope breakdown. During this stage, a highly dynamic bipolar array of microtubules called mitotic spindle is formed. Spindle microtubules are then captured by kinetochores (specialized proteinaceous structures associated with centromere DNA on mitotic chromosomes) (Figure 2b). Subsequently, mono-oriented chromosomes establish an interaction with microtubules from the opposite pole and become bi-oriented. Chromosomes then congress and reach the equator of the spindle forming what it is called the 'metaphase plate'. After all chromosomes have undergone a proper bipolar attachment, a sudden loss in sister-chromatid cohesion triggers the onset of anaphase. This event is called the 'metapahase to anaphase transition'. During early anaphase, chromosomes lose their cohesion, split apart and each chromatid moves towards one spindle pole. At late anaphase, the spindle elongates separating furthermore the two groups of chromatids. In telophase, the two sets of daughter chromosomes reach the poles of the spindle, chromatin starts to decondense and the nuclear envelope reforms around the daughter chromosomes.

Cytokinesis is the process of cytoplasmatic division, and its regulation is intimately linked to mitotic progression. At the end of telophase, a contractile ring assembles at the cortex of the cell to partition the whole cytoplasm into two daughter cells. This contractile ring ultimately gives rise to the midbody (a dense bundle of microtubules derived from the telophase central spindle) that indicates the abscission site. The whole process is finished when abscission completely separates the cytoplasm of the two new daughter cells.

2. Cell cycle checkpoints

2.1 Interphase and the Restriction point

To ensure proper progression through the cell cycle, cells have developed a series of checkpoints that prevent them from entering into a new phase until they have successfully completed the previous one (Malumbres and Barbacid, 2001). The first important decision that a quiescent cell has to make is whether to cycle or not. Different pathways, named as signal transduction pathways, monitor the environment and the size of the cell and inform the cell about the balance between the

mitogenic and anti-mitogenic signals. Considering this information cells will make a decision, which will be reversible until the restriction point is reached (Pardee, 1974). However, once this point is passed, around mid-G1, cells are compromised to replicate its genome and to finish mitosis. This is an extremely important decision since cycling under improper conditions can cooperate with tumor progression. Indeed, cancer cells often show alterations in the signal transduction pathways that lead to proliferation in response to external signals (Hanahan and Weinberg, 2000).

2.2 DNA damage checkpoints

Maintenance of a stable genome is also a critical event to prevent apoptosis, senescence and malignant cell transformation. When mammalian cells contain damaged DNA, a complex mechanism named the DNA Damage Checkpoint is able to sensor this damage and transduce the signal to activate the p53 and the retinoblastoma (pRb) tumor suppressor pathways. Activation of

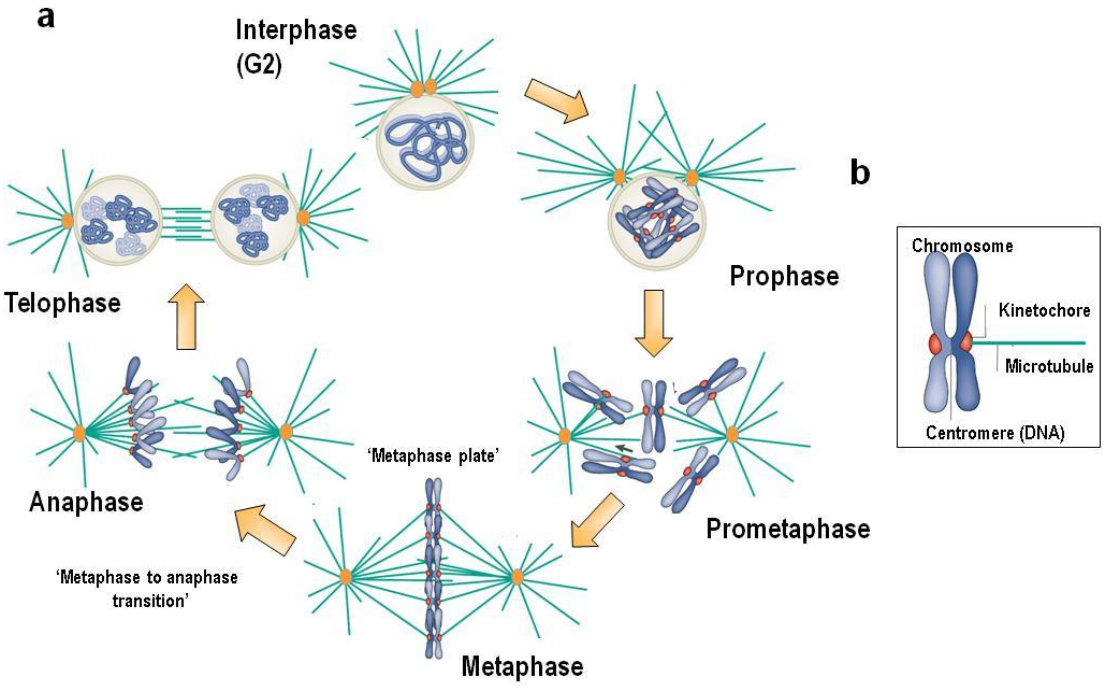

Figure 2. The phases of mitosis and a structural view of a mitotic chromosome. **(a)** Replicated interphase chromatin is condensed and kinetochores assembled during prophase. After nuclear envelope breakdown, during prometaphase, kinetochores interact with microtubules. By metaphase, bi-orientated chromosomes align in the middle of the bipolar spindle. Sister chromatids are pulled apart in anaphase and chromatin decondenses at telophase at the same time that the nuclear envelope is reformed. **(b)** Scheme of a mitotic chromosome. Kinetochores are assembled on the centromere regions of each sister chromatid to interact with microtubules. Microtubules are shown in green, nuclear envelope in grey, centrosomes in orange, chromatin in blue and kinetochores in red. (Adapted from (Cheeseman and Desai, 2008)).

these pathways prevents cells from entering DNA replication or mitosis when DNA is damaged, providing an opportunity for DNA repair (Bartek et al., 2004; Kastan and Bartek, 2004; Lukas et al., 2006). The DNA Damage Checkpoint can arrest cell cycle progression before, during or after S phase.

2.3 The Spindle Assembly Checkpoint

Correct chromosome segregation during cell division is essential to maintain an intact genome. Errors in chromosome partition can result in daughter cells that have inherited too many or too few chromosomes, a condition associated with cancer development that it is known as aneuploidy (Holland and Cleveland, 2009). To ensure high fidelity of chromosome segregation cells have developed a surveillance mechanism called the Spindle Assembly Checkpoint (SAC) that delays the onset of anaphase until all chromosomes are properly bi-orientated on the mitotic spindle (Figure 3). The effector of the SAC, known as the mitotic checkpoint complex (MCC), is located at unattached kinetochores and is composed by three proteins, Mad2, BubR1 and Bub3. The MCC inhibits the ability of Cdc20 to activate the ubiquitin ligase anaphase-promoting complex/cyclosome (APC/C). Once all the chromosomes are properly oriented on the spindle, the SAC is satisfied and Cdc20 is free to activate the APC/C-mediated polyubiquitylation of two key substrates, cyclin B and securin, thereby tagging its destruction by the proteasome. Securin is an inhibitor of a protease known as separase which is required to cleave the cohesin complex that holds sister chromatids together. Cleavage of cohesin is necessary to execute anaphase. On the other hand, proteolysis of Cyclin B is required to inactivate Cdk1 and this event is essential for exiting mitosis.

3. Control of mitosis and cytokinesis by post-translational modifications

The regulation of the last steps of the cell cycle relies predominantly on two post-translational mechanisms: protein phosphorylation and ubiquitin-mediated proteolysis. Both mechanisms are linked together since the proteolytic machinery is controlled by phosphorylation, and many kinases are downregulated by degradation. Deregulation of one of these post-translational modifications will affect the other resulting in uncontrolled proliferation, genomic instability and cancer.

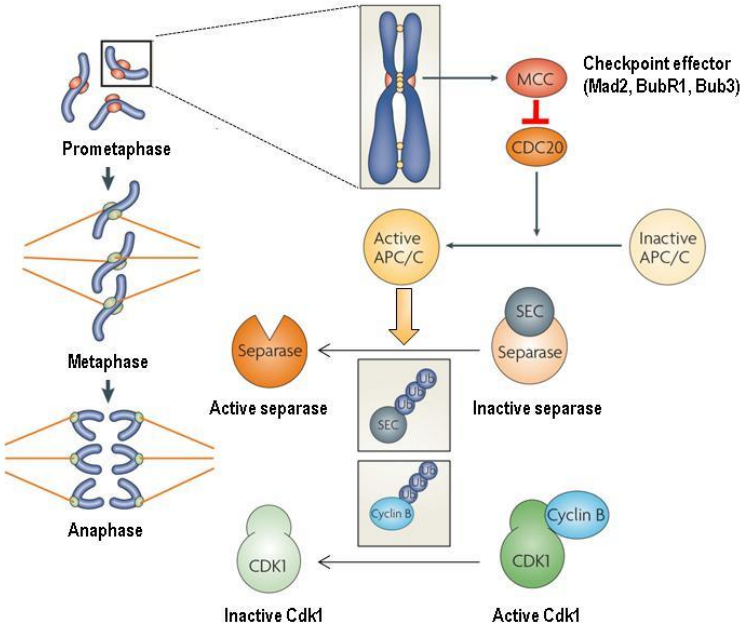

Figure 3. The Spindle Assembly Checkpoint. The checkpoint effector (MCC) is located at unattached kinetochores inhibiting Cdc20 binding to the APC/C. Bi-orientation of all the chromosomes provokes Cdc20 release, which now can activate the APC/C. This results in the polyubiquitination of anaphase substrates such as Cyclin B and Securin, and their subsequent proteolytic degradation, which leads to the activation of separase and the inactivation of Cdk1, respectively. (Adapted from (Musacchio and Salmon, 2007)).

3.1 Ubiquitination and SUMOylation

3.1.1 Ubiquitination

Protein degradation mediated by ubiquitin has emerged to be a very powerful mechanism to regulate cell cycle progression (Nakayama and Nakayama, 2006). This mechanism consists on assembling polyubiquitin chains on substrates to target them for degradation by the 26S proteosome. Ubiquitin is covalently conjugated to a lysine residue of a target protein by an enzymatic cascade involving an ubiquitin-activating enzyme (or E1), an ubiquitin-conjugating enzyme (or E2) and an ubiquitin-ligase (or E3) (Thornton and Toczyski, 2006). The substrate specificity of this pathway relies on the ubiquitin ligases. The main ubiquitin ligases complexes are: the SCF (Skp1 / cullin / Fbox proteins) that regulates the progression through the end of G1 to the beginning of M phase and the APC/C (anaphase-promoting complex/cyclosome) that it is active from mitosis to the end of G1 (Nakayama and Nakayama, 2006).

APC/C complex is regulated by the binding of the two cofactors, Cdc20 and Cdh1. The binding of these cofactors is, in turn, regulated by Cdks in that, phosphorylation of APC/C components is required for Cdc20 binding and impairs Cdh1 binding. Whereas Cdc20 activates APC/C during early mitosis, Cdh1 is responsible for APC/C activity from late mitosis till the G1/S transition (Peters, 2006). Both Cdc20 and Cdh1 recognize APC/C substrates by interacting with specific motifs such as the D-box (Fang et al., 1998), KEN-box (Pfleger and Kirschner, 2000), or

A-box (Littlepage and Ruderman, 2002). By recognition of these motifs, APC/C targets A-type cyclins (during G2/M) and B-type cyclins (metaphase-to-anaphase transition) for degradation, thereby controlling Cdk activity. In addition, APC/C regulates progression through mitosis by ubiquitinating several mitotic kinases such as Plk1, Aurora A, Aurora B and Nek2. Finally, in coordination with the SAC, APC/C-Cdc20 initiates anaphase by targeting the separase inhibitor, securin and cyclin B, for destruction (Peters, 2006).

3.1.2 SUMOylation

SUMOylation is a highly dynamic and reversible type of post-translational modification. Like ubiquitination, SUMOylation modulates protein function through post-translational covalent attachment of small ubiquitin-related modifiers (SUMOs) to lysine residues within targeted proteins (Geiss-Friedlander and Melchior, 2007). In vertebrates at least three SUMO forms (SUMO1, 2 and 3) are expressed. Human SUMO-1 is 45% identical to human SUMO-2 or -3, while SUMO-2 an-3 are 95% identical to each other and phenotypically indistinguishable. SUMO is covalently attached to a lysine residue, usually in the consensus modification site Ψ-Lys-X-Glu (where Ψ is a hydrophobic residue and X is any amino acid), in three enzymatic steps analogous to the ubiquitination cascade. SUMO conjugation requires a SUMO-activating E1 enzyme (SAE1/SAE2), the SUMO-conjugating E2 enzyme Ubc9 and, in some cases, additional E3 SUMO-ligases (Hay, 2005). SUMO modification is reversible by the action of SUMO-specific isopeptidases that belong to the family of ubiquitin-like proteases (Ulps), also known as sentrin-specific proteases (SENPs) (Hay, 2007) (Figure 4).

In contrast to poly-ubiquitination that targets proteins for degradation, SUMOylation has been shown to play a crucial role in the regulation of the activity of numerous cellular processes, including nuclear transport, genome integrity, signal transduction, and transcriptional regulation (Hay, 2005; Ulrich, 2008). The molecular consequences of SUMOylation are target specific, and can positively or negatively influence interactions with proteins, DNA or other macromolecules. Potentially, SUMO can affect any aspect of a target protein, including stability, localization or activity (Geiss-Friedlander and Melchior, 2007). Recent work has revealed the importance of SUMOylation for mitotic progression (Dasso, 2008; Watts, 2007) and has outlined a critical role of SUMO in kinetochore/centromere function (Dawlaty et al., 2008; Di Bacco et al., 2006; Klein et al., 2009; Zhang et al., 2008b).

SUMO can also mediate non-covalent interactions with proteins containing SUMO interaction motifs (SIMs) (Song et al., 2004). An exciting role for SIMs was recently shown for a family of E3 ubiqutin ligases (Rnf4 in mammals and Rfp1/Hex3-Slx8 in yeast) which can specifically recognize SUMO-containing substrates via their SIM motif (Prudden et al., 2007; Sun et al., 2007; Uzunova et al., 2007). This opens up the possibility that SUMOylation can act as a signal for the recruitment of E3 ubiquitin ligases, which leads to the ubiquitylation and degradation of the modified protein (Geoffroy and Hay, 2009).

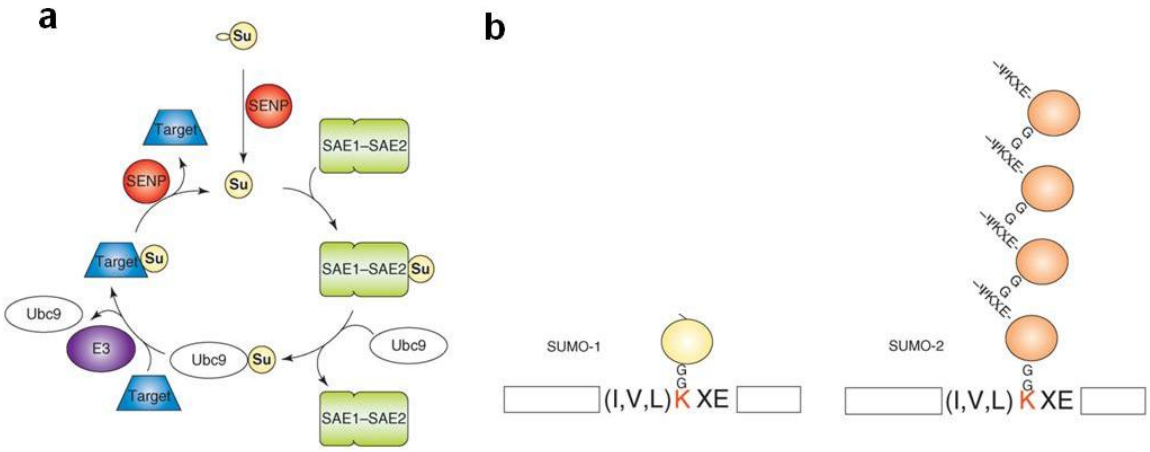

Figure 4. SUMO conjugation and deconjugation. **(a)** SUMO cycle of conjugation and deconjugation. SUMO (Su, yellow) is processed by a SUMO-specific protease (SENP, red) before being activated and covalently linked to the SUMO E1-activating enzyme (SAE1–SAE2, green). SUMO is then transferred to the SUMO E2-conjugating enzyme (Ubc9, white), which carries out target (blue) modification with the aid of a SUMO E3 ligase (E3, purple). Deconjugation to release free SUMO and target is mediated by a SENP. **(b)** SUMO-1 is distinct than SUMO-2 modification. Lysine acceptor residues subject to SUMO modification are usually found in the SUMO modification motif cKxE (where c is I, V or L). This motif is found in the N-terminal region of SUMO-2 and SUMO-3 but not in SUMO-1. Thus, SUMO-2 (and SUMO-3) can form polymeric chains through conjugation at the cKxE motif. (Adapted from (Hay, 2007)).

3.2 Phosphorylation

Progression through the entire cell cycle requires the controlled activation of different families of kinases that regulate by phosphorylation diverse cellular processes required for cell division (Fig 5). Some of them, such as the **Cyclin-Dependent Kinases** (Cdks), are involved in the regulation of different cell cycle phases. Indeed, the Cdks, which are heterodimeric protein kinases composed of a catalytic subunit known as Cdk and a regulatory subunit known as cyclin, regulate cell cycle commitment, DNA synthesis and the onset of mitosis (Malumbres and Barbacid, 2005). Cyclins's expression and degradation impose successive waves of kinase activation and inactivation controlling the progression of the cell cycle. Mitogenic signals are detected by the expression of D-type cyclins that bind and activate Cdk4 and Cdk6 during G1 to prepare the cell for DNA

replication. Activation of the complex Cdk4/6-cyclin D partially phosphorylates and inactivates pRb proteins that in turn allow the expression of E-type cyclins. E-cyclins bind and activate Cdk2 during the beginning of S phase and trigger the initiation of DNA synthesis. At the end of S phase, Cdk2 is then activated by cyclin-A2 to promote progression to G2. Finally, Cdk1 is activated by A-type cyclins to facilitate entry into mitosis. After the nuclear envelope breakdown, A-type cyclins are degraded and Cdk1 is then activated by cyclin-B. The Cdk1/cyclin B complex, also known as MPF (maturation promoting factor) is considered as the 'master regulator' of mitosis. This complex regulates many events at the onset of mitosis including nuclear envelope breakdown, centrosome separation, spindle assembly, chromosome condensation and Golgi fragmentation. Moreover, inactivation of the complex is also necessary to exit from mitosis and occurs upon inactivation of the SAC and degradation of Cyclin B by the APC/C, as mentioned before.

The **DNA damage kinases** are also involved in the mitotic regulation. Among the kinases implicated in the DNA damage checkpoint are included Atm (Ataxia-Telangiectasia Mutated) and Atr (ATM and Rad 3-related) and the checkpoint kinases Chk1 and Chk2 (Figure 5). Activation of these kinases frequently results in the modulation of mitosis through the regulation of other kinases —Wee1 and Myt1, which inactivate Cdks— or phosphatases —such as the Cdc25 family, which activate Cdks by removing the previous inactivating phosphorylations.

A group of cell cycle kinases are almost exclusively related with mitosis. Included in this group of **Mitotic Kinases** are the kinases of the Polo, Nek and Aurora families participate in the centrosome cycle and modulate spindle function and chromosome segregation during mitosis (Figure 5). Polo-like kinase (Plk) family is composed by four members in mammals, with Plk1 being the best known. Plk1 has been implicated in the activation of Cdk1-cyclin B at mitotic entry, centrosome maturation, mitotic assembly, the release of cohesin from chromosome arms in prophase and in the initiation of cytokinesis (Barr et al., 2004). Regarding the other members of the Plk family, Plk2 and Plk3 are mitogen-activated kinases with putative tumor suppressor functions and Plk4, the most divergent Plk family member, plays diverse roles in the generation of centrioles (Eckerdt et al., 2005; Kleylein-Sohn et al., 2007). The NIMA-related kinase family, or 'Nek family', consist of eleven different members (Nek1–11) (O'Connell et al., 2003). Among them, Nek2 is the more deeply characterized member and has been shown to be a core component of the human centrosome throughout the cell cycle. Additional kinases such as Bub1, BubR1 and Mps1 have been shown as major regulators of the spindle assembly checkpoint (Fisk et al., 2004; Logarinho and Bousbaa, 2008). Finally, Aurora kinase family includes key regulators of mitosis that will be described in detail in the next section.

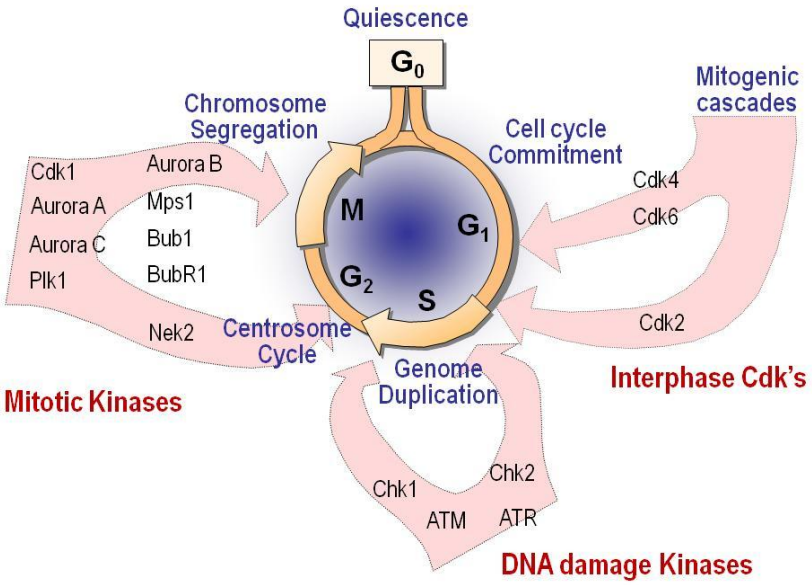

Figure 5. Control of the mammalian cell cycle by phosphorylation. There are three main groups of kinases (in red) that regulate cell cycle progression: Interphase's Cdks, DNA damage kinases and mitotic kinases. The main cell cycle events are shown in blue.

4. The Aurora family of protein kinases

Early work in *Drosophila* led to the identification of aurora mutants, which carry a loss-of-function mutation in a serine/threonine kinase essential for centrosome separation and the formation of bipolar spindles (Glover et al., 1995). A single Aurora protein exists in budding (Ipl1) or fission (Ark1) yeast, whereas two family members, Aurora A and Aurora B, are present in worms, flies and frogs. Three different Aurora family members, known as Aurora A, B and C, exist in mammals (Nigg, 2001). These kinases contain a conserved catalytic domain and N-terminal domains that vary in sequence and in length (Figure 6). Aurora B and C are close paralogues that probably arose from a relatively recent common ancestor (Brown et al., 2004).

4.1 Aurora kinases function and localization

Despite their high level of similarity, the three mammalian Aurora kinases have very distinct localizations and functions.

4.1.1 Aurora A: centrosomes and spindles

Aurora A, the orthologue to the original *Drosophila* kinase, localizes on duplicated centrosomes from the end of S phase to the beginning of the following G1 phase. Aurora A participates in several processes required for building a bipolar spindle including centrosome maturation and

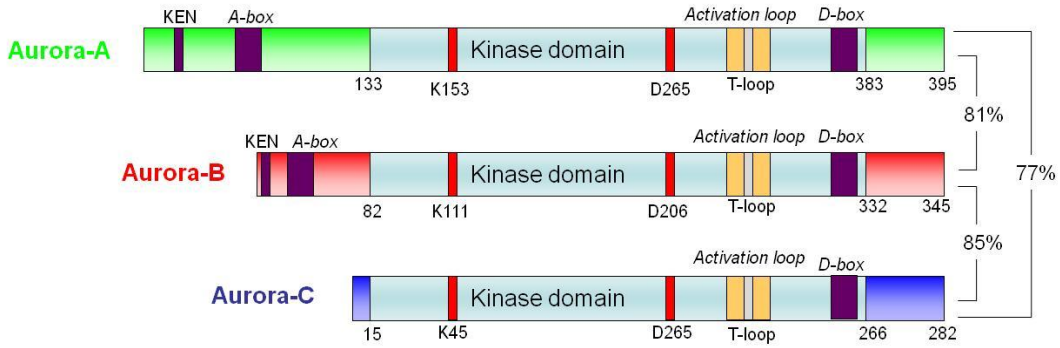

Figure 6. Mammalian Aurora kinases. The catalytic kinase domain (light blue) is highly conserved among the three mouse aurora kinases. The lysine (K) and aspartate (D) residues (in red) are located in the ATP-binding pocket and are in charge of binding to ATP. The T-loop (grey) is located at the activation loop motif (orange). D-box (purple) degradation motif is located at the C-terminal end of the three proteins. Outside the kinase domain, the three proteins differ in the length of the N-terminal domain in where KEN- and A-boxes degradation motifs are present in Aurora A and Aurora B proteins. Aurora B and Aurora C share the biggest homology among them (85% of identity).

separation, mitotic entry and bipolar spindle assembly (Barr and Gergely, 2007; Giet et al., 2005). Aurora A is implicated in all these processes through the interaction with a increasing number of effectors including Tpx2, Eg5, XMap125/chTog, NDel1, Lats and Tacc proteins.

4.1.2 Aurora B: the catalytic member of the chromosomal passenger complex

Aurora B is the enzymatic core of a multiprotein complex, named the chromosomal passenger complex (CPC), which comprises other three non-enzymatic subunits, INCENP, Survivin and Borealin (Ruchaud et al., 2007) (Figure 7). The CPC localization is highly dynamic. It is initially detected along chromosome arms, but is progressively concentrated in inner centromeres through prometaphase and metaphase. At the onset of anaphase, the CPC relocates to the central spindle, and accumulates at the midbody during telophase and cytokinesis (Figure 7).

The CPC is one of the most upstream regulators of centromere/kinetochore function being responsible for the recruitment to the kinetochore and centromere of a growing number of proteins including inner centromeric proteins (Sgo1, Sgo2, Mcak), regulators of the microtubule-kinetochore interaction (such as Ndc80/Hec1, Cenp-E or Plk1 among others) or proteins involved in the Spindle Assembly Checkpoint (SAC; such as Mad2, BubR1 or Mps1) (Kelly and Funabiki, 2009). Some of these molecules, including Ndc80, Dam1 and Mcak, are Aurora B substrates suggesting a critical role for the CPC in the destabilization of aberrant microtubule-to-kinetochore attachments and the SAC-dependent delay in mitotic progression until these defects are corrected. Recent data suggests that substrate phosphorylation depends on the distance of the substrate from Aurora B at the inner centromere, thus indicating that recruitment of the CPC to the kinetochore

prevents the stabilization of improper attachments and activates the SAC to delay the metaphase to anaphase transition (Liu et al., 2009).

During cytokinesis, Aurora B is localized to the midbody where its local inactivation is crucial for completion of abscission (Guse et al., 2005; Steigemann et al., 2009). Aurora B also participates in mitotic phosphorylation of Ser10 and, probably, Ser 28 in histone H3. These events seem to be necessary for chromosome condensation although the correlation between H3S10 phosphorylation and the condensation of chromosomes is not fully established (Johansen and Johansen, 2006; Nowak and Corces, 2004; Prigent and Dimitrov, 2003).

In addition to mitotic roles, Aurora B may also control gene silencing during differentiation by displacing heterochromatin protein 1β (Hp1β) from facultative heterochromatin and marking silent chromatin domains (Amabile et al., 2009; Sabbattini et al., 2007).

4.1.3 Aurora C: only a male meiotic kinase?

Less is known about Aurora C, which is expressed at high levels in the testis (Carmena and Earnshaw, 2003), and at low levels in thyroid and other cell types (Lin et al., 2006; Ulisse et al., 2006). Endogenous Aurora C has been detected in meiotic chromosomes of male mouse germinal cells where is known to play a specific role in spermatogenesis (Kimmins et al., 2007; Tang et al., 2006). In agreement with this, mutations in Aurora C have been shown to cause infertility in humans (Dieterich et al., 2007). In somatic cells, Aurora C, when exogenously expressed, colocalizes with Aurora A during interphase and Aurora B throughout mitosis (Dutertre et al., 2005) where it can bind members of the CPC (Li et al., 2004). Importantly, Aurora C ectopic expression can rescue Aurora B loss of function in cultured cells (Sasai et al., 2004; Slattery et al., 2009; Slattery et al., 2008; Yan et al., 2005), suggesting that Aurora C can perform the same mitotic functions as Aurora B, at least in some cell types. Additional potential roles for Aurora C in somatic tissues could include non-mitotic functions such as gene regulation via phosphorylation of histone H3 (Price et al., 2009).

4.2 Regulation of Aurora kinases

The kinase activity of Aurora family members is controlled by phosphorylation and dephosphorylation events, whereas their protein levels are regulated by ubiquitin-mediated proteolysis.

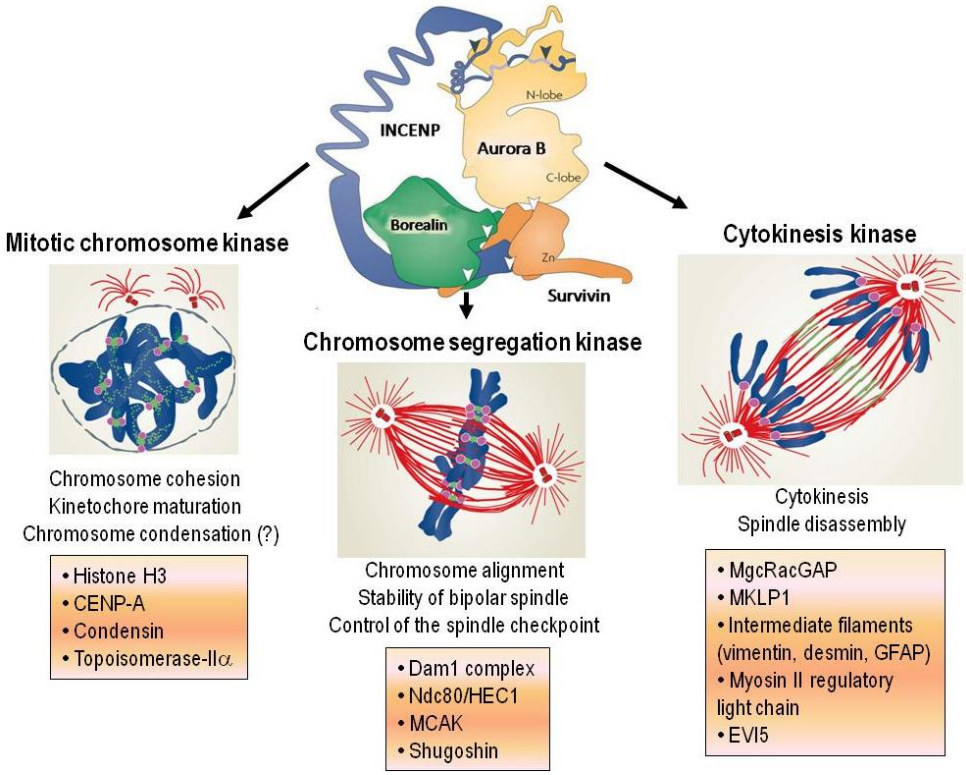

Figure 7. Aurora B and CPC localization and function during mitosis. Schematic representation of the chromosomal passenger complex (CPC) - composed by Incenp, Survivin, Borealin and Aurora B – correlated with its multiple functions and different localizations during mitosis. Aurora B substrates in each case are grouped in orange boxes. Aurora B as the enzymatic core of the CPC can act as a mitotic chromosome kinase during prophase where it is located along chromosomes arms and centromeres. During this stage, it is important for release of arm cohesion, kinetochore maturation and probably for chromosome condensation. During prometaphase / metaphase it concentrates in centromeres where it is involved in chromosome alignment, the stability of the spindle and the spindle checkpoint. Finally, at late mitosis Aurora B translocates to the central spindle where it regulates spindle disassembly and is essential for cytokinesis. The CPC during mitosis is shown in green, kinetohores in purple, chromosomes in blue and the mitotic spindle in red. Adapted from (Ruchaud et al., 2007).

4.2.1 Aurora A is regulated by Tpx2

Aurora A activation depends, in a first place, on the phosphorylarion of a critical threonine residue in the T-loop. Although this residue can be phosphorylated in vitro by protein kinase A (Walter et al., 2000), it has indeed been identified as an autophosphorylation site (Cheeseman et al., 2002). On the other hand, as it was first described in yeast, the phosphatase Pp1 negatively regulates Aurora A (Francisco et al., 1994). However, the best known Aurora A regulator is Tpx2 (Kufer et al., 2002). Binding with Tpx2 induces a conformational change in Aurora A in such a way that the phosphorylated T-loop, inside the activation motif of this kinase, adopts a more compact position, providing a better substrate binding platform and hiding the activating phosphoryl group from attack by the phosphatase Pp1 (Bayliss et al., 2003). In addition, Tpx2 stimulates

autophosphorylation and autoactivation of Aurora A, suggesting that Tpx2 can indirectly regulate Aurora A activity (Eyers et al., 2003). Ajuba and Pak1 have also been reported to regulate Aurora A activity (Hirota et al., 2003).

Aurora A is degraded in an APC/C-Cdh1 dependent-manner during mitotic exit (Castro et al., 2002). This mechanism is tightly regulated since D-box degradation motif of Aurora A (Figure 6) is only functional in the presence of a non-phosphorylated amino-terminal A-box (Littlepage and Ruderman, 2002).

4.2.2 Aurora B is regulated in a CPC-dependent manner

Aurora B regulation is principally mediated by the interaction with the CPC components: Incenp, Survivin and Borealin. Indeed, the CPC members are physically and functionally interpendent in that knock-down of any member of the complex delocalizes the others, disrupts mitotic progression and may destabilize one or more subunits (Gassmann et al., 2004; Jeyaprakash et al., 2007). The CPC non-enzymatic members control the targeting, enzymatic activity and stability of Aurora B (Ruchaud et al., 2007)

Aurora B activation is triggered by autophosphorylation of the T-loop residue after association with its substrate Incenp. Full activation occurs also by autophosphorylation in a positive feedback loop after Aurora B phosphorylation of Incenp in the conserved IN-box region (Bishop and Schumacher, 2002; Honda et al., 2003). In addition, phosphorylation of Borealin by Mps1 has been shown to be essential to control Aurora B activity and chromosome alignment (Jelluma et al., 2008), revealing a new way to regulate Aurora B activity through a member of the CPC and the mitotic kinase Mps1. Althoug some authors have pointed out that Survivin might contribute to Aurora B regulation (Bolton, 2002) this possibility has been ruled out by others (Honda et al., 2003). Finally, another inner centromere protein, Td-60, has been shown to enhance Aurora B activity in the presence of microtubules (Rosasco-Nitcher et al., 2008).

Aurora B activity is negatively regulated by the action of phosphatases. Although little is known about dephosphorylation processes of the CPC, it is thought that, as occurred for Aurora A, the major counteracting phosphatase of Aurora B is Pp1 (Emanuele et al., 2008; Francisco et al., 1994; Hsu et al., 2000). Indeed, Pp1α and Pp1γ are localized to the outer kinetochore where they could be able to remove Aurora B phosphorylation marks (Trinkle-Mulcahy et al., 2006). In addition, dephosphorylation of Incenp in budding yeast by Cdc14 phosphatase upon activation by separase has been described to be important for the transfer of Aurora B/Incenp to the central

spindle (Pereira and Schiebel, 2003). Clearly, dephosphorylation of the CPC and Aurora B substrates seems to be crucial for completion of mitosis but needs further study.

Regarding Aurora B degradation, this kinase is regulated by ubiquitin post-translational modifications in different ways. Firstly, Aurora B is targeted by a Cul3-containing SCF ubiquitin ligase during early mitosis (Sumara et al., 2007). Interestingly, this modification is necessary to remove a fraction of Aurora B from mitotic chromosomes allowing its accumulation on the central spindle during anaphase. In the absence of this SCF-Cul3 ubiquitin ligase, Aurora B spreads along chromosomes and fails to dissociate from them during anaphase. Secondly, Aurora B requires APC/C-Cdh1 activity to efficiently translocate to the spindle midzone in anaphase. Thus, in APC/C-Cdh1 depleted cells Aurora B and the CPC are not targeted to the spindle midzone and prematurely accumulate in the equatorial cortex resulting in a weak anaphase spindle (Floyd et al., 2008). Finally, after completion of cytokinesis, the remaining pool of Aurora B is targeted for degradation by APC/C-Cdh1 (Floyd et al., 2008; Garcia-Higuera et al., 2008). The requirements for the proteolysis of Aurora B by APC/C-Cdh1 are less well understood than in the case of Aurora A, but they are likely to involve a KEN-box and a motif similar to the A-box (Nguyen et al., 2005) (Figure 6).

4.2.3 Aurora C, the unknown member of the family

How Aurora C is regulated is almost completely unknown. It has been described that Aurora C interacts with Incenp and therefore, one possibility is that Aurora C activation may also be triggered by association with Incenp (Li et al., 2004). Despite the functional similarity between Aurora B and Aurora C, both proteins present structural differences in the N- and C- terminal domains. For instance, Aurora C do not have the KEN-box and A-box motifs that are present in Aurora A and Aurora B proteins (Figure 6), suggesting that Aurora C may be less susceptible to degradation than the other Auroras. Supporting this idea, it has been described that Aurora C expression in HeLa cells persists after Aurora B degradation near the end of mitosis (Sasai, 2004). In addition, the mechanisms by which Aurora C expression is only found in some specific tissues remain still undiscovered.

4.3 Mouse models of Aurora kinases

Different mouse models have been generated for the study of Aurora A. In three of them Aurora A gene has been genetically ablated using different approaches (Cowley et al., 2009; Lu et al., 2008; Sasai et al., 2008). Aurora A disruption, in all these cases, leads to early embryonic lethality at

embryonic day 3.5 (E3.5) due to severe defects in the formation of the mitotic spindle, indicating that Aurora A is an essential regulator of mitosis since the first embryonic divisions. On the other hand, different transgenic mouse models have been generated to study the effects of Aurora A overexpression in different tissues. In the transgenic models that overexpress Aurora A in the mammary gland hyperplasias or malignant tumors were detected after a long latency (Wang et al., 2006; Zhang et al., 2008a). On the other hand, over-expression of Aurora A in transgenic liver led to a low incidence of hepatic tumors (Li et al., 2009).

Aurora B has been poorly studied using mouse models. The only transgenic mouse model generated and published so far, analyzes the role of Aurora B specifically in spermatogenesis (Kimmins et al., 2007). This model, in which expression of either wild-type Aurora B or an inactive form of the kinase is driven by a pachytene-stage-specific promoter, confirms the important role of Aurora B during male meiosis.

Aurora C knock-out mouse model has been recently published (Kimmins et al., 2007). Aurora C-null mice were viable and appear nearly normal. The unique reported defect is reduced male fertility due to morphological defects of the sperm. This mouse model suggests that Aurora C appears to play unique functions during spermatogenesis and therefore, it is not required for somatic mitosis.

4.4 Aurora kinases and cancer

One century ago, Theodore Boveri predicted that chromosome alterations may be associated with cancer development and progression. In the last few years, a significant number of genetic alterations in mitotic regulators have been described to induce chromosomal instability (CIN) and aneuploidy, two related conditions associated with tumour development (Holland and Cleveland, 2009; Perez de Castro et al., 2007). Given the importance of mitotic kinases in the spindle assembly checkpoint, centrosome cycle and chromosomal segregation, it is not surprising that these kinases are frequently deregulated in cancer. This fact has opened new therapeutic opportunities to battle against cancer by inhibiting mitotic kinases (de Carcer et al., 2007; Perez de Castro et al., 2008).

The first data to implicate Aurora family of kinases in tumorigenesis came with the observation that Aurora A and Aurora B are overexpressed in primary breast (Bischoff et al., 1998) and colon tumour samples (Sen et al., 1997). Importantly, Aurora A has been found to be located on human chromosome 20q13, a hotspot of amplification in tumours that has also been associated with poor prognosis in patients (Sen et al., 1997). Many subsequent studies identified other tumour

types, including breast, pancreatic, ovarian and gastric tumours, in which Aurora A was amplified or otherwise overexpressed (Bischoff et al., 1998; Gritsko et al., 2003; Li et al., 2003; Miyoshi et al., 2001; Moreno-Bueno et al., 2003; Sakakura et al., 2001; Sen et al., 2002). A third evidence came from *in vitro* studies in which overexpression of wild-type Aurora A, but not a catalytically inactive form, is able to cause malignant transformation in primary rodent cells pointing Aurora A as an oncogene (Bischoff et al., 1998).

The role of Aurora B in tumourigenesis is less clear. A recent study, has included both Aurora A and Aurora B in the top-70 list of genes of the CIN signature (Carter et al., 2006) meaning that they may act as a driving force in tumor initiation (Shih et al., 2001). Some *in vitro* studies have shown that forced expression of wild-type Aurora B, but not a catalytically inactive form, can enhance Ras-induced cell transformation (Kanda et al., 2005). Furthermore, overexpression of Aurora B in CHO cells was reported to promote aneuploidy and increase invasiveness in xenograft experiments suggesting a possible role of Aurora B as a promoter of metastasis (Ota et al., 2002).

Aurora C is also overexpressed in cancer cell lines, but there is just one study that analyzes its expression in tumours. In this work, the three Aurora kinases were analyzed in parallel and the three of them appear to be overexpressed at the protein level in thyroid carcinomas (Ulisse et al., 2006).

All these evidences, have shown Aurora kinases to be promising clinically relevant anti-cancer targets. Numerous small molecule inhibitors against Aurora kinases have been developed in the last years (Taylor and Peters, 2008). The first and best described compounds are Hesperadin, VX-680 and ZM447439 (Ditchfield, 2003; Harrington et al., 2004; Hauf et al., 2003). Treatment of cells with these inhibitors causes very similar phenotypes than the ones observed upon inhibition of Aurora B. All three compounds show a marked decrease in mitotic phosphorylation of histone H3 on serine 10, accompanied with cytokinesis failure and the appearance of polyploidy cells. In addition, VX-680 treatment of mice bearing established xenografted tumours caused significant regression of tumour size associated with the induction of apoptosis and reduction of histone H3 phosphorylation (Harrington et al., 2004). Confirming their potential in anti-tumoral therapies, the clinical use of a new generation of Aurora kinase inhibitors is currently being tested in phase I and phase II trials (Perez de Castro et al., 2008) (Keen and Taylor, 2009).

Aim of the work

The aim of the project presented in this thesis was to determine the relevance of Aurora B in the regulation of cell cycle and tumour development in mammals. The work has focused on the identification of new regulatory mechanisms of Aurora B and in the functional characterization caused by complete or partial inactivation of Aurora B gene in mice and primary cells.

With this intention we proposed the following objectives:

1. Understand the regulation of Aurora B by new posttranslational modifications.

2. Study the consequences of partial inactivation of Aurora B during development and tumor formation.

3. Determine the essential roles of Aurora B and putative complementation by Aurora C during the first embryonic cell cycles.

4. Explore novel roles of Aurora B using primary cells in which Aurora B can be completely eliminated in a conditional manner.

Materials & Methods

1. Genetically modified mouse models

1.1 Animal housing

All the mice used in this study were housed in the pathogen-free animal facility of the Centro Nacional de Investigaciones Oncológicas (Madrid) following the FELASA (Federation of European Laboratory Animal Science Associations) recommendations and the current legislation of the European Union. All the mice experiments carried out in this memory were previously approved by the Bioethics Committee of the Instituto de Salud Carlos III. These animals were observed on a daily basis by our specialized technicians (Sheila Rueda and Isabel Moreno) and sick mice were killed humanely in accordance with the Guidelines for Humane End Points for Animals used in biomedical research. All animals were maintained in a mixed 129/Sv (25%) × CD1 (25%) × C57BL/6J (50%) background.

1.2 Generation of mouse models

1.2.1 Construction of targeting vectors

The conditional targeting vector was constructed by Gene Bridges by flanking exons 2-6 of the murine *Aurkb* locus with loxP sequences (Figure 18). The genomic sequences containing Aurora B gene were obtained from two bacterial artificial chromosomes (BACs) named RP23-153N12 and RP23-26L2. A neomycin resistance-gene (neo^r) driven by the phosphoglycerate kinase (PGK) promoter was used for positive selection of clones.

The knock-in targeting vector that expresses the β-galactosidase (lacZ) gene was constructed in our lab using the pFLEx backbone (Schnutgen et al., 2003). Genomic sequences of 5' and 3' homology arms, exons 2-4 and splicing acceptor (SA) were amplified by PCR from previous BACs and cloned in the intermediate vectors pCRII-Zero-blunt and pCR4 using the TOPO cloning system (Invitrogen). The thymidine kinase gene driven by the PGK promoter (PGK-TK cassette) was amplified from pPNT vector (Tybulewicz et al., 1991) and was used for negative selection of clones after ganciclovir addition. The SA was then cloned in pFLEx using *Pme*I/*Pme*I restriction sites, exons 2-4 were cloned in *Nru*I/*Nru*I, the 5' arm in *Not*I/*Xho*I, the 3'arm in *Sal*I/*Sal*I and the PGK-TK cassette in *Mfe*I/*Mfe*I.

The knock-in targeting vector that gives inducible expression of Aurora B gene under a minimal tetracycline promoter was constructed in collaboration with Earnshaw's lab in Edinburgh using a modified version of pTRE-tight vector (Clontech). This modified pTRE-tight vector contains the puromycin gene sequences driven by the β-actin promoter for positive selection of clones. Genomic sequences of 5' and 3' homology arms, were amplified by PCR from previous BACs and cloned in pGEM-T (Promega) intermediate vector. The cassette PGK-TK was amplified from pPNT vector and was used for negative selection of clones. The 5'arm was then cloned in pTRE modified vector using *Avr*II/*Spe*I restriction sites, the 3'arm was cloned in *Pvu*II/*Not*I and the PGK-TK cassette in *Cla*I/*Cla*I.

1.2.2 Generation of quimeras

To facilitate homologous recombination, mouse ES cells V6.4 obtained from a hybrid (129 x C57BL/6J) strain were electroporated with 100ug of linearized DNA from the corresponding targeting vectors. Recombinant ES cells and clones were selected in the presence of G418 (neomycin) and, if possible, with ganciclovir. This step was done by the Transgenic Unit of the CNIO. The identification of the recombinant clones was performed by Southern blot analysis using new restriction sites from the recombinant alleles and probes external to the homology arms. Positive recombinant clones were either aggregated with morulas CD1 or microinjected into C57BL/6J blastocysts by the Transgenic Unit of the CNIO. The male quimeras obtained (Figure 8) were crossed with wild-type females for transmission of the recombinant allele.

1.2.3 Generation of Aurora B conditional, knock-in and null alleles

Heterozygous recombinant mice *Aurkb*(+/loxfrt) (conditional knock-out model) and *Aurkb*(+/Zloxfrt) (knock-in model) were first crossed with TgpCAG–Flpe transgenic mice (Rodriguez et al., 2000) that ubiquitously expressed Flp recombinase, to remove the neo selection marker and thus, to generate either the conditional *Aurkb*(lox) allele (conditional knock-out model)

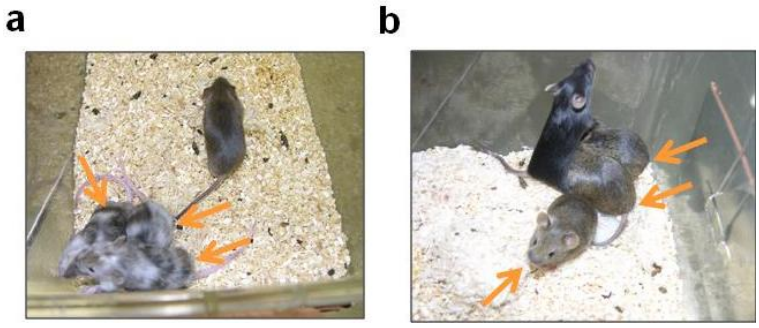

Figure 8. Generation of quimeras. (a) Quimeras (arrows) obtained from aggregation of ES cells (129/ C57BL/6J – agouti/black) with morulas (CD1 – white). (b) Quimeras (arrows) obtained from microinjection of ES cells (129/ C57BL/6J – agouti/black) into blastocysts (black).

or a non-functional conditional *Aurkb*(Zlox) allele (knock-in model). To generate the null alleles, we crossed *Aurkb*(+/lox) mice and *Aurkb*(+/Zlox) with TgCMV–Cre transgenic mice (Schwenk et al., 1995) that ubiquitously expressed Cre recombinase. In the *Aurkb*(lox) allele, Cre-mediated recombination between the two loxP sites excises exons 2-6; whereas, in the *Aurkb*(Zlox) allele, Cre-mediated recombination between the two wild-type loxP sites, or between the two mutant lox511 sites, eliminates exons 2-4 and produces an inversion of the IRES (internal ribosome binding site)-lacZ cassette. In the final *Aurkb*(Z) allele, the IRES-lacZ cassette is transcribed downstream the *Aurkb* exon 1 resulting in a truncation of the *Aurkb* transcript and expression of β-galactosidase from the IRES.

On the other hand, heterozygous recombinant mice *Aurkb*(+/lox-tet) were crossed with TgCMV–Cre transgenic mice to remove the puromycin selection cassette, obtaining the final *Aurkb*(tet) allele.

Table 1. Genetic modifications of Aurora B locus.

Aurora B alleles	Description
***Aurkb*(lox)**	Conditional allele
***Aurkb*(–)**	Null allele , germline deletion
***Aurkb*(Δ)**	Null allele, deletion by adenovirus infection of Cre
***Aurkb*(Z)**	Knock-in allele, *Aurkb* gene is replaced by lacZ transcripts
***Aurkb*(tet)**	Knock-in allele, *Aurkb* promoter is replaced a minimal tetracycline inducible CMV promoter

1.3 Mouse crosses

The mouse strains shown in Table 2, were crossed at some point with the different mouse models generated for Aurora B.

Table 2. Mouse strains used in this study.

Mouse line	Description	Origin
TgCMV-Cre	Transgenic line expressing Cre recombinase under ubiquitous CMV promoter	(Schwenk et al., 1995)
TgpCAG–Flpe	Transgenic line expressing the Flpe recombinase under the control of the pCAG element (beta-actin promoter-CMV enhancer)	(Rodriguez et al., 2000)
TgMMTV-Erbb2	Transgenic line expressing the activated rat Erbb2 (c-neu) oncogene under the direction of the mouse mammary tumor virus promoter	Jackson Laboratories (Muller et al., 1988)
Rosa26-M2rtTA	Knock-in line expressing a reverse tetracycline-controlled transactivator (rtTA)	(Beard et al., 2006)

1.4 Mouse genotyping

For genotyping *Aurkb*(lox), *Aurkb*(–) , *Aurkb*(Z) and *Aurkb*(tet) alleles we isolated tail DNA from 3-4-week old mice and we performed a PCR amplification reaction using the oligonucleotides

shown in Table 3 and following this conditions: 94 ºC during 4 minutes followed by 35 cycles of DNA denaturalization at 94 ºC during 30seconds, primer annealing at 60 ºC during 30 seconds and polymerase extension at 72 ºC during 60 seconds ending with a single elongation cycle of 7 minutes at 72 ºC.

Table 3. Oligonucleotides used for *Aurkb* locus genotyping. (cKO:conditional knock-out, F:forward and R, reverse primers, asterisk (*) indicates size too big for genotyping purposes).

Mouse Model	Name	Sequence (5'-3')	*Aurkb* allele and size
cKO	F-1	AGAGGTCTCCCTGCCTCTG	*Aurkb*(+) : 1520bp*
	R-3	GGGCATGAATTCTTGAGTCG	*Aurkb*(–) : 364bp
cKO	F-2	AGGGCCTAATTGCCTCTTGT	*Aurkb*(+) : 358bp
	R-3	GGGCATGAATTCTTGAGTCG	*Aurkb*(lox) : 491bp
lacZ knock-in	F-Z1	AGAGGTCTCCCTGCCTCTG	*Aurkb*(+) : 247bp
	R-Z2	GGAGCAAAGGGTGACTCTGA	*Aurkb*(Z) : 435bp
tet knock-in	F-Tet1	AGTAGTCTCTGCCCCCTGGT	*Aurkb*(+) : 482bp
	R-Tet2	GAGATGGGTTGGGTAGCAGA	
tet knock-in	F-Tet1	AGTAGTCTCTGCCCCCTGGT	*Aurkb*(tet) : 368bp
	R-Tet3	GCCTCGTGATACGCCTATTT	

1.5 Treatments in live animals

1.5.1 Wound healing

To analyze the ability of *Aurkb*(+/+) and *Aurkb*(+/–) mice to repair wounds we introduced 4-mm punch biopsy wounds into the dorsal skin of anesthetized mice. We performed two wounds per mouse, one per flank. For a period of five days, we measured wound diameters using a digital caliper and we took pictures of all the wounds. We repeated the same protocol to collect skin samples from wounded-mice for immunohistochemistry and hispathological analysis.

1.5.2 Hepatectomy

To study the ability of hepatocytes to enter the cell cycle and regenerate the liver after tissue loss we performed 2/3 partial hepatectomy following the guidelines described in (Mitchell and Willenbring, 2008). The mass of the resected liver tissue was measured after the operation, and that of the remnant liver was determined after killing of the animals six days after surgery. After hepatectomy, *Aurkb*(+/+) and *Aurkb*(+/–) mice were injected intraperitoneally (i.p) with 50mg/kg BrdU (Sigma) 2 h before mice were sacrificed for samples. This surgery was done in collaboration with Dr. Cristopher Heeschen.

1.5.2 Tumor induction

1.5.2.1 Skin carcinogenesis: DMBA-TPA

Seven-day-old *Aurkb*(+/+) and *Aurkb*(+/–) mice were painted with a single dose of 0.5 mg of 7,12-dimethylbenz[α]anthracene (DMBA). Two weeks later, tumor growild-typeh was promoted by treating with 5 mg of 12-O-tetradecanoylphorbol-13-acetate (TPA) twice a week for twelve weeks. Mice were shaved before each treatment to allow a better distribution of the chemicals. Animals were observed on a daily basis, and the size and characteristics of the skin lesions were annotated. Tumors were measured weekly in two using a digital caliper. Most mice developed multiple lesions. The position and number of each tumor were recorded, and each lesion was followed individually.

1.5.2.2 Fibrosarcomas: 3-methylcholanthrene (3-MC)

For the induction of fibrosarcomas *Aurkb*(+/–) and *Aurkb*(+/+) mice of 3–5 months of age, received a single intramuscular injection, in one of the rear legs, of a 50 µl solution containing 3MC (Sigma), at a concentration of 20 µg/µl, and dissolved in sesame oil (Sigma). Mice were observed on a daily basis until tumors of >1.5 cm in diameter developed in the injected leg, at which point the animals were killed humanely and the tumors were extracted for further analysis.

2. Histological and immunohistochemical analysis

For histological observation, dissected organs were fixed in 10%-buffered formalin (Sigma) and embedded in paraffin wax. Sections of 3- or 5-µm thickness were stained with haematoxylin and eosin (H&E). Additional immunohistochemical examination of the tissues and pathologies analysed were performed using the antibodies noted as IHQ that are shown in the Table 4.

The quantification of DNA ploidy in sections was performed using ImageJ software (National Institutes of Health, Bethesda, Maryland, USA, http://rsb.info.nih.gov/ij/). The pathology analysis was performed by Marta Cañamero, head of the Comparative Pathology Unit of the CNIO.

3. Embryos

3.1 Embryo culture and extraction

Zygotes were extracted by ripping the ampula of pregnant females from crosses between *Aurkb*(+/–) mice. The zygotes obtained were then treated with hyalurodinase (Sigma) to remove the cumulus cells and washed with Hepes-buffered Medium 2 (M2; Sigma). Fertilized embryos at E1.5-E2.5 were collected by flushing the uteri of pregnant females with M2 (Sigma). Zygotes and embryos

Table 4. Primary antibodies used in different assays. (IHQ: immunohistochemistry ; IF: immunofluorescence ; IP: immunoprecipitationWB: Western-blot).

Antibody	Host Species/Clonality	Application	Dilution	Source / Clone
ACA	Human Polyclonal	IF	1:100	Antibodies Incorporated
Akt	Rabbit Polyclonal	WB	1:500	Cell Signaling
α-tubulin	Mouse Monoclonal	IF, WB	1:2000	Sigma / DM1A
α-tubulin	Rat Monoclonal	IF	1:1	ATCC / YL1/2
Aurora B	Mouse Monoclonal	IF, WB	1:200	BD Transduction / AIM-1
Aurora B	Rabbit Polyclonal	IF, IHQ	1:200/1:100	Abcam
Aurora C	Rabbit Polyclonal	IHQ	1:250	Zymed
β-Actin	Mouse Monoclonal	WB	1:2000	Sigma / AC-40
Bromo-deoxyuridine	Mouse Monoclonal	IF	1:50	BD Pharmingen / 3D4
Bromo-deoxyuridine	Mouse Monoclonal	IHQ	1:50	GE Healthcare / BU-1
Caspase 3 Active	Rabbit Polyclonal	IHQ	1:200	RYD Systems
Cyclin B1	Mouse Monoclonal	IHQ	1:175	Millipore / U152
Cyclin B1	Rabbit Polyclonal	IF	1:200	Santa Cruz Biotech.
γ-tubulin	Mouse Monoclonal	IF	1:500	Sigma / GTU88
HA	Rabbit Polyclonal	WB	1:4000	Abcam
Incenp	Human Polyclonal	IF	1:100	Hospital Puerta del Mar
Ki67	Rat Monoclonal	IHQ	1:100	GE Healthcare
Mad2	Rabbit Polyclonal	IF	1:500	E. Salmon laboratory
$p21^{Cip1}$	Mouse Monoclonal	WB	1:100	Santa Cruz Biotech.
Phospho-CENP-A (Ser7)	Rabbit monoclonal	IF	1:200	Upstate Biotech. / NL41
Phospho-Histone H2A.X (Ser139)	Mouse Monoclonal	IHQ	1:2000	Millipore / JBW30
Phospho-Histone H3 (Ser10)	Rabbit Polyclonal	IF	1:500	Upstate Biotechnology
Phospho-p53 (Ser15)	Rabbit Polyclonal	IHQ	1:25	Cell Signaling
Phospho-P70-S6K (T389)	Mouse Monoclonal	WB	1:500	Cell Signaling / 1A5
Phospho-Rb (S780)	Rabbit Polyclonal	WB	1:500	Cell Signaling
V5	Mouse Monoclonal	IF, IP	1:2000/1-2ug	Invitrogen

were cultured in vitro in potassium simplex optimized medium (KSOM, Chemicon International Inc.). Embryos were treated with the Aurora kinase inhibitor ZM447439 (Tocris, Biosciences) at a 2 or 20 μM final concentration of the drug during 12 hours. To perform embryo "hatching", blastocyts were transferred into gelatinized p96-well plates and cultured in ES cells medium (DMEM+GlutaMAX, 15% fetal bovine serum, non-essential aminoacids) for several days. This process can be visualized in Figure 9.

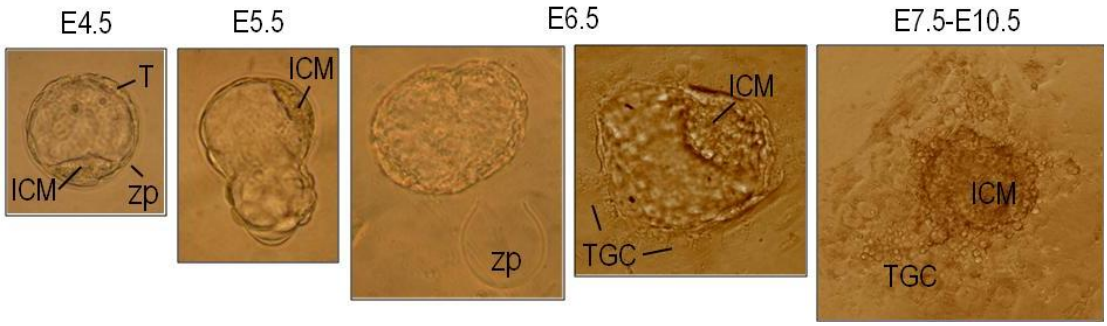

Figure 9. Culture of blastocysts – Embryo "hatching". A blastocyst at E4.5 display a clear inner cell mass (ICM) a layer of trophoblast cells (T) and it is surrounded by a thick membrane called zona pellucid (zp). After one day in culture the blastocyst's growild-typeh starts to deform the zp until it finally breaks (E6.5). At this moment, the embryo attaches to the plate with the help of a cell lineage derived from the trophoblast called trophoblast giant cells (TGC). Once attached, and after several days in culture (E7.5-E10.5) the blastocyst's ICM form a robust mass of ES cells surrounded by a big population of TGC.

3.2 Embryo microinjection

For RNA interference against Aurora B and C in early embryos, wild type zygotes were microinjected with a combination of three distinct shRNAs for each kinase that were cloned in a modified Gateway® (Invitrogen) compatible version of pSuper-Retro plasmid, along with a reporter H2B-GFP expression vector at a final concentration of 20ng/ul. Forty eight hours after microinjection, embryos were observed under the confocal microscope to confirm H2B-GFP expression and then fixed for immunostaining or maintained in culture one day more. At 72h after microinjection, embryos were used for RNA extraction or fixed for immunostaining. The targeted sequences for Aurora B and C are shown in Table 5. Embryo microinjection was performed by Javier Martín (Transgenic Unit, CNIO)

Table 5. siRNA sequences to interfere against Aurora B and Aurora C.

Vector	Target sequence (5'-3')
sh***Aurkb*-1**	GTTGGCTGAGAACAAGAGT
sh***Aurkb*-2**	GAGCCGTTTCATCGTGGCA
sh***Aurkb*-3**	CAAGAGTCAGGGCTCCACT
sh***Aurkc*-1**	GGAAAATCATTTCATCGTG
sh***Aurkc*-2**	CCAGGAAGCATTTCACCAT
sh***Aurkc*-3**	GCTTCTTAGGTACCATCCT

4. Cell culture

4.1 MEFs culture, extraction and infection

Mouse embryonic fibroblasts (MEFs) were prepared from E14.5 embryos and cultured using standard protocols. E14.5 embryos were extracted from the uterus of pregnant females from *Aurkb*(+/–) intercrosses, the placenta was removed and embryos were isolated from the yolk salk. The embryo without the liver and the head was minced, and dispersed in 0.1% trypsin (5 min at 37°C). Cells were grown for two population doublings and then frozen. All cultures were maintained in Dulbecco's modified Eagle's medium (DMEM; Gibco) supplemented with 2 mM glutamine, 1% penicillin/streptomycin and 10% foetal bovine serum (FBS). To analyze S phase entry, passage 2 MEFs (10^6 cells per 10 cm dish) were deprived of serum for 48 hr and restimulated with 10% FBS to enter the cell cycle. MEFs were pulsed for 30 min with 10 μM BrdU and stained using an anti-BrdU antibody (BD Pharmingen). BrdU incorporation was measured by immunofluorescence and DNA content. MEFs infection was performed using adenoviruses expressing GFP or the Cre recombinase (Ad5 CMV-Cre) obtained from The University of Iowa (Iowa City, IA). Infection was carried out during 2 days in a cell culture synchronized in G0 by serum deprivation and/or confluence.

4.2. Human and mouse cell lines

HEK293, U2OS and HeLa human cells were maintained in DMEM medium supplemented with 10 % fetal bovine serum and antibiotics and were grown at 37ºC in a humidified 5% CO_2 atmosphere. NIH-3T3 mouse cells were maintained in the same conditions with 10% calf serum. Human Aurora B was silenced using validated siRNA oligos from Qiagen with the following sequence: 5'-AACGCGGCACTTCACAATTGA-3'. HEK293, U2OS and HeLa cells were transfected with 1 μg of plasmid DNA using Effectene transfection reagent (Qiagen) according to the manufacturer´s instructions. For silencing experiments, siRNA oligos were nucleofected in HeLa cells using Amaxa kit and the conditions provided by Amaxa I13 program. In focus formation assays, NIH-3T3 cells were transfected with 10ug of V5-Aurora B plasmids and 1ug of HRasG12V following standard calcium phosphate transfection protocol, maintained in culture during three weeks and then stained with crystal violet solution for foci quantification.

Cell cycle distribution of MEFs and human cell lines were determined by flow cytometry after DNA staining with propidium iodide (Sigma) and analysed on a FACSCanto flow cytometer (Becton Dickinson). Data were processed using FACSDiva software (Becton Dickinson). MEFs and HeLa cells were treated with ZM447439 (Tocris, Biosciences) at a 2μM final concentration of the drug

5. Biochemical procedures

5.1 RNA extraction and Real-time-PCR

To quantify expression of Aurora transcripts, total RNA from embryos at different stages was isolated using Trizol (Invitrogen). Expression of Aurora B and Aurora C was quantified by real-time quantitative amplification with the SuperScript® III Platinum assay kit (Invitrogen), according to the manufacturer's instructions, in a BioRad iCycler Real-Time PCR apparatus. Amplification of GAPDH was used for normalization. The oligonucleotides used for amplification of Aurora B, Aurora C and GAPDH are shown in Table 6.

Table 6. Oligonucleotides used for RT-PCR of Aurora B and Aurora C (F, forward and R, reverse primers).

RT-PCR Oligos	Target sequence (5'-3')
***Aurkb*-F**	ATGGCTCAGAAGGAGAACGC
***Aurkb*-R**	CCAGTTCCCACCCCTTCT
***Aurkc*-F**	ATGGAGCCCAGCACCTCAAC
***Aurkc*-R**	ACAGAGCCTGGAGACCTTCC
GAPDH-F	GCCACCCAGAAGACTGTGGATGGC
GAPDH-R	CATGATGGCCATGAGGTCCACCAC

5.2 DNA cloning

Mouse Aurora B cDNA was amplified by PCR from the plasmid mAA0155 (Mammalian Gene Collection), cloned into pENTR-D-TOPO vector using TOPO technology (Invitrogen) and transferred to a destiny vector coexpressing GFP or V5 tag by a LR recombination reaction of the Gateway system (Invitrogen). Aurora B mutants (K111M, D205A and K207R) were prepared using the Quick-Change site-directed mutagenesis kit (Stratagene) and were verified by DNA sequencing. The additional plasmids pcDNA3.1-HA-SUMO-1,/-2 and /-3 and pcDNA3-Ubc9 were kindly provided by Ron Hay (Wellcome Trust Centre for Gene Regulation and Expression, Dundee, UK); whereas, HRas-G12V expression vector was from Barbacid's laboratory (CNIO).

5.4 Immunofluorescence

For immunofluorescence, embryos were fixed with cold methanol during 1 h at –20ºC, rinsed with M2 medium, washed in PBS containing 0.1% BSA (Sigma) and incubated with 0.1% Triton X for permeabilization. Alternatively, embryos were fixed with 5% paraformaldehyde (PFA). MEFs and human cell lines were fixed with 4% PFA and permeabilized with 0.15% Triton X. Embryos or MEFs were then blocked with 3% BSA and incubated with the primary antibodies noted as IF that are shown in Table 4. The matching secondary antibodies, with different Alexa dies (488, 594, 647), are from Molecular Probes (Invitrogen). Images were obtained using a confocal ultra-spectral microscope (Leica TCS-SP5).

5.4 X-Gal detection in embryos and cells

To detect β-galactosidase activity, embryos were fixed for 5 min in PBS containing 1% formaldehyde, 0.2% glutaraldehyde and 1% serum. After fixation, embryos were rinsed with 1% serum in PBS and then transferred to a β-galactosidase reaction mixture (4 mM $K_3Fe(CN)_6$, 4 mM $K_4Fe(CN)_6$, 2 mM $MgCl_2$ and 1 mg/ml X-gal in PBS) at 37ºC overnight. Embryos were washed once in PBS and kept at 4ºC. Positive embryos were scored 48h after the reaction was initiated. Alternatively, ES cells were fixed with 0.2% glutaraldehyde and treated overnight at 37ºC with the same β-galactosidase reaction mixture.

5.5 Protein extraction and analysis

For immunodetection in protein lysates, cells were washed twice with ice-cold PBS and lysed in RIPA lysis buffer (37 mM NaCl, 0.5% NP-40, 0.1% SDS, 1% TX-100, 20 mM Tris-HCl pH 7.4, 2 mM EDTA, 10% glicerol 1 mM PMSF) supplemented with protease and phosphatase inhibitory

cocktails (Sigma). Additionally, for detecting SUMOylated proteins an inhibititor of SUMO-proteases, called N-ethylmaleimide (NEM), was added at 10mM final concentration. After 30 min on ice, samples were cleared by centrifugation. Proteins were separated on SDS-PAGE, transferred to nitrocellulose membranes (BioRad), probed using specific antibody and detected using fluorescent donkey (Rockland) or goat (Invitrogen) anti rabbit or anti mouse secondary antibodies followed detection using the Odyssey Infrared Imaging System (Li-Cor Biosciences). After transfer of the protein lysates, we probed nitrocellulose membranes with primary antibodies noted as WB that are shown in Table 4. Secondary antibodies were coupled to Alexa 680 and 800 dies (Invitrogen) for immunodetection.

5.6 Immunoprecipitation and in vitro kinase assays

Total protein lysates extracted from HEK293 cells transiently transfected with V5-tagged Aurora B vectors were precleared with protein G-agarose bead suspension for 1hour (Amersham). Supernatants were first incubated for 2h at 4ºC on a rotating wheel with mouse anti-V5 (Invitrogen) and later with 50 µl of the blocked bead suspension for an additional hour. Immunoprecipates were then washed three times in RIPA buffer and, in case of the kinase assay, one extra wash was performed with RIPA plus 0.5M NaCl to remove possible bound unspecific kinases. One fifth of the immunoprecipitates bound to the beads were used for V5 detection by western blot. For the kinase assay, four fifths of the beads were washed in kinase assay buffer [10 mM HEPES-NaOH (pH 7.4), 150 mM NaCl, 10 mM MgCl2, and 1 mM EGTA] supplemented with 0.5 mM DTT and phosphatase inhibitor cocktail (Calbiochem) and later incubated in 25 µl of 2x kinase buffer supplemented with 0.2 mM ATP, 2,5 uCi [γ-32P]ATP and 3 ug of MBP as Aurora substrate. The reactions were incubated for 30 min at 30° C, stopped by addition of 5 µl of 5x Laemmli sample buffer, separated on a 12.5 % SDS-PAGE and analyzed by autoradiography.

Results

1. SUMO regulation of Aurora B

1.1 Aurora B is modified by SUMO

Aurora B regulation is principally mediated by the interaction with the CPC components: Incenp, Survivin and Borealin. Recent work has emphasized the importance of post-translational modification for proper activity and control of the dynamic behavior of the CPC. For example, phosphorylation of Borealin by Mps1 kinase is essential to activate Aurora B (Jelluma et al., 2008); ubiquitination controls the dynamic association of Survivin and Aurora B to the chromatin (Ramadan et al., 2007; Vong, 2005); and SUMOylation has been very recently shown to modified Borealin (Klein et al., 2009).However, the participation and the functional impact of these and other post-translational regulatory mechanisms of Aurora B remains to be elucidated.

1.1.1 Identification of a putative SUMOylation motif conserved in Aurora B proteins

To find new regulatory mechanisms of Aurora B we performed an *in silico* bioinformatic analysis of this kinase. We first used ELM (Eukaryotic Linear Motif, http://elm.eu.org) site prediction software that predicts the presence of 136 motifs in the sequence of a given protein. These motifs among other functions, promote protein-protein interactions, are recognized for post-translational modifications and regulate protein transport. In mouse Aurora B protein sequence we identified motifs already described in the regulation this kinase, thus validating the *in silico* analysis. This motifs are emphasized in a black box in figure 10a and are responsible for Aurora B degradation (KEN-box and D-box motifs), and Aurora B activity (PP1 binding motif). Interestingly, a consensus motif for SUMO modification (Ψ-Lys-X-Glu, in which Ψ means hydrophobic aminoacid residue and X any residue) that has not been previously related with Aurora B, is present in the kinase domain (Figure 10a, red box). To further confirm the presence of this motif we used the specific SUMO prediction software SUMOplot™ Analysis Program, (http://www.abgent.com/tools/SUMOplot) and we identified the same consensus motif for SUMO modification.

To evaluate the importance of SUMO motif in Aurora B regulation, we analysed the evolutionary conservation of this motif among Aurora B orthologues (Figure 10b). Importantly, the Aurora B sequence I-K-P-E (Ile – Lys – Pro – Glu) that constitutes the SUMO motif is completely

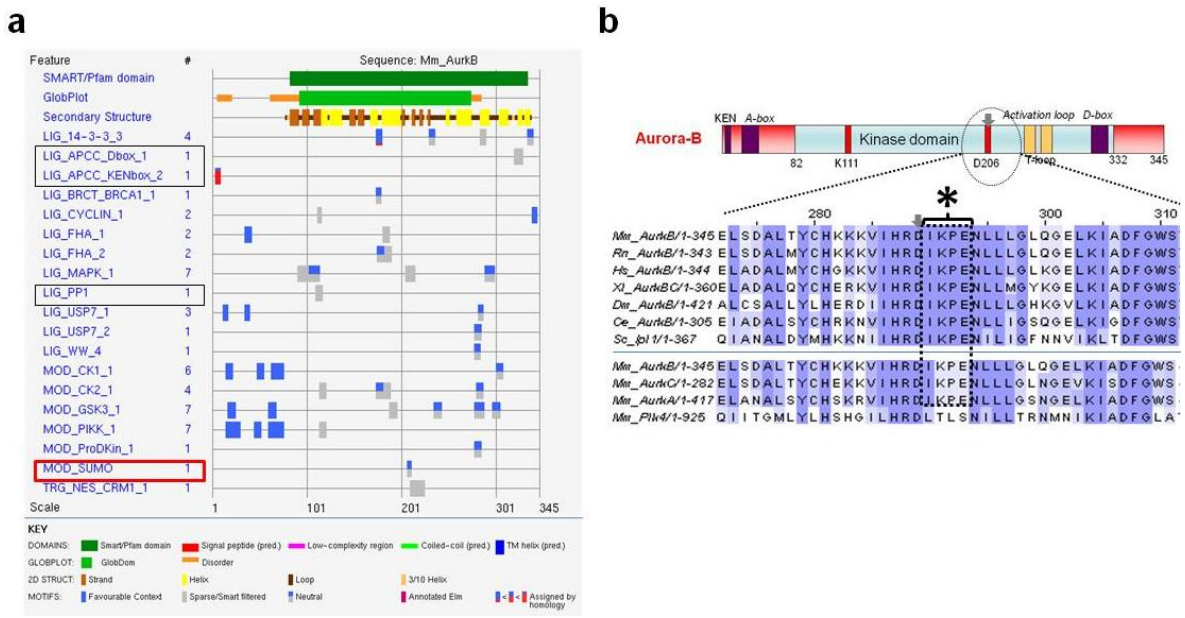

Figure 10. Identification of a putative SUMOylation motif conserved in Aurora B proteins. **(a)** Bioinformatic analysis of mouse Aurora B protein using ELM (Eukaryotic Linear Motif Resource for Functional Sites in Proteins: http://elm.eu.org) site prediction program. At the top of panel (SMART/Pfam line) appears in dark green the prediction of Aurora B kinase domain. The next line (GlobPlot) predicts a central region of globularity (light green) within Aurora B, flanked by disordered regions (orange). Then, the secondary structure is predicted based on the presence of α-helixes (yellow) and β-strands (light brown). Finally, the predicted motifs (blue, gray or partial red) are shown in the following lines. The motifs already described to regulate Aurora B are inside a black rectangle (D-box and KEN-box motifs regulate Aurora B degradation and PP1 binding regulate its activity). An interesting non-described motif, recognized for modification by SUMO peptides, is contained in a red rectangle. For a detailed description of each motif visit: http://elm.eu.org/browse.html **(b)** Multiple sequence alignment of Aurora B proteins from different species (*Mm: Mus musculus ; Rn: Rattus norvegicus ; Hs: Homo sapiens ; Xl: Xenopus laevis ; Dm: Drosophila melanogaster ; Ce: Caenorhabditis elegans ; Sc: Saccharomyces cerevisiae*) using ClustalView software (http://www.ch.embnet.org). SUMO modification motif (black asterisk) is highly conserved in Aurora B proteins, as well as in Aurora kinases, but it is not present in the closest mitotic relatives of these mitotic kinases (PLK4 proteins). Note that the SUMO motif is located one residue downstream the aspartate residue (D205, grey arrow) that binds to ATP.

conserved in all Aurora B orthologues from yeast to human (Figure 10b). The SUMO motif is also present in the other mammalian members of the Aurora family but not in the closest mitotic kinases (Plk family).

1.1.2 Aurora B mouse protein is SUMOylated at K207 residue

To confirm whether the SUMOylation site of Aurora B corresponds to the predicted lysine residue (K207 in mouse), we mutated this residue into the charge-conservative arginine residue. K207R mutation impedes SUMO covalent binding affecting as less as possible the kinase structure. Next, we expressed V5 epitope tagged versions of mouse Aurora B wild-type and K207R mutant along with an Ubc9 expression vector and HA-tagged versions of the three SUMO isoforms by transient transfection of HEK293 cells (Figure 11). The ectopically expressed proteins were immunoprecipitated using α-V5 antibodies, and detected by western-blotting with an antibody

directed against HA epitope. Consistant with our previous hypothesis we detected a band at the predicted SUMO-Aurora B conjugate size of 50 kDa when the three SUMO isoforms were expressed (Figure11, double asterisk). Importantly, SUMO-Aurora B conjugates were only present in cells expressing the non-mutated Aurora B form demonstrating that K207 residue is required for SUMO covalent modification of Aurora B.

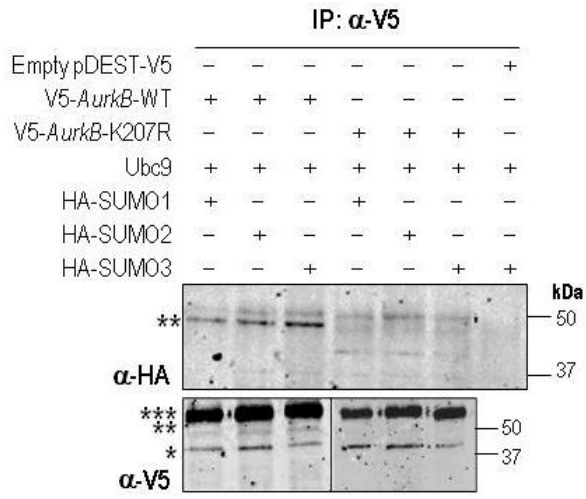

Figure 11. *In vivo* SUMOylation of Aurora B at K207 residue. HEK293 asynchronous cells were transiently transfected with V5-*Aurkb*-WT/-K207R, HA-SUMO-1/-2/-3 and E2-ligase Ubc9 expression vectors. Transfection with the empty pDEST-V5 vector was used as negative control. V5-Aurora B proteins were immunoprecipitated 48h after transfection using α-V5 antibodies and immunoblotted with α-HA and α-V5 antibodies. α-HA western blotting shows detection of Aurora B-SUMO conjugates (double asterisk) in the cells transfected with V5-*Aurkb*-WT at approximately 50 kDa, which is the expected size for V5-Aurora B-HA-SUMO1/2/3, and not in the cells transfected with V5-*Aurkb*-K207R mutant form. α-V5 western blotting detects V5-Aurora B immunoprecipated proteins in all lanes (single asterisk) and an additional band (double asterisk) only present in the V5-*Aurkb*-WT transfected cells that corresponds to the SUMO-modified V5-Aurora B form. The mouse IgGs are shown as triple asterisk.

1.2. Ectopic expression of a SUMO-dead Aurora B protein induces cellular defects

1.2.1 Lack of Aurora B SUMOylation at K207R induces polyploidy and nuclear defects

To address whether SUMOylation of Aurora B is important for cell cycle progression, we transiently transfected HEK293 cells with GFP tagged vectors for Aurora B wild-type, putative kinase-dead mutants (K111M and D205A) and a SUMO-dead form (K207R). As previously described (Tatsuka, 1998), over-expression of Aurora B wild-type slightly increases the percentage of 4N and >4N cells indicating mitotic arrest and defects in completion of cytokinesis. These defects are more pronounced upon the expression of Aurora B K111M kinase-dead mutant and, even at a higher degree, after expression of Aurora B D205A kinase-dead mutant where a dramatic increase in the >4N cell population is also observed (47.6% of >4N GFP-AurkB-D205A cells vs. 19.1% of >4N GFP-AurkB-K111M cells, Figure 12b). This phenotypic difference between K111M and D205A mutants may suggest distinct grades of inhibition of kinase activity and/or kinase-independent defects in D205A mutant. Interestingly, over-expression of a SUMO-dead Aurora B protein (K207R) induces polyploidy at the same level as D205A mutant (44.1% of >4N GFP-AurkB-K207R cells vs. 47.6% of >4N GFP-AurkB-D205A cells, Fig 12b). A more detailed

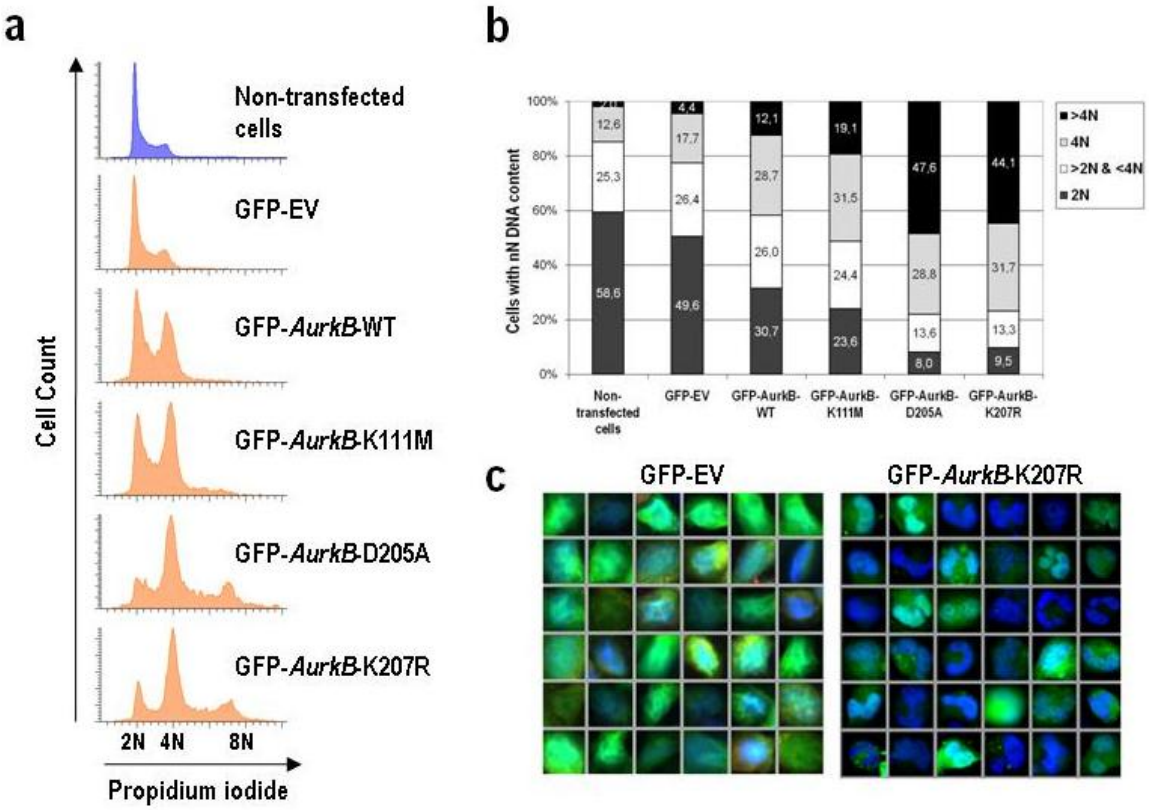

Figure 12. Transient expression of Aurora B K207R mutant form induces poliploidy and nuclear defects. **(a)** DNA content histograms of HEK293 cells transiently transfected with a GFP empty vector (EV) and GFP tagged vectors for Aurora B wild-type and Aurora B mutants – K111M, D205A and K207R – and fixed 72h after transfection. HEK293 GFP-positive cells were cytometry detected and used for cell cycle analysis. Over-expression of a SUMO-dead Aurora B protein (K207R) deregulates cell cycle progression inducing polyploidy in the same way as D205A kinase-dead form. **(b)** Bar graph quantification of cellular DNA content, showing a dramatic increase of polyploidy in cells overexpressing Aurora B-D205A and -K207R mutants. **(c)** Immunofluorescence collection of images obtained with the Olympus ScanR system revealing that cells over-expressing Aurora B-K207R mutant are mostly multinucleated and display nuclear aberrancies.

examination of these cells using the Olympus ScanR system allowed us to determine that the >4N cells over-expressing K207R mutant are mostly multinucleated and display severe nuclear abnormalities (Figure 12c).

1.2.2 Lack of Aurora B SUMOylation compromises cell viability

We next analyzed the cellular consequences of stably expressing Aurora B K207R in a long-term manner. For this purpose, we transfected U2OS cells with a GFP-empty vector and the previously described GFP-tagged vectors for Aurora B forms (wild-type, K111M, D205A and K207R) and we cultured GFP-positive cells with G418 selection during 12 days (Figure 13a). Stable expression of D205A and K207R in these cells severely reduces the number of colonies suggesting that mutations in these residues impair Aurora B function in a way that it is incompatible with cell viability (Figure 13b). A detailed inspection of these colonies reveals that expression of K207R

mutant promotes polyploidy, cellular fragmentation and cell death (Figure 13c). The presence of these poliploid cells is consistant with the cell cycle defects observed upon GFP-Aurora B-K207R transient expression (Figure 12). In addition, GFP-Aurora B-K207R colonies display bigger mitotic cells and less cytokinesis bridges than GFP-Aurora B-wild-type colonies suggesting abnormal mitosis and defects in completion of cytokinesis (Figure 13c).

1.3. Aurora B is regulated by SUMO

Deregulation of Aurora B function by chemical inhibition, small interference RNA (siRNA) treatment or overexpression of a kinase-dead form leads to very similar phenotypes including chromosome misalignment with subsequent arrest in prometaphase and fail to execute cytokinesis resulting in multinucleated cells (Ruchaud et al., 2007). To gain insight into the role of SUMOylation in Aurora B regulation, we generated and analyzed HeLa stable cell lines for GFP-Aurora B-WT /-D205A and /-K207R fusion proteins.

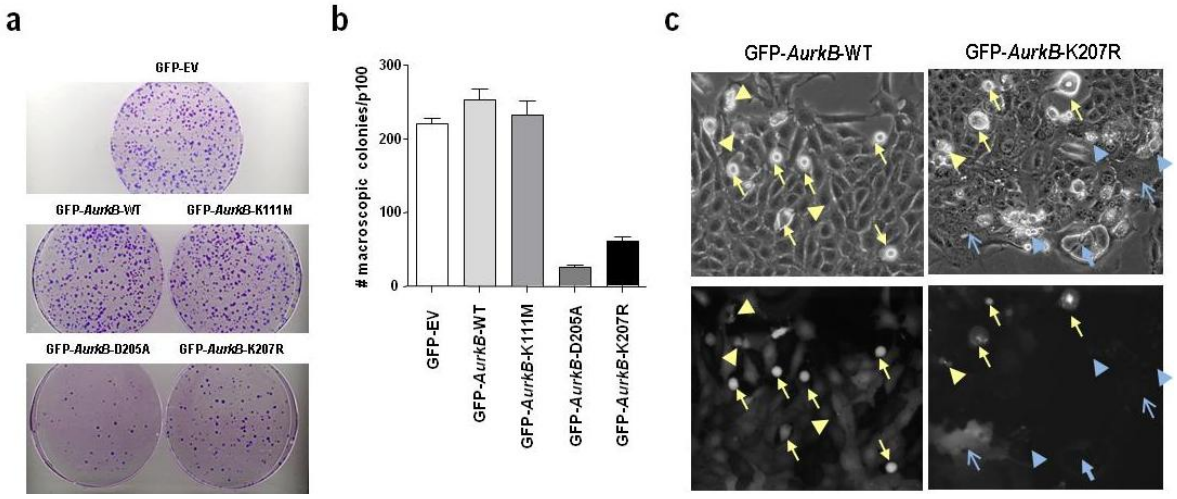

Figure 13. Stable expression of Aurora B K207R mutant form compromises cell viability. (a) Colony formation assay of U2OS cells stably expressing GFP empty vector (EV) and GFP tagged vectors for Aurora B (wild-type, K111M, D205A and K207R). U2OS GFP-positive cells were sorted 48h post-transfection, replated in the presence of G418 1mg/ml, then fixed 12 days later and stained with crystal violet to determine colony number. $50*10^3$ GFP-positive cells were sorted and plated per p100. (b) Bar graph quantifying the number of macroscopic colonies per p100 plate showing a clear reduction of colonies in cells expressing Aurora B-D205A and -K207R mutants. (c) Representative colonies stably expressing GFP-Aurora B-WT and GFP-Aurora B-K207R. Colonies expressing GFP-Aurora B-K207R mutant present multinucleated cells (light blue open arrows), cellular fragmentations (light blue arrow) and dead cells (light blue arrowheads). These colonies also display bigger mitosis (light yellow arrows) and few cytokinesis bridges (light yellow arrowheads) than colonies expressing GFP-Aurora B wild-type form.

1.3.1 SUMOylation of Aurora B is important for correct mitotic progression and completion of cytokinesys

We first validated the generated stable cell lines by selecting the total and the GFP-positive cell population for cell cycle profile analysis (Figure 14a). Proliferation of the clones stably expressing GFP-Aurora B fusion proteins is normal, although cells expressing D205A and K207R mutants display slightly fewer cells in a supposed G2/M stage (4N DNA content) probably due to a premature exit for mitosis. Importantly, GFP-Aurora B-WT expression is cell cycle regulated and the corresponding 5% of GFP-positive cells are mainly at a presumptive G2/M stage (4N). The percentage of GFP-positive cells in the mutant stable clones is slightly lower than in the case of the wild-type (4.3% and 3.0% of GFP-Aurora B-D205A and –K207R positive cells, respectively) and strikingly, expression of the mutants is not restricted to G2/M but also present in G1/S phases, especially in the case of D205A mutant. This altered expression of the mutants may be explained by a higher stability of the mutant proteins and/or by the existence of aneuploid cells in mitosis with a DNA content distinct than 4N.

To study the cellular effect of expressing a SUMO-dead Aurora B form we depleted in HeLa cells the endogenous human Aurora B by siRNA treatment and we let the cells grow during 36h with exogenous siRNA-resistant mouse Aurora B-GFP fusion proteins (Figure 14b). GFP-Aurora B-WT efficiently counteracts the formation of multinucleated cells after depletion of endogenous Aurora B and progress normally through mitosis, whereas expression of D205A and K207R mutants was unable to rescue mitosis and arrest cells at prometaphase, failing to execute cytokinesis and resulting in multinucleated cells. Similar results are observed after chemical inhibition of Aurora B kinase activity with ZM447439 (ZM1) (Figure 14c,d and pictures). A detailed examination of the mitotic distribution of these stable cell lines after depletion of endogenous Aurora B confirms that expression of GFP-Aurora B-D205A and -K207R provokes an arrest at prometaphase and a reduction in cells telophase (Figure 14e). This reduction in cells exiting mitosis is accompanied by a decrease in the percentage of cells in cytokinesis (Figure 14f). In addition, the remaining cells in cytokinesis are mostly aberrant and frequently display chromosomal bridges between the two daughter cells.

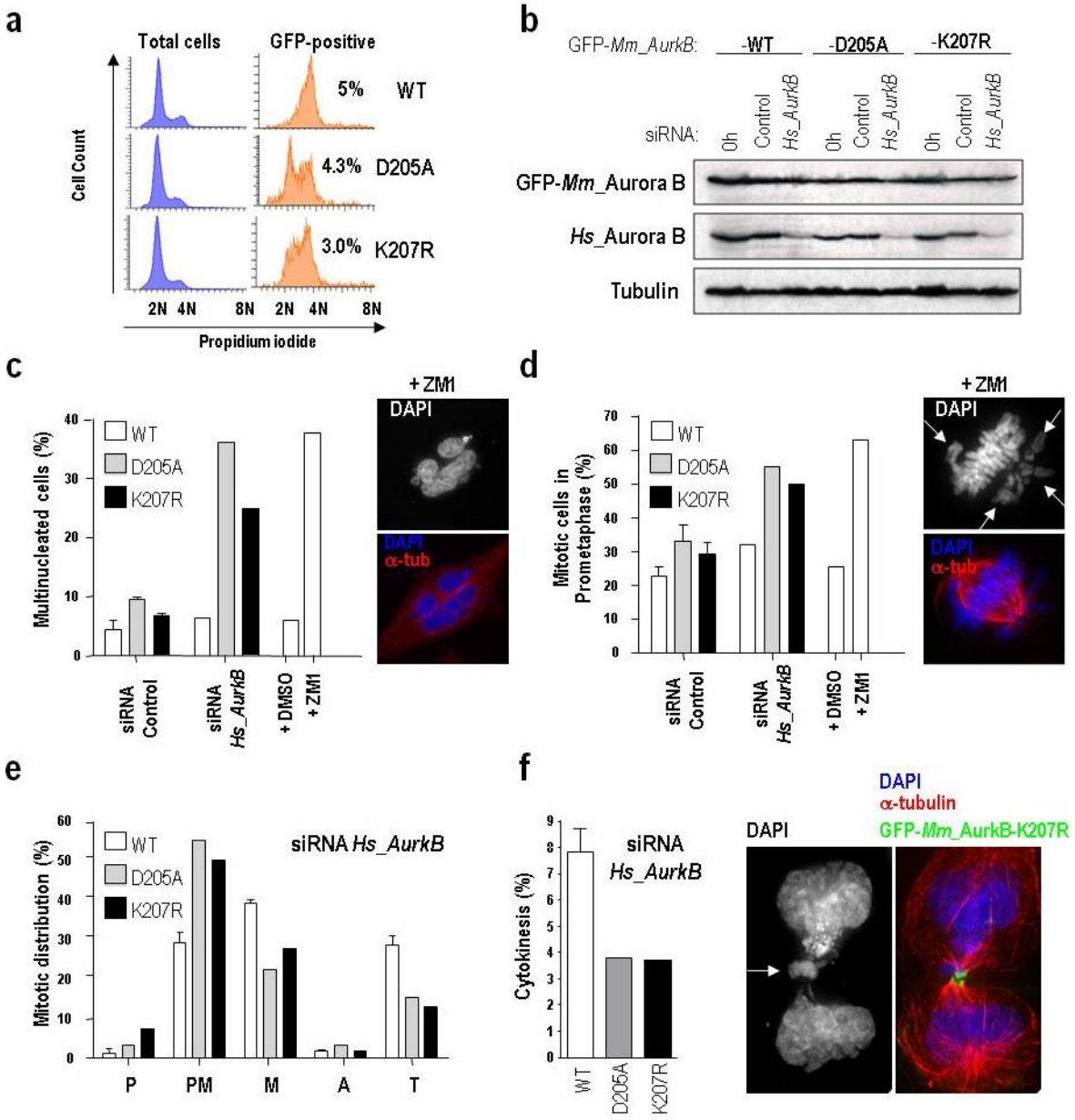

Figure 14. Lack of Aurora B SUMOylation disrupts mitotic progression and cytokinesis. HeLa cells stably expressing siRNA-resistant mouse Aurora B fused to GFP were first validated by flow cytometry, then nucleofected with human Aurora B siRNA oligonucleotides or a control siRNA and analyzed 36h after nucleofection by immunoblotting and immunofluorescence. **(a)** Generation and validation of HeLa stable cell lines by cytometry cell cycle analysis. The analysis of the total cell population is shown in blue histograms, while the analysis of the GFP-positive population is shown in orange histograms accompanied by the percentage of these cells over the whole population. At least three different stable clones were generated for each GFP-Aurora B fusion protein. Depicted histograms are from representative stable clones. **(b)** Western blot showing efficient depletion of human endogenous Aurora B and siRNA-resistance of GFP-Aurora B proteins in HeLa stable cell lines. Tubulin was used as loading control. **(c)** Bar graph quantification of the percentage of interphase multinuclei cells. Stable expression of GFP-Aurora B-D205A and -K207R induces accumulation of multinucleated cells (see picture) upon depletion of endogenous Aurora B. Around 1000 interphase cells were counted per point. **(d)** Bar graph quantification of the percentage of mitotic cells in prometaphase revealing a significant arrest at this stage caused by chromosome misalignment (see picture) in the abscence of endogenous Aurora B in cells stably expressing GFP-Aurora B-D205A and -K207R. At least 50 mitotic cells were counted per point. Chemical inhibition of Aurora B kinase activity with ZM447439 (ZM1) was included in (c) and (d) as

positive control. **(e)** Mitotic distribution of stable cell lines after depletion of endogenous Aurora B. Expression of GFP-Aurora B-D205A and -K207R provokes an arrest at prometaphase and a reduction in cells at telophase. P: prophase, PM: prometaphase, M: metaphase, A: anaphase, T: telophase. **(f)** Bar graph quantification of interphase cells in cytokinesis. GFP-Aurora B-D205A and -K207R stable cell lines show a decrease percentage of cells in cytokinesis. The remaining cytokinesis figures are usally abnormal with chromosomal bridges (arrows). α-tubulin (α-tub) staining is in red, GFP-Aurora B in green and DAPI (DNA) in blue.

1.3.2 SUMO regulates Aurora B and Incenp centromeric localization

To further investigate the mitotic defects caused by the expression of a SUMO-dead Aurora B protein we performed immunofluorescence analysis of HeLa stable cell lines 36 hours after depletion of endogenous Aurora B. Fluorescence microscopy analysis shows that Aurora B-K207R mutant was distributed along the entire chromosome arms in prometaphase (PM) and metaphase (M) cells (Figure 15a). Interestingly, the CPC component Incenp was also dispersed on chromatin failing to concentrate in inner centromeres suggesting localization defects of the whole complex upon lack of Aurora B SUMOylation. A similar delocalization behavior, albeit less dramatic, was observed for the Aurora B-D205A kinase-dead mutant where additional chromosome alignment defects are present. In contrast, Aurora B-wild-type remained focused at the centromere region upon chromosome condensation, as visualized by the dotted localization pattern on PM/M chromosomes (Figure 15a). Quantification of the percentage of PM/M cells with delocalized Aurora B / Incenp signal revealed that this phenotype only appears in the absence of endogenous Aurora B when K207R mutant and, in a less extent, D205A are expressed (Figure 15b). Further analysis of Aurora B dispersion using pseudocolour images treated with metamorph software confirms D205A and K207R signal dispersion on chromosomes (Figure 15c and insets). Quantification of the integrated optical density (OD) which is used to analyze the opacity of an object when exposed to transmitted light, shows that the chromosomal staining of a SUMO-dead Aurora B form is significantly (p<0.001) less opaque than Aurora B-WT staining meaning that Aurora B-K207R does not concentrate at any chromosomal region (Figure 15d).

To address whether Aurora B kinase activity is important for proper Aurora B localization in the centromere, we treated GFP-Aurora B-WT stable cell line with ZM1 inhibitor. Consistant with previous reports (Ditchfield et al., 2003), chemical inhibition of Aurora B kinase activity does not perturb Aurora B or Incenp localization in the centromere indicating that an active kinase is not required for their centromeric localization (Figure 15e). All together, our data indicate that SUMO modification of Aurora B is crucial to regulate Aurora B and Incenp dynamics at centromeres.

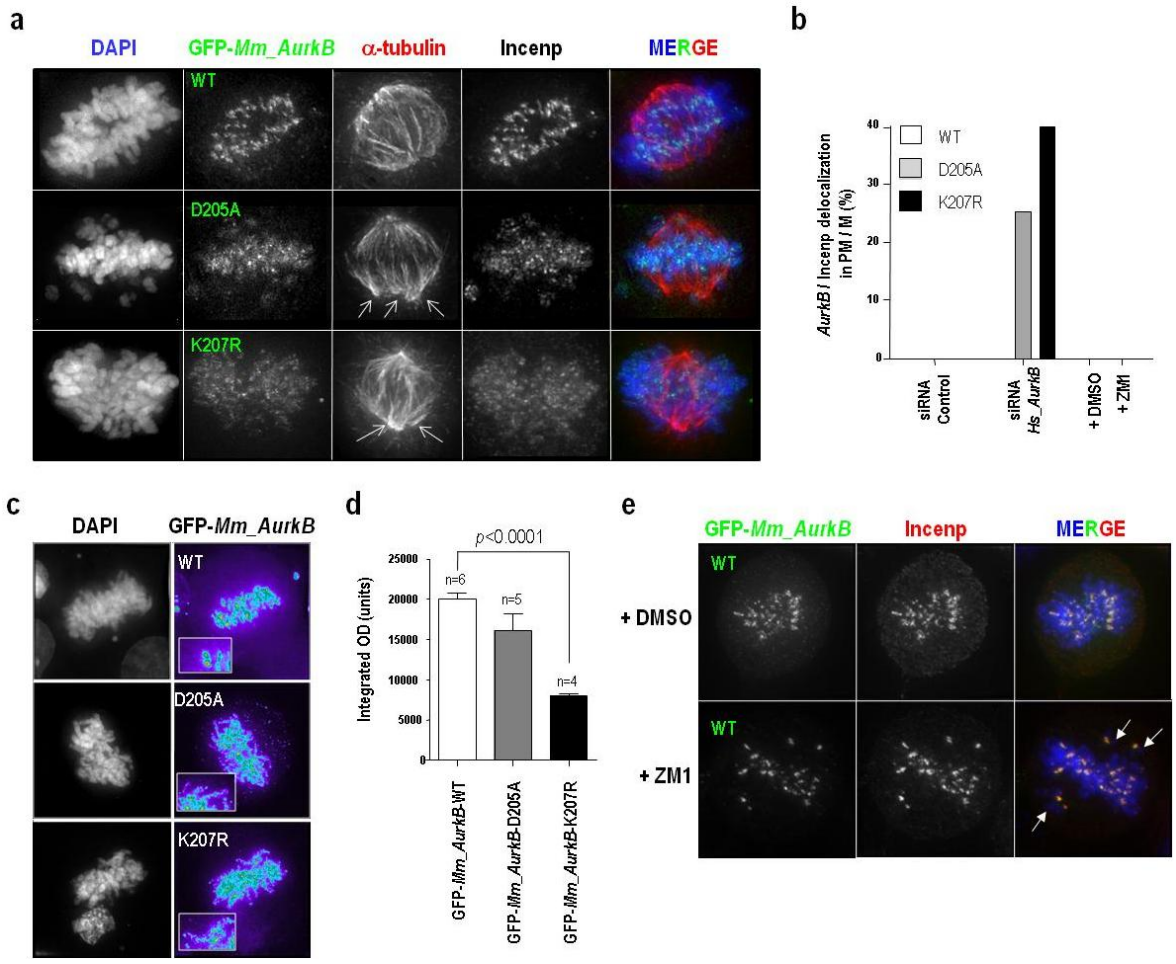

Figure 15. SUMOylation of Aurora B is important for AuroraB/Incenp localization in the centromere. **(a)** Immunofluorescence images of HeLa stable cell lines after depletion of endogenous Aurora B. GFP-Aurora B-D205A and -K207R mutants together with Incenp display a disperse localization over the chromatin in PM/M cells. Multipolar spindles are also present in these mutant cells (white open arrows). **(b)** Bar graph quantification of the percentage of PM/M cells in which GFP-Aurora B fusions and Incenp are delocalized. Delocalization of Aurora B is only observed in D205A and K207R mutants after depletion of the endogenous protein. At least 50 mitotic cells were counted per point. **(c)** Image pseudocolour treatment with metamorph software to visualize the distribution of GFP-Aurora B signal in stable cell lines after depletion of endogenous Aurora B. Intensity of the signal is represented in a colour scale: (low) purple, blue, green, yellow, red (high). **(d)** Bar graph quantification of the integrated optical density (OD) of GFP-Aurora B signal over the chromatin shows a significant reduction (p<0.0001) of GFP-Aurora B-K207R signal density. **(e)** Chemical inhibition of Aurora B with ZM1 does not mislocalize the protein although it provokes chromosome misalignment (white arrows). α-tubulin staining is in red, Incenp in (e) is also in red, GFP-Aurora B in green and DAPI (DNA) in blue.

1.3.3 SUMOylation affects Aurora B function without reducing its kinase activity

Next, we asked whether a SUMO-dead Aurora B form was able to rescue the mitotic functions of the CPC. For this purpose we analyzed the phosphorylation status of CENP-A, a known Aurora B substrate, in our stable cell lines 36 hours after depletion of endogenous Aurora B. The staining with phospho-specific antibodies against CENP-A reveals that delocalized D205A and K207R mutants are unable to phosphorylate CENP-A (Figure 16a). In contrast, GFP-Aurora B-WT which is concentrated in the centromeres efficiently phosphorylates CENP-A resulting in positive staining

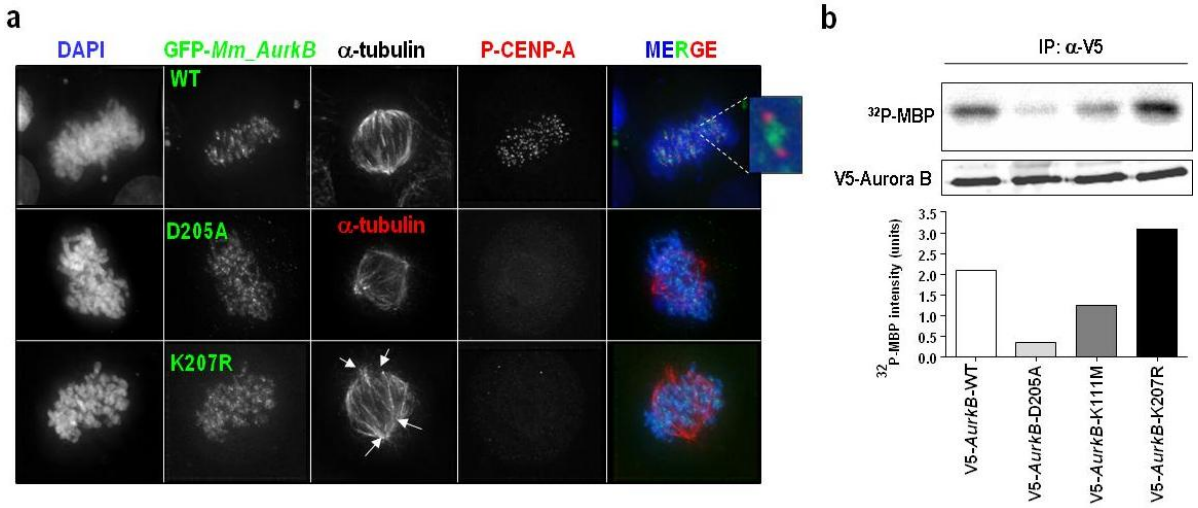

Figure 16. Centromeric mislocalization of Aurora B-K207R mutant prevents CENP-A phosphorylation without reducing its kinase activity. **(a)** Immunofluorescence images from HeLa stable cell lines treated with siRNA against endogenous Aurora B. GFP-Aurora B-D205A and -K207R accumulate along chromosome arms and fail to phosphorylate CENP-A. α-tubulin staining is in red, P-CENP-A if present is in red, GFP-Aurora B in green and DAPI (DNA) in blue. **(b)** *In vitro* kinase activity toward recombinant MBP of V5 tagged Aurora B proteins. HEK293 cells were transiently transfected with the indicated V5-*Aurkb* expression vectors and the resulting exogenous expressed proteins were immunoprecipitated with α-V5 antibody. The kinase activity of a SUMO-dead (K207R) Aurora B form is not reduced but partially increased. Aurora B kinase-dead mutants K111M and D205A were included as negative controls of MBP phosphorylation. Quantification of ^{32}P-MBP signal was calculated considering the total amount of V5-Aurora B protein in each case.

for P-CENP-A at the inner kinetochores flanking GFP-Aurora B-WT signal (Figure 16a, inset). To determine the reason by which lack of SUMOylation perturbs Aurora B function, we tested the kinase activity of V5 tagged Aurora B proteins immunoprecipitated from transiently transfected HEK293 cells (Figure 16b). Consistant with structural predictions, K111M and D205A mutants fail to efficiently phosphorylate MBP substrate *in vitro*, although K111M still present some kinase activity. Strikingly, the kinase activity of Aurora B-K207R mutant is not reduced but increased if compared with Aurora B wild-type activity. Therefore, these data support the idea that lack of SUMOylation perturbs Aurora B function by impeding its proper localization in centromeres and not by reducing its kinase activity.

1.3.4 An abnormal SUMOylation of Aurora B affects its oncogenic properties

It has been reported that elevated Aurora B activity promotes cellular transformation *in vitro* by enhancing oncogenic Ras signaling (Kanda et al., 2005). To test the oncogenic properties of a SUMO-dead Aurora B form, we performed focus formation assays in NIH-3T3 cells, a well known cell line susceptible to transformation with various oncogenes (Clark et al., 1995).We stably transfected NIH-3T3 cells with V5-Aurora B expression vectors in combination or not with oncogenic HRas-G12V expression vector and examined its effect on the frequency of cellular foci

resulted from HRas-G12V-induced transformation (Figure 17). As previously reported, although Aurora B wild-type expression alone is not able to promote malignant cell transformation it significantly augments the frequency of HRas-G12V transformation. Importantly, this potentiation was suppressed by cotransfection with Aurora B-D205A kinase-dead vector, confirming that Aurora B kinase activity promotes cell transformation in combination with HRas (Kanda et al., 2005). On the contrary, cooperation with HRas is significantly increased (p<0.05) upon expression of Aurora B-K207R, suggesting that lack of SUMOylation facilates cell transformation. Finally, to address if genetic instability contributes to the formation of a transformed phenotype, we counted the number of chromosomes of the resulted foci. In all cases, the analyzed cells displayed a similar number of chromosomes suggesting that chromosomal instability is not supporting HRas oncogenic activity.

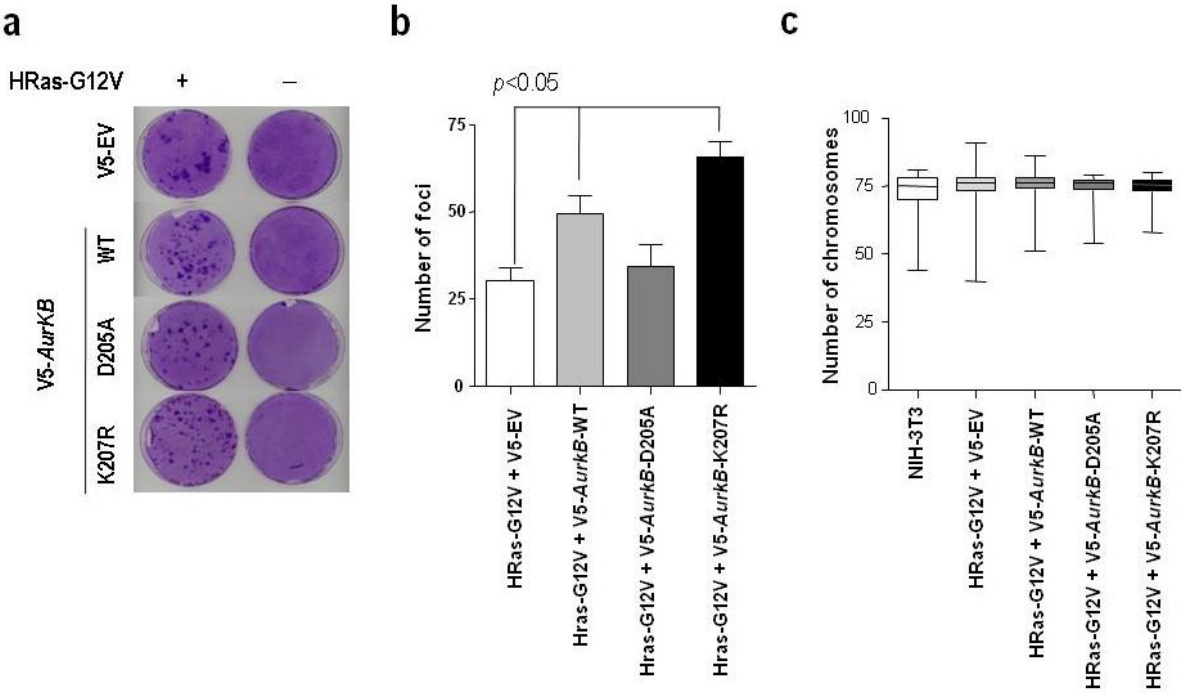

Figure 17. An abnormal SUMOylation of Aurora B affects its oncogenic properties. **(a)** Focus formation assay in NIH-3T3 cells. Depiction of transformed foci in Giemsa-stained dishes in NIH-3T3 cells cotransfected with HRasG12V and V5-*Aurkb* expression vectors. An empty V5-vector was used as control. **(b)** Bar graph quantification of the number of transformed foci. Expression of SUMO-dead Aurora B significantly increases (p>0.05) the number of HRas-induced foci when compared with Aurora B-WILD-TYPE counterpart. **(c)** Chromosome quantification of transformed and normal 3T3 cells. Lack of SUMOylation of Aurora B does not induce genetic instability in 3T3 cells.

2. Development of mouse models

Aurora B function has been extensively studied in yeasts, nematodes, insects and cold-blood vertebrates but very limited information concerning Aurora B role in mammals and in its implication in tumorigenesis is available. To study the in vivo function of Aurora B in mammals we have generated three different mouse models: a conditional knock-out model (Figure 18), a knock-in model (Figure 19) and a tetracycline inducible model (Figure 20 and 21).

2.1 Generation of a conditional knock out mouse model

To generate a conditional knock-out model we first constructed a targeting vector in which Aurora B exons 2-6 are flanked with loxP sequences and a frt-neo^r (neomycin-resistant gene)-frt cassette for selection purposes (Figure 18). At both ends of the construct we cloned two homology arms to facilitate homologous recombination in ES cells. After homologous recombination, we selected clones carrying the recombinant alleles *Aurkb*(loxfrt) (Figure 18b) and the corresponding ES cells were microinjected into wild-type blastocysts to generate *Aurkb*(+/loxfrt) mice. The neo^r cassette was first removed by crossing with transgenic mice expressing the Flp recombinase (see Methods) resulting in the conditional *Aurkb*(lox) allele. Germline deletion of exons was achieved by additional crosses with CMV-Cre transgenic mice to generate the *Aurkb*(–). Note that elimination of exons 2-6 in *Aurkb*(–) allele ensures total inactivation of Aurora B gene since we are removing almost completely the kinase domain of Aurora B protein. Moreover, in case of alternative splicing between exon 1 and 7 the codified protein is not going to be related with Aurora B since there is a change in the reading frame between these exons. Genotyping of these alleles was done by PCR using DNA extracted from the tails of these mice and two distinct combination of primers (1+3 and 2+3, Figure 18a,c).

2.2 Generation of a β-Galactosidase knock-in mouse model

In addition, we followed the FLEx strategy (Schnutgen et al., 2003) to generate a knock-in allele, *Aurkb*(Z), in which expression of the endogenous *Aurkb* gene is replaced by lacZ transcripts encoding β-galactosidase. A detailed description of the strategy followed is shown in Figure 19a. To confirm activity of Aurora B promoter by the β-galactosidase reporter we performed X-Gal staining of *Aurkb*(+/Zloxfrt) and *Aurkb*(+/Z) ES cells (Figure 19d). Both the *Aurkb*(–) and *Aurkb*(Z) alleles are null for Aurora B expression, as detected by immunofluorescence (see below), and lead to similar phenotypes.

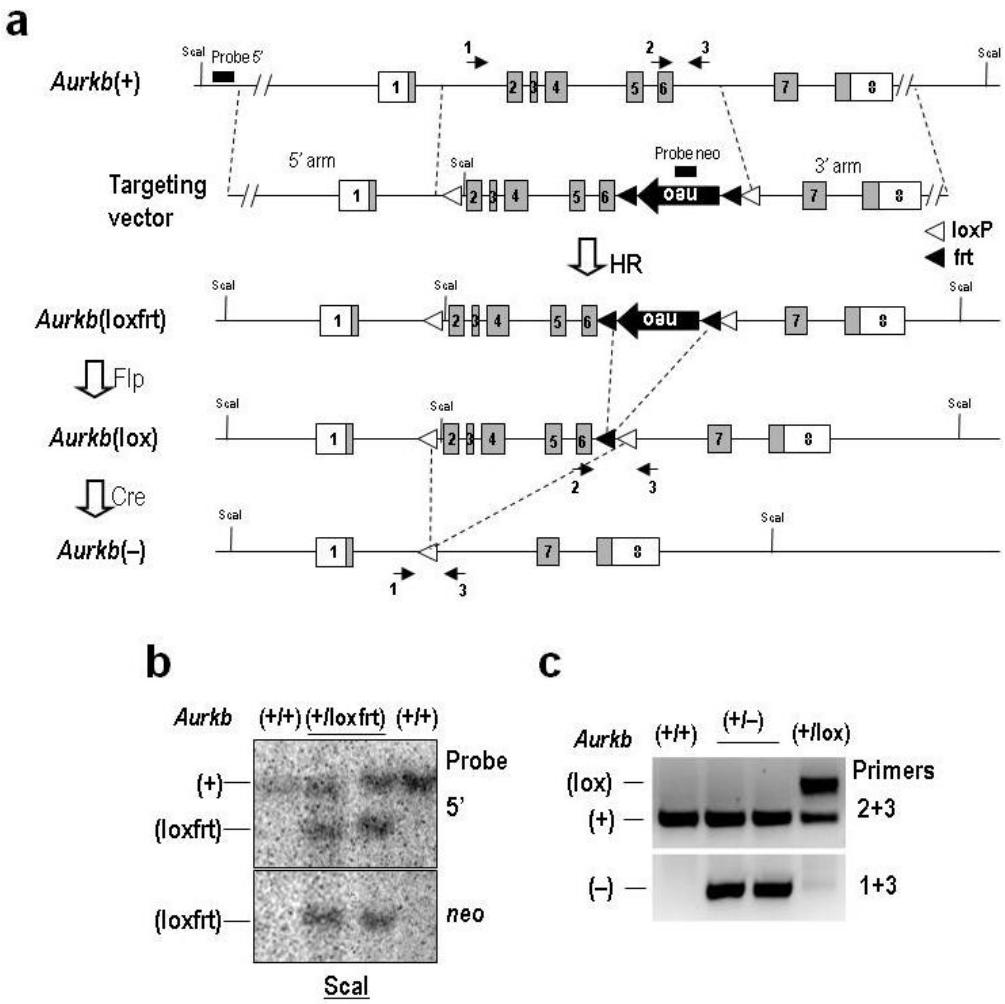

Figure 18. Generation of conditional and null Aurora B alleles. **(a)** Schematic representation of the *Aurkb* knock-out alleles. The mouse *Aurkb* locus encoding Aurora B contains 8 exons (boxes) containing noncoding (open boxes) or protein-coding (filled boxes) sequences. Wild-type (white triangles) loxP sites and frt (black triangles) sites are used to flank Aurora B exons or the neo-resistance in the targeting vector. This neo cassette (black) contains promoter and poly-A sequences and it is used for selection of clones after homologous recombination (HR) in ES cells. The neo cassette is eliminated in vivo by crossing *Aurkb*(+/loxfrt) mice with transgenic mice expressing the Flp recombinase. Further excision of exons 2-6 is mediated by expression of the Cre recombinase resulting in the *Aurkb*(–) null allele. Also shown are the ScaI restriction sites, 5' and neo probes and primers 1, 2 and 3 used for genotyping. **(b)** Southern blot analysis of recombinant ES cells showing two *Aurkb*(+/loxfrt) clones that underwent HR. DNA was digested with ScaI and hybridized with the probe 5' or neo specific sequences **(c)** PCR genotyping of tail DNA using primers 1, 2 and 3, confirming the presence of *Aurkb*(lox) and *Aurkb*(–) alleles.

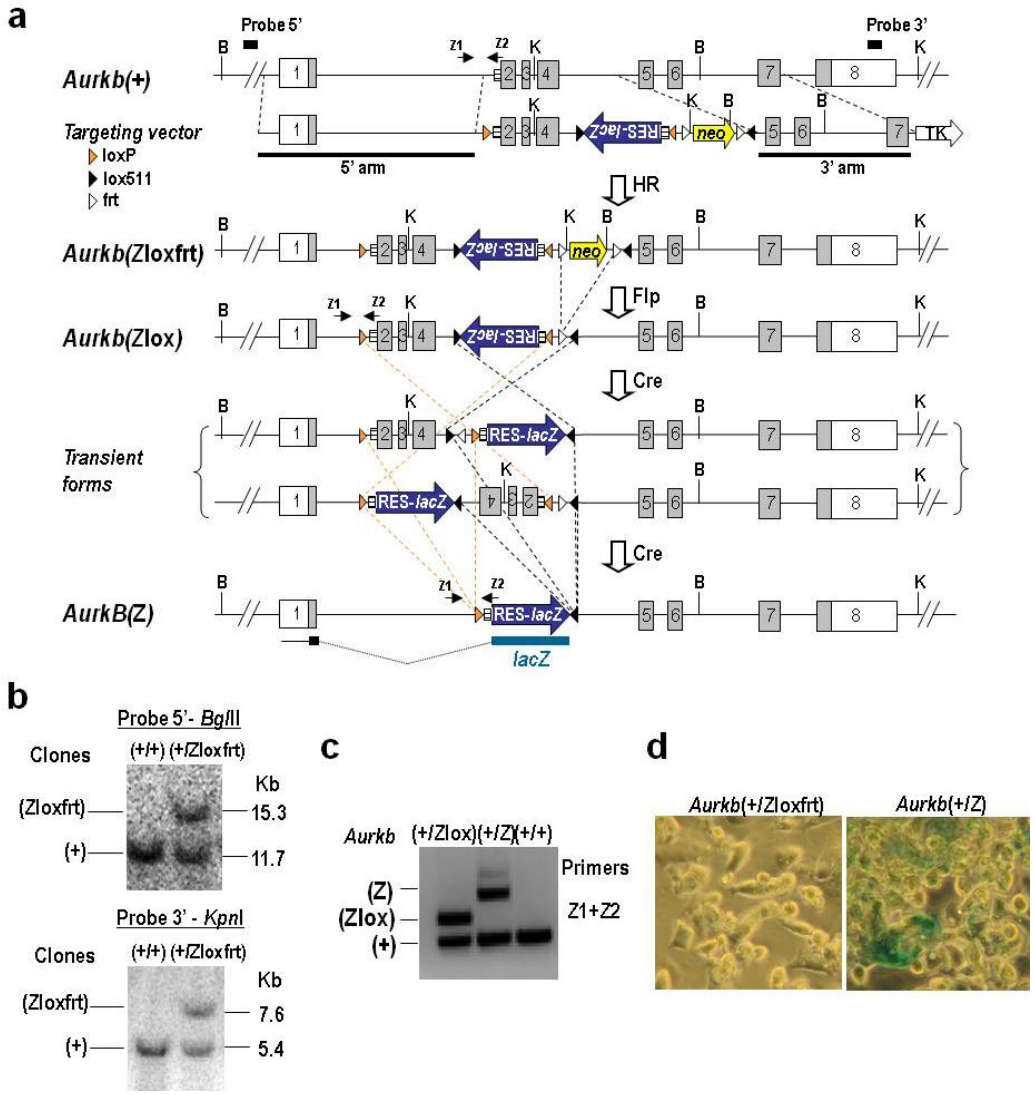

Figure 19. Generation of knock-in mice in which Aurora B expression has been replaced by β-Galactosidase . **(a)** Schematic representation of the *Aurkb* knock-in alleles generated following FLEx strategy (Schnutgen et al., 2003). Aurora B exons 2-4 were flanked with wild-type and mutant loxP sequences following the FLEx strategy. An internal ribosome binding site (IRES)-*lacZ* cassette is placed in the opposite orientation between exons 4 and 5. This cassette contains the splicing acceptor of *Aurkb* exon 2 (lined box) upstream of the IRES sequence and the SV40 polyA sequence (not indicated) downstream of the *lacZ* gene. The corresponding targeting vector was electroporated into ES cells. After homologous recombination in ES cells, we selected clones carrying the recombinant allele *Aurkb*(Zloxfrt) and the corresponding ES cells were aggregated to generate *Aurkb*(+/Zloxfrt) mice. The neomycin-resistant cassette was first removed by crossing with transgenic mice expressing the Flp recombinase. This results in the *Aurkb*(Zlox) allele carrying an inverted IRES-lacZ cassette. After expression of Cre recombinase, this cassette is inverted due to the presence of opposite loxP or lox511 mutant sites as described previously (Schnutgen et al., 2003). The resulting *Aurkb*(Z) allele expresses the *lacZ* gene downstream of the *Aurkb* exon 1 resulting in a truncated Aurora B transcript and the concomitant expression of β-galactosidase. (**b**) Southern blot analysis of ES cell clones after homologous recombination indicating the presence of the recombinant allele *Aurkb*(+/Zloxfrt) in some of these clones. The situation of the probes 5' and 3' is indicated in (a). (**c**) Representative genotyping of the *Aurkb*(+), *Aurkb*(Zlox) and *Aurkb*(Z) alleles corresponding to (a). The position of oligonucleotides (Z1 and Z2) used for PCR genotyping is represented in panel (a). (**d**) Expression of β-galactosidase from the *Aurkb*(Z) but not *Aurkb*(Zloxfrt) alleles. *Aurkb*(+/Zloxfrt) ES cells were infected with a vector expressing the Cre recombinase to generate *Aurkb*(+/Z) cells. Both infected and non-infected cells were stained for β-galactosidase activity (blue colour).

2.3 Generation of a tetracycline-inducible mouse model

Finally, in collaboration with Professor Earnshaw's laboratory at the Wellcome Trust Centre for Cell Biology in Edinburgh we generated an inducible mouse model in which Aurora B gene expression can be potentially modulated by the addition of tetracycline (Figure 20 and 21). This approach centers on a 'promoter-hijack' strategy first described by Earnshaw's laboratory for DT40 cells (Samejima et al., 2008) in which the gene's promoter is replaced with a minimal cytomegalovirus (CMV) promoter upstream-linked with seven in-tandem repeats of tetO sequences. This construction leads to a Tet-responsive minimal promoter (Tet-P) that is only active in the presence of binding of the transactivator regulatory proteins (tTA or rtTA) to the tetO sequences. We also generated a targeting vector to modify the remaining Aurora B allele in order to drive expression of a tTA from the Aurora B endogenous promoter (Figure 21b). Thus, in a mouse harboring both modified alleles, *Aurkb*(tet/tTA), Aurora B gene will be essentially regulated by its own promoter but through the intermediary tTA. Alternatively, we crossed *Aurkb*(+/tet) mice with knock-in mice expressing an M2rtTA under the ubiquitious Rosa26 promotor (Beard et al., 2006) (Figure 21b). In this other case, *Aurkb*(+/tet);Rosa26(+/rtTA) mice will be used to induce Aurora B ubiquitous expression in vivo in a conditional way. Modulation of this system is achieved by addition of tetracycline as depicted in Figure 21c.

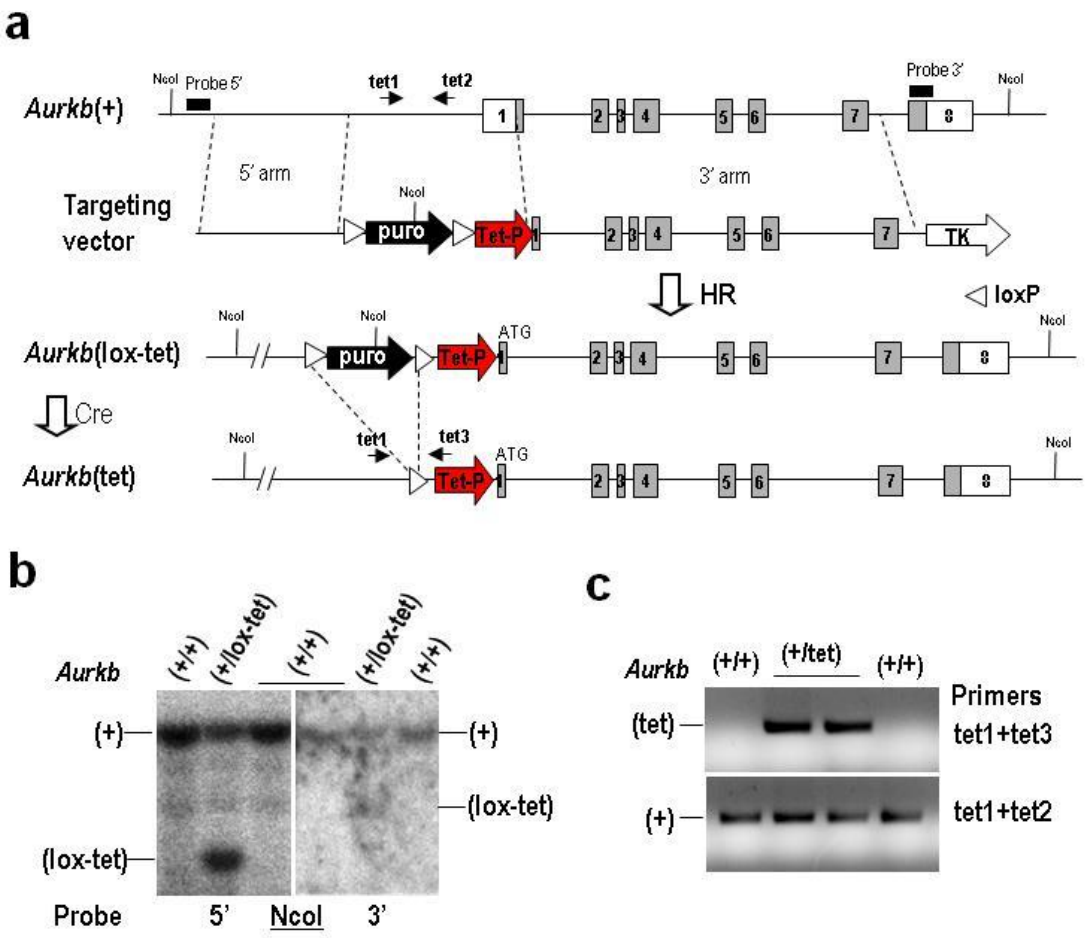

Figure 20. Generation of inducible mice in which Aurora B promoter has been replaced by a tetracycline-responsive minimal promoter. **(a)** Schematic representation of the alleles generated in the inducible mouse model. Aurora B endogenous promoter was replaced by tet-P which is a minimal CMV promoter that contains seven in-tandem repeats of tetO sequences recognized by the transactivator regulatory proteins tTA and rtTA. The corresponding targeting vector was electroporated into ES cells. After homologous recombination in ES cells, we selected clones carrying the recombinant allele *Aurkb*(lox-tet) by positive and negative selection using puromycin and thymidine kinase resistance genes, respectively. The corresponding ES cells were aggregated to generate *Aurkb*(+/lox-tet) mice. The puromycin-resistant cassette was then removed *in vivo* by crossing with transgenic mice expressing the Cre recombinase. This results in the *Aurkb*(tet) that contains a minimal tetO-CMV promoter (Tet-P) instead of Aurora B endogenous promoter. (**b**) Southern blot analysis of ES cell clones after homologous recombination indicating the presence of the recombinant allele *Aurkb*(+/lox-tet) in one of the clones. The situation of the probes 5' and 3' is indicated in (a). (**c**) Representative genotyping of the *Aurkb*(+) and *Aurkb*(tet). The position of oligonucleotides (tet1, tet2 and tet3) used for PCR genotyping is represented in panel (a).

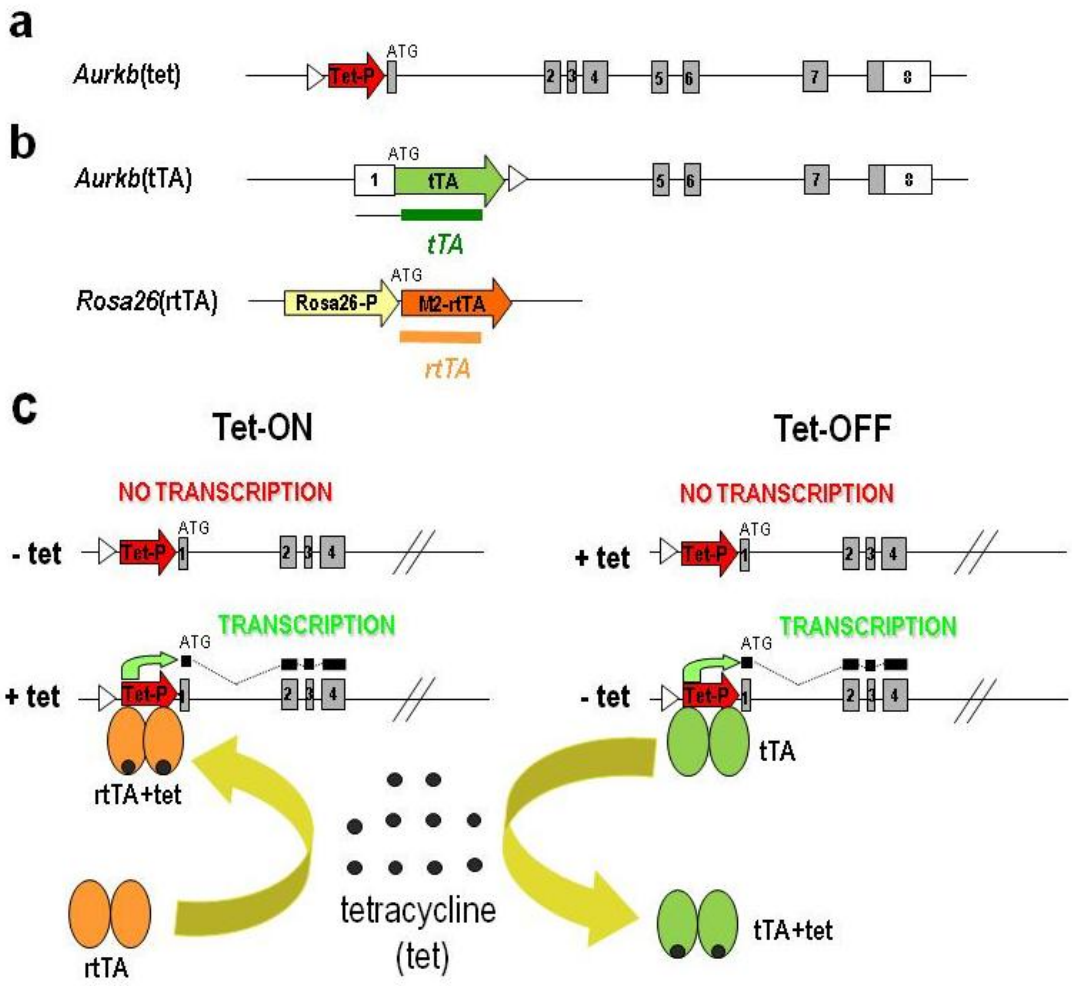

Figure 21. Promoter-hijack approach for inducible expression of Aurora B. **(a)** The *Aurkb*(tet) allele contains a minimal tetO-CMV promoter (Tet-P) instead of Aurora B endogenous promoter. This cassette contains seven in-tandem repeats of tetO sequences recognized by transactivator regulatory proteins (tTA and rtTA). In the absence of binding of these regulatory proteins to tetP Aurora B gene is silenced. White triangle is a remaining loxP site after the targeting strategy (see Figure 12a). **(b)** Recombinant alleles expressing transactivator regulatory proteins under different promoters. The *Aurkb*(tTA) allele contains a tTA cassette (green) instead of Aurora B codifying exons 1-4. The tTA cassette contains a fusion sequence of the tet repressor and the activation domain of VP16 protein, as well as poly-A sequences for termination of transcription. Expression of this cassette is driven by Aurora B regulatory sequences. The Rosa26(rtTA) allele generated in (Beard et al., 2006) expresses a tetracycline-inducible M2rtTA transactivator driven from the endogenous ubiquitous Rosa26 promoter. **(c)** Addition of tetracycline modifies the configuration and binding of tTA and rtTA to the tetO sequences. rtTA binds to and activates expression of tet-P in the presence of tetracycline (Tet-ON system); whereas, tTA only binds to tet-P in the absence of tetracycline (Tet-OFF system).

3. Partial *in vivo* inactivation of Aurora B

3.1 Lack of one allele of Aurora B does not result in major alterations during mouse development

After generation of the mice colony we observed that Aurora B heterozygous null mice are healthy during adult life suggesting that mice can develop normally with reduced allele dosage of Aurora B.

3.1.1 Aurora B heterozygous MEFs proliferate well in culture

To further confirm that Aurora B heterozigosity does not lead to defects in cell cycle progression we extracted *Aurkb*(+/+) and *Aurkb*(+/–) mouse embryonic fibroblasts (MEFs) from embryos at E14.5 (Methods) and we analysed the cell cycle profile of asynchronic cultures of these primary cells. Similarly to *Aurkb*(+/+) control MEFs, *Aurkb*(+/–) MEFs proliferate well in culture and do not display obvious defects during cell cycle progression (Figure 22).

3.1.2 Aurora B heterozygous mice are fertile although few of them develop hypospermia

To check if heterozygous mice were fertile, we crossed *Aurkb*(+/–) mice and we observed that heterozygous males and females were able to reproduce normally. However, few *Aurkb*(+/–) males (16,6% incidence) develop hypospermia by 12 months of age, in agreement with a relevant role of Aurora B during spermatogenesis (Figure 23) as suggested previously (Kimmins et al., 2007). To further explore this phenotype we analysed testis sections from *Aurkb*(+/+) mice (n=4) and

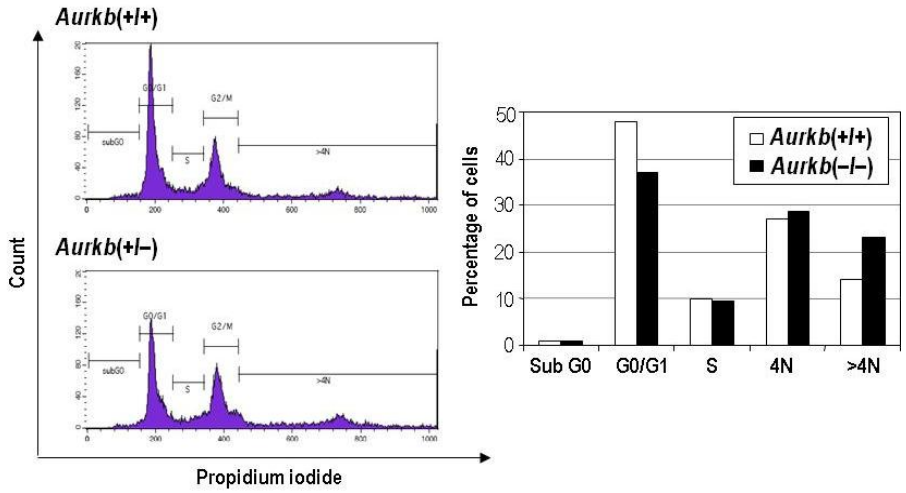

Figure 22. Normal cell proliferation in *Aurkb*(+/–) embryonic fibroblasts. DNA content profile of primary (passage 2) asynchronous *Aurkb*+/+ and *Aurkb*+/– MEFs in complete medium with 10% FBS. Percentage of cells in each phase of the cell cycle is shown at the right panel.

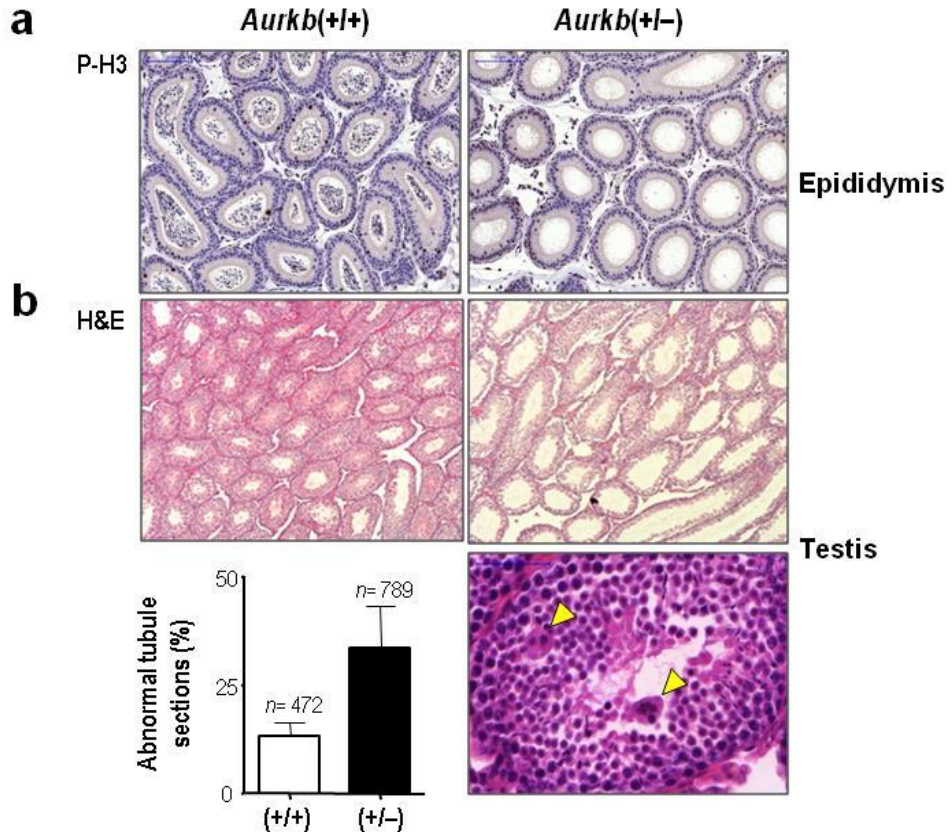

Figure 23. Hypospermia in *Aurkb*(+/–) males. **(a)** Immunohistochemical analysis of phosphorylated Ser10 of histone H3 (P-H3) in epididymis sections revealing absence of spermatozoa in *Aurkb*(+/–) male. **(b)** Hematoxylin/eosin-stained testes sections showing aberrant tubule morphology in *Aurkb*(+/–) male. Bar graph quantitating the percentage of abnormal tubules per mouse at 12 months of age (down left panel), and detail of a tubule from a *Aurkb*(+/–) male with two multinucleated aberrant cells (down, right panel).

Aurkb(+/–) mice (n=6) by 12 months and we found a significant increase in defective tubules in *Aurkb*(+/–) that correlates with empty seminiferous tubules in the epididymis (Figure 23). Interestingly, few multinucleated cells were only present in *Aurkb*(+/–) tubules suggesting spermatogenesis defects specifically in mice with reduced levels of Aurora B.

3.2 Lack of one allele of Aurora B results in impaired proliferation and slight protection against tumour induction

Aurora B is an essential regulator of cell division in yeasts, nematodes, insects, cold-blood vertebrates and in most of the cell lines tested (Ruchaud et al., 2007). In mammals, Aurora B is expressed in the majority of the proliferative tissues (Terada, 1998). However, the requirement of Aurora B for in vivo proliferation in mammals is not known.

3.2.1 Impaired in vivo proliferation in Aurkb(+/–) mice

To investigate if the lack of one Aurora B allele may result in specific proliferative alterations in vivo, we first performed wound healing assays in the skin of *Aurkb*(+/+) and *Aurkb*(+/–) mice. As depicted in Figure 24a, *Aurkb*(+/–) mice display a delay in wound closure in the skin. Whereas wild-type animals take about 2.5 days to heal 50% of the wound area, *Aurkb*(+/–) mice require one additional day (40% more time). This delay correlates with a decrease in proliferation in skin keratinocytes as measured by Ki67 immunodetection in these samples (Figure 24b) indicating that complete protein levels of Aurora B are required for skin proliferation when animals are submitted to challenging proliferative conditions.

3.2.2 Slight protection against tumour induction in Aurkb(+/–) mice

To analyse whether the impaired proliferation observed in the skin of *Aurkb*(+/–) has any relevance in cancer progression, we submitted *Aurkb*(+/–) mice to two different routine carcinogenic

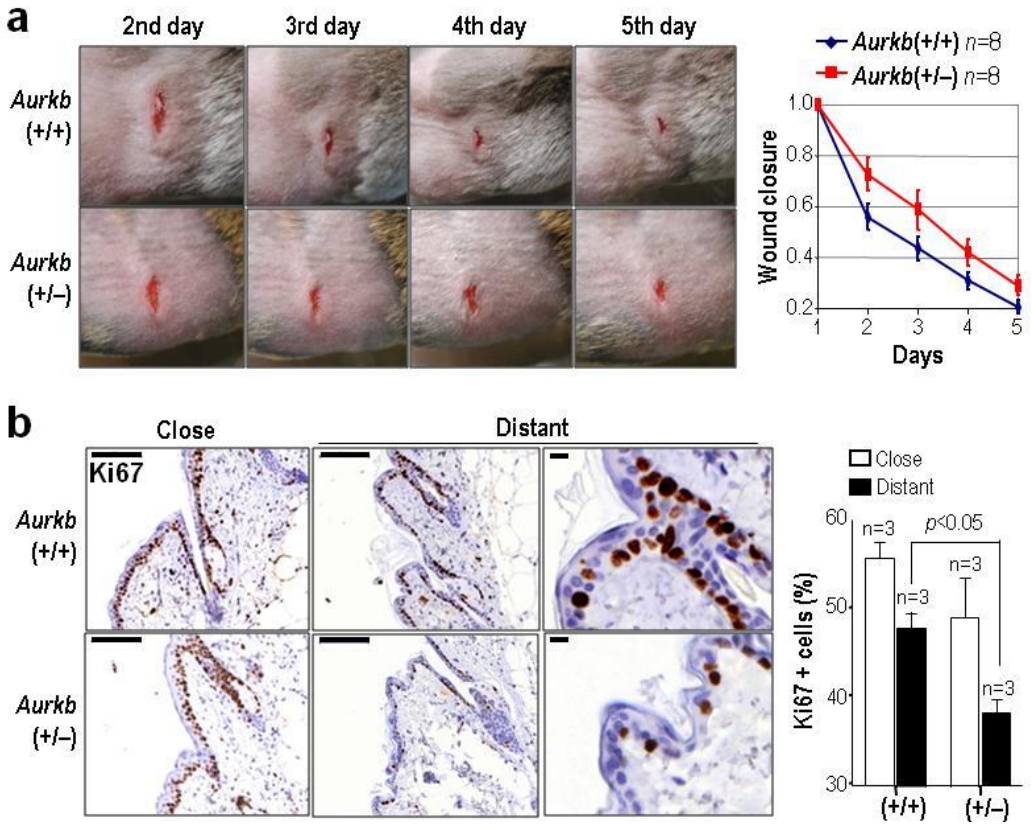

Figure 24. Delayed closure of biopsy wounds in *Aurkb*(+/–) mice. **(a)** Images showing 4mm-wounds closing 2, 3, 4 and 5 days after biopsy in *Aurkb*(+/+) and *Aurkb*(+/–) 12 months-old mice. Line graph plotting the rate of wound closing showing that *Aurkb*(+/–) mice needs more time to close the wound than *Aurkb*(+/+) mice. **(b)** Immunohistochemical analysis of ki67 proliferation marker in skin sections close and distant (approximately 150mm away) to the wound (large and short scale bar: 100 and 10 m, respectively). Bar graph quantification of ki67 positive keratinocytes showing significantly less proliferation in distant areas to the wound in *Aurkb*(+/–) mice.

treatments, 3-MC and the two-stage carcinogenesis protocol using DMBA and TPA (Methods). As indicated in Figure 25a, lack of one allele of Aurora B results in a slight, although not significant, protection against 3-MC-induced fibrosarcomas. Similar results are obtained using the DMBA+TPA protocol (Figure 25b). Thus, the incidence of DMBA-TPA-induced papillomas in *Aurkb*(+/–) mice is reduced, in comparison with control mice, by one unit during the first three weeks of the treatment and from week 12 to week 15. Finally, we also induced tumours in the mammary gland in *Aurkb*(+/–) females by crossing these animals with transgenic mice expressing the Erbb2 oncogene under the mouse mammary tumour virus (MMTV) promoter sequences. As in the previous assays, lack of one allele of Aurora B did not significantly modify the survival of these transgenic mice although *Aurkb*(+/–) mice tend to survive longer as in the case of 3-MC induced tumours (Figure 25c). We conclude that lack of one allele of Aurora B has a minor protective effect against tumour induction.

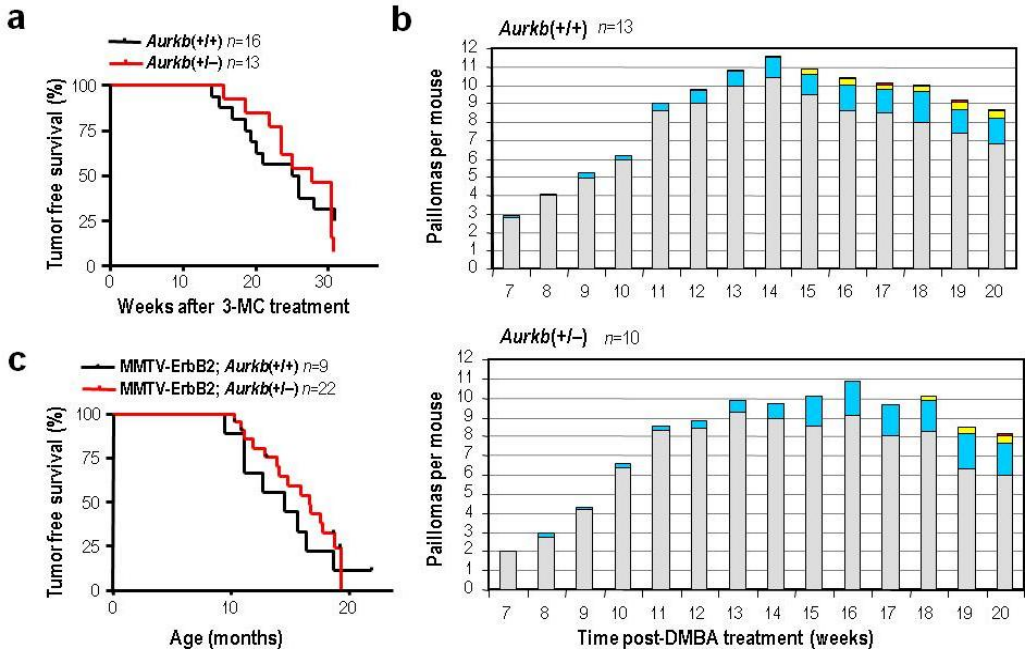

Figure 25. Minor protective effect against tumor induction in *Aurkb*(+/–) mice. **(a)** Incidence of 3MC-induced fibrosarcomas in mice (see Materials and methods). The time of appearance of tumors (>1.5 cm diameter) was scored for each genotype *Aurkb*(+/+) n=16 and *Aurkb*(+/–) n=13. **(b)** Incidence and latency of DMBA-TPA induced papillomas in mice (see Materials and methods). Papillomas's size is represented using a coloured scale (grey for < 3mm, blue for 3-6mm, yellow for 6-9mm and red for > 9mm) for each genotype *Aurkb*(+/+) n=13 and *Aurkb*(+/–) n=10 **(c)** Incidence of Erbb2 genetically-induced mammary tumors in female mice. Erbb2 oncogene is expressed under the mouse mammary tumour virus (MMTV). The time of appearance of tumors (>1.5 cm diameter) was scored for each genotype *Aurkb*(+/+) n= 9 and *Aurkb*(+/–) n=22.

3.3 Lack of one allele for Aurora B increases susceptibility to spontaneous tumour development in aged mice

Although *Aurkb*(+/–) mice do not show gross abnormalities during adult life, we observed that these heterozygous mutant mice display a decreased survival at later ages (Figure 26a). Thus, whereas 83,3% of *Aurkb*(+/+) mice are alive by 26-months of age, only 11,8% of *Aurkb*(+/–) survive by this age. Indeed, the half-life span of these mutant mice is reduced by 6 months compared to their wild-type littermates (half-life of 24.2 months in mutant mice versus 30.5 months in wild-type mice). This lethality is accompanied by a significant increase in the percentage of heterozygous mice with spontaneous tumours by 24 months of age (Figure 26b). In particular, these mutant mice display a tumour spectrum (mainly pituitary, liver adeno/carcinomas and skin papillomas) that is not observed in the control group (Table 7). In addition, about 33% of *Aurkb*(+/–) mice develop B-cell lymphomas, a type of tumour that it is commonly observed in wild-type mice. These data indicate that *Aurkb*(+/–) mice display a significant tumour susceptibility with age.

Table 7. Tumours observed in aged *Aurkb* mutant mice

Tumours	*Aurkb*(+/+)		*Aurkb*(+/–)	
	Incidence (%)	Latency (months)	Incidence (%)	Latency (months)
B-cell Lymphoma	66.6 (4/6)	29	33.3 (3/9)	23
Lung Adenoma	16.6 (1/6)	26	22.2 (2/9)	21
Pituitary Adenoma	0	-	22.2 (2/9)	22
Papilloma	0	-	22.2 (2/9)	18
Liver Adeno/carcinoma	0	-	22.2 (2/9)	28
Thymic angioma	0	-	11.1 (1/9)	22
Hemangioma	16.6 (1/6)	30	0	-
Sarcoma	16.6 (1/6)	26	0	-
Bile duct adenoma	16.6 (1/6)	26	0	-

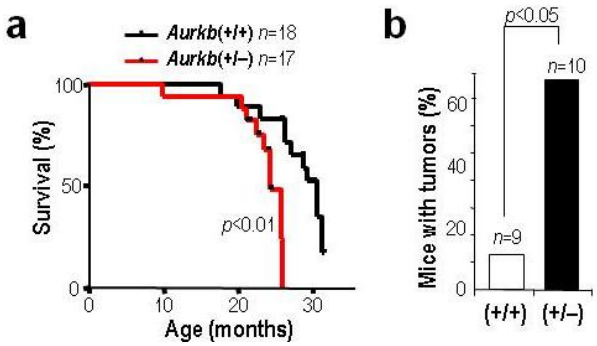

Figure 26. Increased susceptibility to tumour development in aged *Aurkb*(+/–) mice. **(a)** Survival curve of *Aurkb*(+/+) and *Aurkb*(+/–) mice indicating a slight but significant reduction in the life span of these mutant mice. **(b)** Bar graph quantification of percentage of mice with tumours at 24 months of age revealing a significant increase in tumour appearance in *Aurkb*(+/–) mice. (c) Representative pathology of the tumours observed in *Aurkb*(+/–) mice. Images of pituitary and liver carcinomas and skin papillomas

4. Lethality and complementation by Aurora C

4.1 Genetic ablation of Aurora B does not disturb early embryonic divisions

4.1.1 Aurora B-deficient embryos progress normally to a blastocyst stage

To generate homozygous mutants, we intercross *Aurkb*(+/–) or *Aurkb*(+/Z) mice and analyzed their progeny. No homozygous mutant mice were observed from any of these crosses suggesting embryonic lethality (Table 8). Similarly, no homozygous embryos are observed at mid gestation (E10.5-E14.5) indicating that Aurora B is required for completing embryonic development. Since genetic ablation of the other CPC components, Incenp, Survivin or Borealin prevents embryonic cell divisions as early as E2.5 (Cutts et al., 1999; Uren et al., 2000; Yamanaka et al., 2008), we decided to isolate fertilized embryos at E2 (Methods). By this stage most embryos are at the 4-cell stage (Figure 27a). After four additional days in culture, wild-type and heterozygous embryos form normal morulas and blastocysts. Unexpectedly, the mendelian ratio of *Aurkb*(–/–) embryos (27 out of 121 embryos, Table 8) also form normal blastocysts by E5.5 without any evident sign of decreased size or cellular death (Figure 18a). Same results are observed in *Aurkb*(Z/Z) embryos which are able to form blastocysts similar to their wild-type littermates (Figure 27b).

4.1.2 Aurora B is expressed during first cell divisions

To test whether Aurora B is expressed at these early developmental stages, we took advantage of the β-galactosidase reporter expressed in the *Aurkb*(Z) allele. As shown in Figure 27b, we detected positive staining for β-galactosidase suggesting that the *Aurkb* regulatory sequences are active in these early embryonic cycles. Expression of Aurora B was also confirmed at different early developmental stages by immunofluorescence. As depicted in Figure 28, Aurora B is detected at

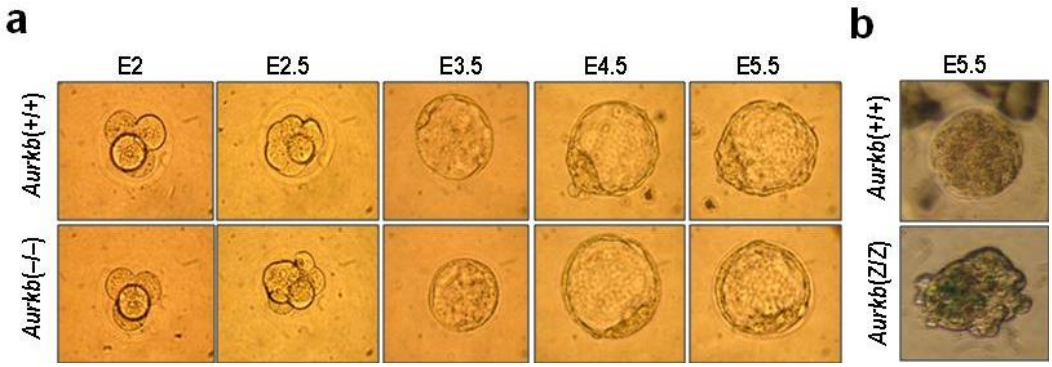

Figure 27. Normal development of pre-implantation embryos lacking Aurora B. **(a)** E2 embryos were isolated from intercrosses between *Aurkb*(+/–) mice and cultured for 4 additional days. These embryos were genotyped by PCR analysis at E5.5. **(b)** Analysis of β-galactosidase expression in *Aurkb*(+/+) and *Aurkb*(Z/Z) embryos by E5.5 showing lacZ expression from the endogenous *Aurkb* promoter sequences.

the expected cellular structures (centromeres, midbody and cytokinesis bridges) in early wild-type embryos at all stages tested. Aurora B, however, is not detected in fertilized *Aurkb*(–/–) embryos as early as the 2-cell stage or later developmental phases (see below). Thus, the lack of defects in *Aurkb*(–/–) morulas or blastocysts is not a consequence of uncontrolled expression of Aurora B or maternal contribution but rather an indication of dispensability of Aurora B in the cell division cycle, at least during these stages.

Table 8. Analysis of mice and embryos obtained from *Aurkb*(+/–) intercrosses

Genotypes of live births and embryos					
Age	*Aurkb*(+/+)	*Aurkb*(+/–)	*Aurkb*(–/–)	Reabsorbed	Total
Newborns	48 (33.8%)	94 (66.2%)	0	0	142
E10.5 - E14.5	16 (29.1%)	31 (56.4%)	0	8 (14.5%)	55
Embryos grown in culture					
Stage	*Aurkb*(+/+)	*Aurkb*(+/–)	*Aurkb*(–/–)		Total
Blastocysts E5.5	39 (32.2%)	55 (45.5%)	27 (22.3%)		121
Healthy at E8.5	7	9	0		16
ICM atrophied	1	1	7		9
Histological analysis of embryos in utero					
Stage		*Aurkb* (+)	*Aurkb* (-)	Empty	Total
E9.5		18 (72.0%)	4 (16.0%)	3 (12.0%)	25
E7.5		13 (68.4%)	5 (26.3%)	3 (5.3%)	19

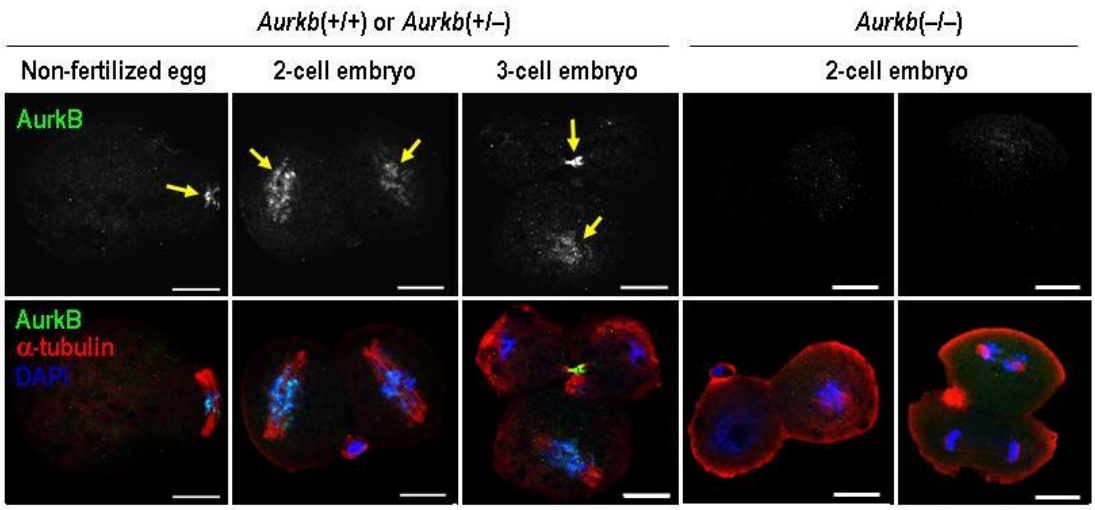

Figure 28. Aurora B is expressed during early embryonic development. Immunofluorescence images of oocytes and 2-3 cell embryos stained for α-tubulin (red), Aurora B (*Aurkb*, in green) and DAPI (DNA, in blue). Aurora B localizes to the chromosomes during prometaphase and to the midbody in cytokinesis. No staining is observed in Aurora B-deficient embryos despite the normal mitotic figures observed. Scale bars, 20 μm.

4.1.3 Histone H3 is properly phosphorylated and Incenp is correctly localized in early embryos lacking Aurora B

Aurora B as part of the CPC phosphorylates Histone H3 at Ser10 to facilitate chromosome condensation at the beginning of mitosis. To study Aurora B activity in early embryos we used a phospho-specific antibody against histone H3-S10. Intriguingly, Aurora B-null morulas display normal mitosis with phosphorylated histone H3 (P-H3), indicating normal chromosome condensation (Figure 29a) in the absence of Aurora B.

As it has been described that the CPC members are physically and functionally interdependent and that disruption of any member of the complex delocalizes the others (Gassmann et al., 2004; Jeyaprakash et al., 2007) we decided to analyse the stability of the CPC in the absence of Aurora B by checking Incenp localization. Interestingly, Aurora B-null embryos display the expected localization of Incenp, which co-localizes with Aurora B in wild-type cells but it is also properly located despite the lack of Aurora B (Figure 29b). These results suggest that Aurora B typical functions are carried out normally in early mutant embryos.

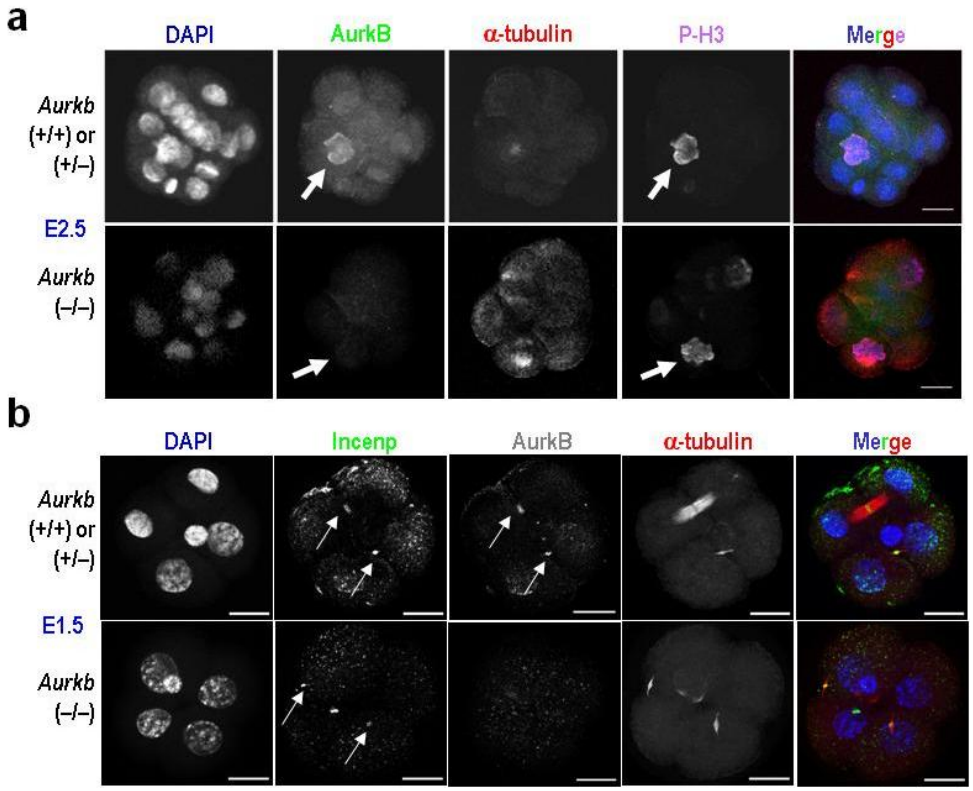

Figure 29. Normal phosphorylation of Histone H3 and localization of the CPC component Incenp in Aurora B-null pre-implantation embryos. Immunofluorescence images of embryos extracted at E1.5 and E2.5 days. **(a)** Expression of Aurora B (*Aurkb* in green) indicating its colocalization with phospho-histone H3 (P-H3 in pink) in mitotic cells of E2.5 pre-implantation embryos. In the absence of Aurora B, mitotic cells are also present in the same frequency and display normal staining for P-H3. **(b)** Incenp (green) is also properly localized (arrows) in early embryos in the presence or absence of Aurora-B. α-tubulin staining is shown in red and DAPI (DNA) in blue. Scale bars, 20 μm.

4.1.4 Aurora B-null blastocysts display normal size and cell number

To explore at the cellular level if Aurora B is also dispensable to form a functional blastocyst, we performed immunofluorescence studies in normal and in Aurora B-deficient embryos at E4.5. As expected from the previous result (Figure 27), Aurora B-null blastocysts display similar size and cell number than normal blastocysts with the typical localization of Aurora B in wild-type but not in mutant embryos (Figure 30).

4.2. Genetic ablation of Aurora B results in mitotic aberrations and lethality after implantation

Since Aurora B-null blastocysts develop normally, we next asked whether Aurora B is required for the implantation of embryos in vivo. As indicated in Table 2, we identified 26.3% of Aurora B-negative implanted embryos by E7.5, as assayed by immunohistochemistry for Aurora B, and a more limited number of Aurora B-negative embryos (16%) by E9.5. All these Aurora B-deficient embryos display a smaller size and several histological abnormalities (see below) that prevented proper identification by PCR. In addition, the embryonic structures were absent in a percentage of deciduas (5.3% and 12% of empty deciduas at E7.5 and E9.5, respectively) suggesting additional dead embryos after implantation (Table 8).

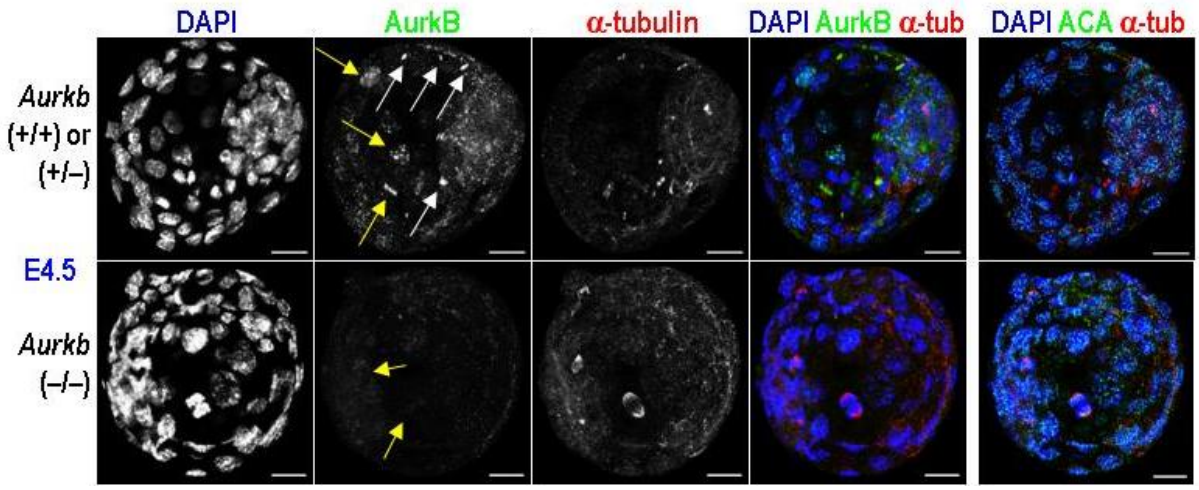

Figure 30. Aurora B-null blastocysts do not show cellular defects. Immunofluorescence images of wild-type and Aurora B-null blastocysts at E4.5 showing similar structure and size including normal PM and M (yellow arrows) and cytokinesis bridges (white arrows) despite the absence of Aurora B. Aurora B (*Aurkb*) staining is shown in green, α-tubulin in red and DAPI (DNA) in blue. Alternatively, we used ACA, anti-centromeric antigen antibody shown in green. Scale bars, 20 μm.

4.2.1 Histological examination of abnormal implanted Aurora B-null embryos

Histological examination by hematoxilin and eosin (H&E) staining of E7.5 embryos revealed defective embryos with hemorrhagia in the ectoplacental cone and frequent oedemas and apoptotic cells (Figure 31). Whereas there is a clear amniotic cavity in wild-type embryos by this stage, Aurora B-deficient embryos accumulate apoptotic cells in a small, atrophic lumen. A significant increase in mitotic (15.8% in Aurora B-null embryos vs. 4.4% in wild-type embryos; $p < 0.001$) and apoptotic (14.6% in Aurora B-null embryos vs. 0% in wild-type embryos; $p < 0.001$) cells is found in Aurora B-deficient embryos (Figure 31).

4.2.2 DNA damage and activation of the p53 pathway leads to apoptosis in implanted embryos lacking Aurora B

To determine which mechanisms are related with the apoptosis observed in Aurora B-deficient ES cells by E7.5, we analysed possible DNA damage or activation of p53 pathway in these cells. After immunohistochemistry detection, we observed that many of the mutant ES cells display a significant positive staining for γH2AX (8.7% in Aurora B-null embryos vs. 0.7% in wild-type embryos; $p < 0.001$) or p53 (2.0% in Aurora B-null embryos vs. 32.9% in wild-type embryos; $p < 0.001$) suggesting DNA damage and activation of the p53 pathway in these apoptotic cells (Figure 32). Finally, to confirm that the apoptotic pathway is activated in Aurora B-deficient cells we examined the activated form of caspase 3 (C3A). In accordance to the presence of apoptotic cells observed in the H&E staining, there is a significant increase in positive C3A cells (14.9% in Aurora B-null embryos vs. 0.8% in wild-type embryos; $p < 0.001$) (Figure 32).

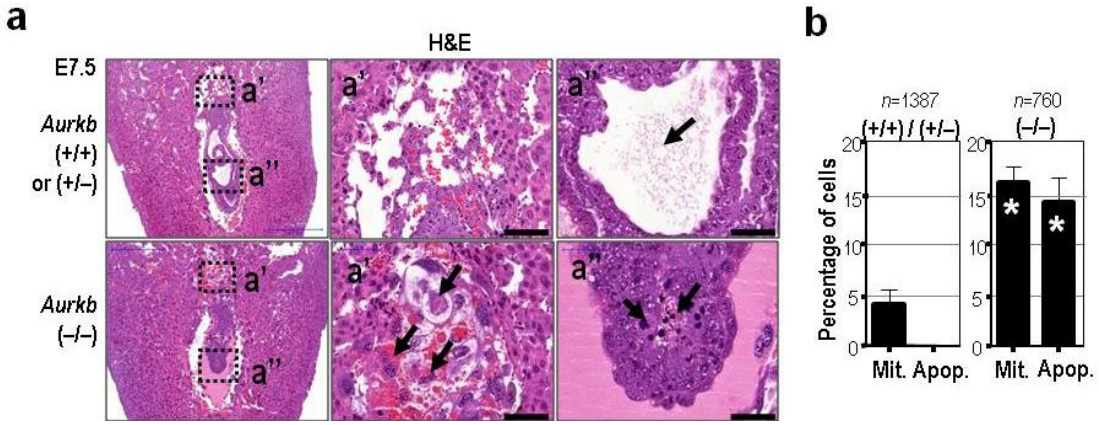

Figure 31. Abnormal embryonic development of Aurora B-null embryos by E7.5. **(a)** Hematoxylin/eosin-stained uterine decidua sections at E7.5 showing *Aurkb*(+/+) or (+/–) and *Aurkb*(–/–) implanted embryos. Aurora B-null embryos display a defective ectoplacental cone (a') with aberrant trophoblasts (arrows) and hemorrhagia. Furthermore, the amniotic cavities are atrophic in Aurora B-null embryos (a") and accumulate apoptotic cells (arrows). The implanted embryo is surrounded by a big oedema (*). **(b)** Bar graph showing the significant increase of mitotic and apoptotic cells in *Aurkb*(–/–) implanted embryos ($p < 0.001$ in all cases). Scale bars, 100 μm

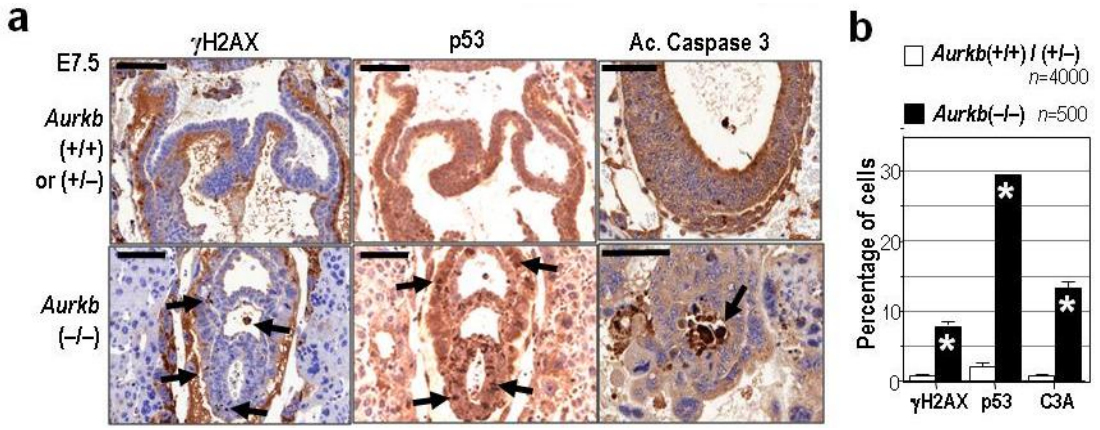

Figure 32. Activation of p53 pathway in the presence of DNA damage leads to apoptosis in Aurora B-null embryos by E7.5. **(a)** Immunohistochemical analysis of H2AX, p53 and C3A in uterine decidua sections at E7.5 showing minimal staining of these markers in *Aurkb*(+/+) or (+/–) embryos and positive staining (arrows) of the three markers in *Aurkb*(–/–) implanted embryos. **(b)** Bar graph showing the significant increase in γH2AX, p53 and C3A positive cells in *Aurkb*(–/–) implanted embryos ($p < 0.001$ in all cases). Scale bars, 100 μm

4.2.3 Aurora B-deficient cells arrest at prometaphase/metaphase with an active SAC

Aurora B is clearly detected by immunostaining in mitotic and other (possibly G2) cells in wild-type embryos (Figure 33). This clear staining in wild-type embryos lead us to easily identify the Aurora B-null embryos as they show completely negative staining in all the embryonic structures. Interestingly, most of the mitotic figures observed in the Aurora B negative embryos represent cells in prometaphase (PM) or metaphase (M), including a significant proportion of abnormal PM/M figures with misaligned chromosomas (Figure 33). In addition, all these cells display a positive signal for Cyclin B1, suggesting that Aurora B-null cells do not progress to anaphase and arrest at a stage where the Anaphase-promoting complex (APC/C) is inactive probably due to a functional Spindle Assembly Checkpoint (SAC).

4.2.4 Embryos fully degenerate at E9.5 in the absence of Aurora B

By E9.5, wild-type embryos are at the beginning of mid-gestion and many of the future adult structures can already be distinguished (Figure 34a). On the contrary, most Aurora B-null embryos are degenerated at this stage with only few cells left that are mostly arrested in M/PM or apoptotic (Figure 34ab). This massive cellular death observed in the mutant embryos is also accompanied with a significant increase in aberrant multinucleated giant trophoblast cells (Figure 34c-e) suggesting defects in the endoreplicative cycles of these particular cells of the placenta.

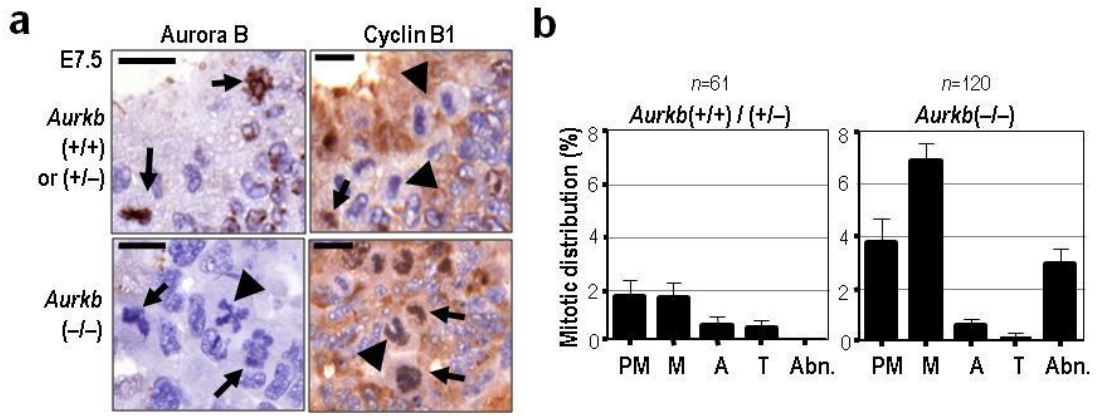

Figure 33. Aurora B negative cells arrest at PM/M with accumulation of Cyclin B1 in E7.5 implanted embryos. **(a)** Immunohistochemical analysis of Aurora B and Cyclin B1 in uterine decidua sections at E7.5. Aurora B is readily detectable in mitotic figures (arrows) of *Aurkb*(+/+) or (+/–) cells but not in *Aurkb*(–/–) cells. Abnormal mitotic figures are frequently observed in Aurora B-null embryos (arrowhead). In wild-type cells, Cyclin B1 is present in prometaphase figures (arrow) but not in advanced metaphase or anaphase stages (arrowheads). Normal (arrows) or abnormal (arrowhead) mitotic figures in *Aurkb*(–/–) embryos display a positive staining for Cyclin B1 in agreement with an arrest in prometaphase. **(b)** Bar graph quantification of the distribution of mitotic cells in the different phases of mitosis indicating an arrest in prometaphases (PM) or metaphases (M) in *Aurkb*(–/–) embryos. Note that due to the low resolution of these paraffin sections where individual chromosomes are not detectable, many M may actually correspond to PM and prophases were difficult to distinguish. PM: prometaphase, M: metaphase, A: anaphase, T: telophase, Abn: abnormal. Scale bars, 20 μm

4.3 Genetic ablation of Aurora B results in abnormal advanced blastocysts

To gain an insight of the cellular defects caused by the lack of Aurora B we mimicked the implantation process using an in vitro approach called embryo "hatching" (Methods). This approach consists on growing blastocysts in culture for 2 to 5 days until they hatch from the zona pellucida and attach to the plate, and is ideal to study at the cellular level the functionality of ES and TGC cells

4.3.1 Aurora B-null advanced blastocysts display an aberrant ICM surrounded with abnormal TGC

To test the possible defects that Aurora B-null blastocysts may present after "hatching", we carried out immunofluorescence analysis at different points. After four days in culture, wild-type blastocysts hatched from the zona pellucida, attached to the culture dish and generated a normal proliferative (as indicated by P-H3) inner cell mass surrounded by trophoblast giant cells (Figure 35a and Methods). Aurora B-deficient embryos, on the other hand, at this stage (E9.5) displayed a deficient and apoptotic inner cell mass (Figure 35a) surrounded with aberrant trophoblasts with significant morphological alterations (Figure 35b).

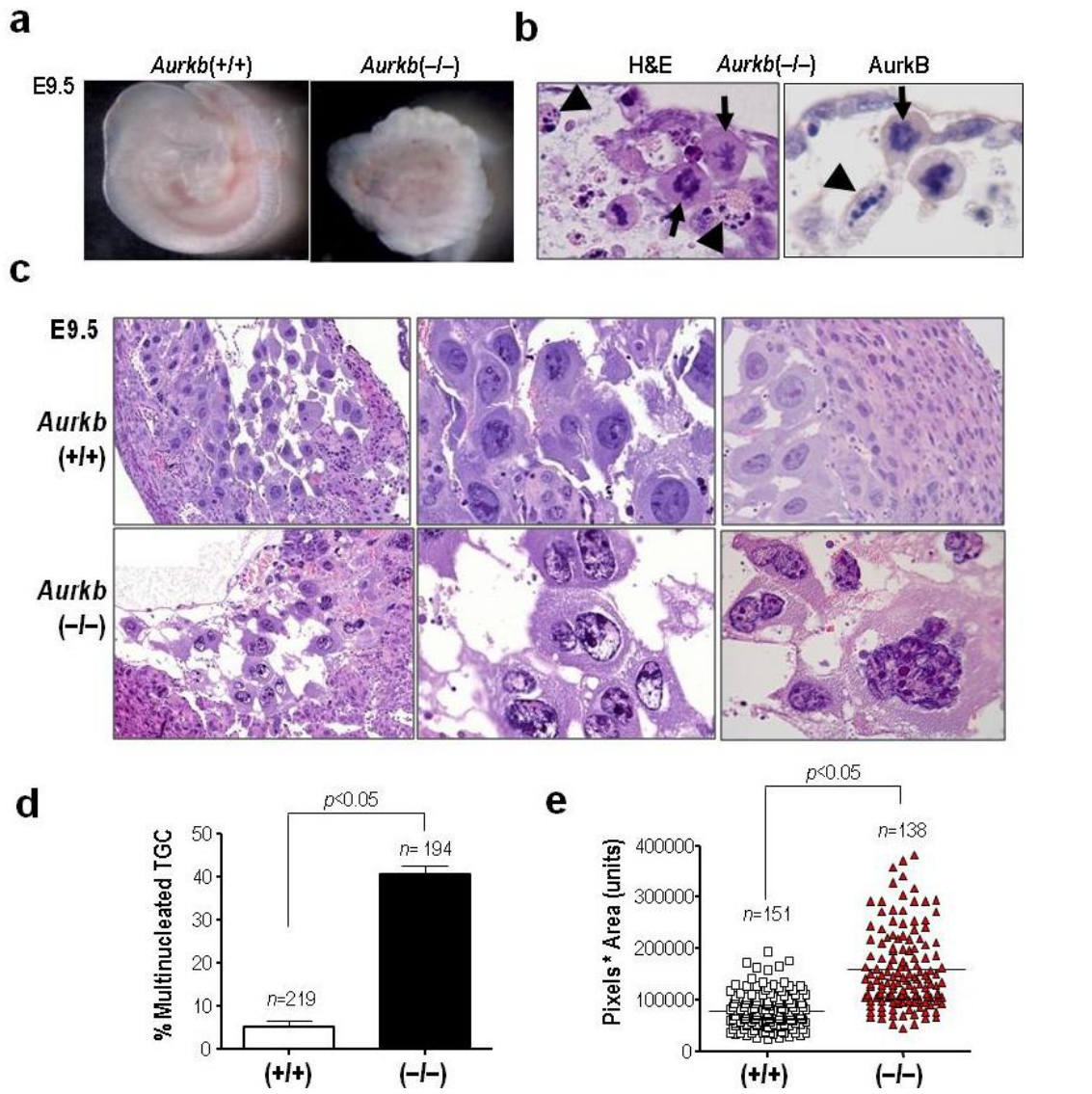

Figure 34. Aurora B-null embryos degenerate completely at E9.5 with aberrant TGC. **(a)** Whole embryos extracted at E9.5 from *Aurkb*(+/–) intercrosses showing atrophic structure of Aurora B-null embryos. **(b)** Hematoxylin/eosin and Aurora B immune staining of *Aurkb*(–/–) embryos revealing that the few cells remaining in the embryo are either apoptotic (arrowheads) or arrested in a prometaphase-like state (arrows). **(c)** Hematoxylin/eosin stained sections of placentas from E9.5 embryos showing aberrant polyploidy TGC. **(d)** Bar graph quantification of percentage of multinucleated TGC in *Aurkb*(+/+) n=2 and *Aurkb*(–/–) n=2. (e) Scatter dot-plot quantification of DNA content of TGC in *Aurkb*(+/+) n=2 and *Aurkb*(–/–) n=2.

4.3.2 Lack of Aurora B prevents proper chromosome segregation in ES cells

To analyse in detail the causes that lead to a deficient ICM in the lack of Aurora B we examined these ES cells at earlier stages. By E7.5, we detected numerous cells in PM or M in Aurora B-null embryos that were less frequently observed in control cultures. As a consequence of this arrest in PM/M we hardly observed cells exiting mitosis in Aurora B-deficient embryos in contrast to control embryos were we observed Aurora B positive cells in metaphase and cytokinesis (Figure

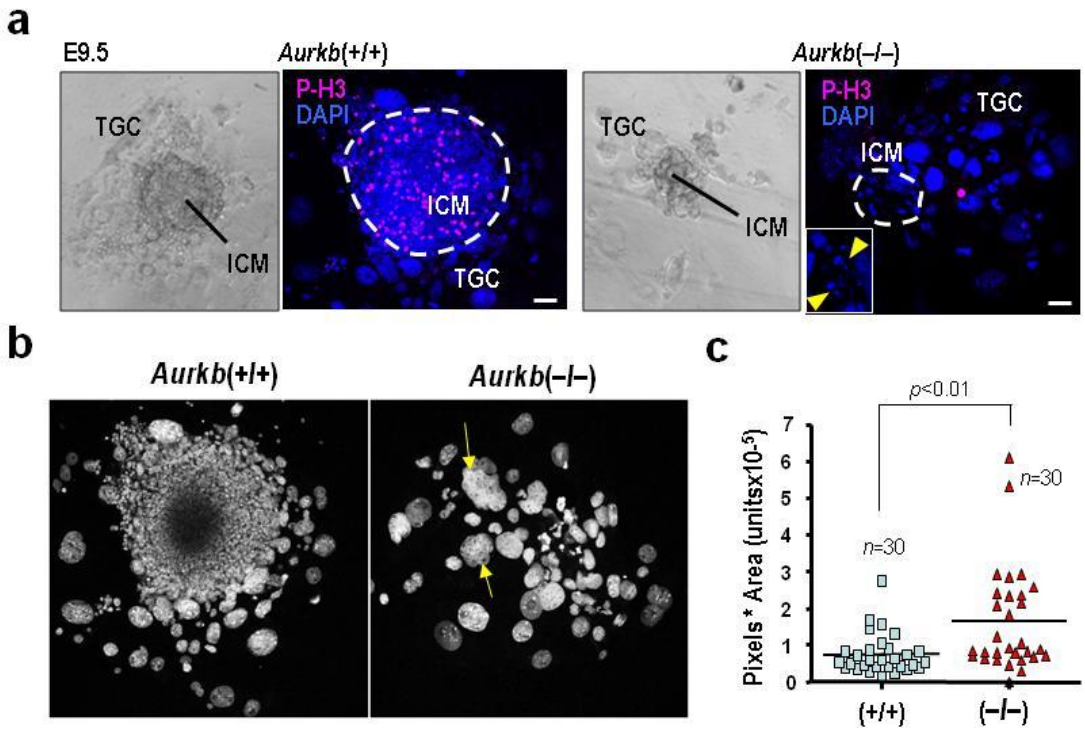

Figure 35. In vitro culture of blastocysts leads to degeneration of Aurora B-null embryos at E9.5. Phase-contrast and immunofuorescence images of embryos harvested at E2.5 and cultured in vitro for 7 days. **(a)** *Aurkb*(+/+) embryos form a robust and proliferative (as indicated with P-H3) inner cell mass (ICM) upon a layer of trophoblasts giant cells (TGC); whereas, Aurora B-null embryos only present few apoptotic cells (yellow arrowheads) surrounded with TGC. DAPI (DNA) staining is in blue and phospho-histone H3 (P-H3) in pink. **(b)** A proportion of TGC cells display nuclear aberrancies (yellow arrows) in *Aurkb*(–/–) embryos. **(c)** Scatter dot-plot quantification of DNA content of TGC in *Aurkb*(+/+) n=2 and *Aurkb*(–/–) n=2. DAPI (DNA) staining is in blue and phospho-histone H3 (P-H3) in pink Scale bar, 50 μm.

36a). During mitosis, Aurora B-deficient cells display abnormal spindles with a strong concentration of tubulin in the poles and lack of bipolar fibers (Figure 36b). Multipolar spindles are also frequently observed suggesting either a defect in organizing bipolar spindles or the presence of polyploidy cells. In addition, all these mitotic figures display misaligned chromosomes (Figure 36b) confirming the role of Aurora B in promoting proper chromosome alignment during mitosis.

4.3.3 Aurora B-deficient ES cells arrest at prometaphase with a functional SAC and mislocalization of the CPC

To check if the arrest in prometaphase is a consequence of having a functional SAC we performed immunofluorescence to detect Mad2 in unattached kinetochores. Indeed, we observed that Mad2 is present at the kinetochores of misaligned chromosomes in mutant cells indicating a functional and robust SAC in these cells (Figure 37a). In addition, we detected positive staining for Cyclin B1 indicating that the APC/C is not active as a consequence of the SAC. Finally, to determine whether these phenotypes are a consequence of an abnormal CPC distribution we tested Incenp localization.

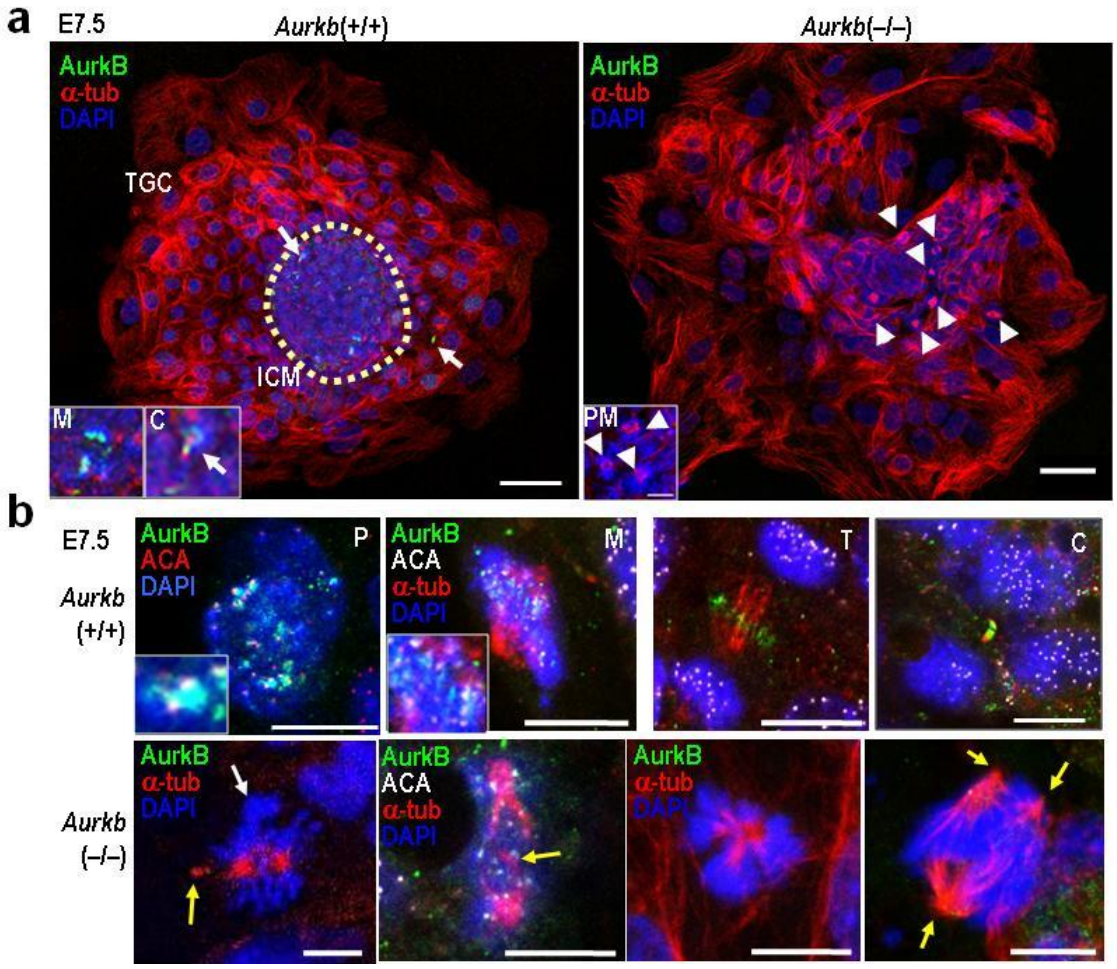

Figure 36. Aurora B-null ES cells arrest at PM with misaligned chromosomes and spindle abnormalities. Immunofuorescence images of embryos harvested at E2.5 and cultured in vitro for 5 days. **(a)** Aurora B (green signal) is present in mitotic, mainly in metaphases (M), and cytokinesis (C) figures in wild-type (arrows and inset) but not in *Aurkb*(–/–) embryos. In the absence of Aurora B, there is an evident accumulation of mitotic cells, mainly prometaphases (PM), (arrowheads and inset) in the ICM . Scale bars, 50 m**(b)** Mitotic distribution in the inner cell mass. In wild-type cells, Aurora B (green) localizes internal to ACA spots (red or white) during prophase (P) or metaphase (M) due to its localization to the inner centromere. Aurora B moves to the central spindle during telophase (T) or to the midbody during cytokinesis (C). In *Aurkb*(–/–) embryos, Aurora B is not detected and these cells display aberrant bipolar spindles with misaligned chromosomes (white arrow), as well as monopolar or multipolar spindles. Note the presence of multiple poles or isolated α-tubulin spots (yellow arrows). Aurora B (*Aurkb*) staining is shown in green, α-tubulin (α-tub) in red, anti-centromeric antigen antibody (ACA) in red or white and DAPI (DNA) in blue. Scale bars, 10 μm.

Whereas Incenp is properly located at the metaphase plate and midbodies of wild-type cells, we were unable to find normal localization of Incenp in Aurora B-null cells (Figure 37b), thus suggesting that Aurora B deficiency results in impaired CPC function in advanced blastocysts but not in earlier developmental stages.

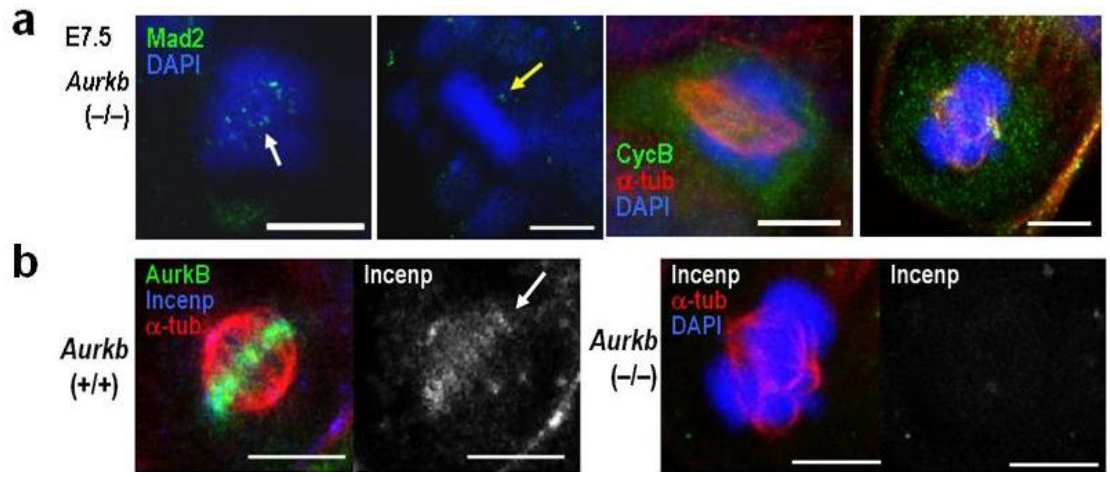

Figure 37. Aurora B-null ES cells arrest at PM with an active SAC and a non-functional CPC. Immunofuorescence images of embryos harvested at E2.5 and cultured in vitro for 5 days. **(a)** *Aurkb*(–/–) cells show the presence of Mad2 (green) at the kinetochores during prometaphase (white arrow) or in misaligned chromosomes in incomplete metaphases (yellow arrow). Cyclin B1 (CycB-green) is also present in these mitotic figures showing a diffuse expression in some cases accompanied by enrichment at the poles. **(b)** Whereas Incenp is properly localized at the centromeres (arrow), midbodies or cytokinesis bridged (not shown) colocalizing with Aurora B (*Aurkb*-green) in wild-type cells, no Incenp signal is observed in Aurora B-null cells. α-tubulin (α-tub) staining is in red and DAPI (DNA) in blue. Scale bars, 10 μm.

4.4. Aurora C compensates for Aurora B function during early embryonic development

Since lack of the other CPC components, Incenp, Survivin or Borealin results in early lethality by E2.5 (Cutts et al., 1999; Uren et al., 2000; Yamanaka et al., 2008), we wondered whether Aurora B can be compensated by other Aurora kinases during early embryonic development. In terms of homology, Aurora C is closer to Aurora B than Aurora A (Figure 6). Indeed, Aurora C has been previously shown to bind other CPC components and to rescue cellular defects due to lack of Aurora B when overexpressed in specific cell lines (Sasai et al., 2004; Slattery et al., 2008; Yan et al., 2005).

4.4.1 Aurora C is highly expressed in early embryos

To determine whether Aurora C is able to compensate Aurora B during early development, we first checked if Aurora C is expressed during early cell divisions. Since currently available antibodies did not work in whole-mount immunofluorescence in mouse embryos, we quantified Aurora C expression in early embryos by real-time PCR or in post-implantation embryos by immunohistochemistry. As depicted in Figure 38a,b, Aurora C is detected in early embryos (2-cell stage and morulas) but it is not expressed in late embryos (E14.5) or implanted embryos (E7.5) as examined by RT-PCR or immunostaining in sections. As control, we detected Aurora C expression in testis by both techniques, RT-PCR and immunostaining, as reported previously (Hu et al., 2000; Kimmins et al., 2007; Tang et al., 2006). Similar data indicating expression of Aurora C in early

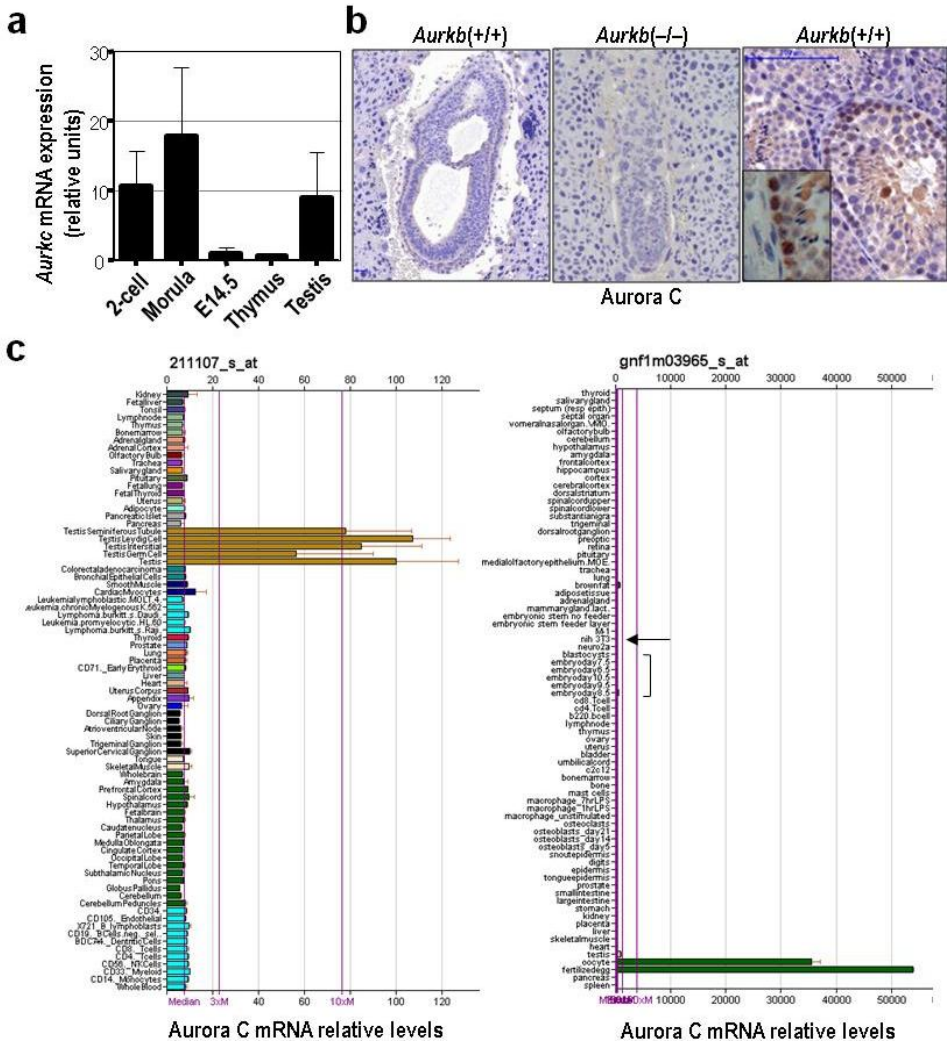

Figure 38. Aurora C is expressed in the early embryonic divisions. **(a)** Expression of Aurora C at the 2-cell stage, morula, mid-gestation or adult tissues as measured by real-time RT-PCR. mRNA levels were normalized versus the expression of GADPH. **(b)** Detection of Aurora C by immunohistochemistry in sections (E7.5) from wild-type (left) or Aurora B-deficient (middle) post-implantation embryos indicating lack of expression at this stage. Aurora C is not detected in most adult tissues but it is highly expressed in germ cells of the testis. **(c)** Published expression profiles from GNF SymAtlas (http://biogps.gnf.org/) showing Aurora C expression specifically in the testis and testis cell lines (left), and in oocytes and fertilized eggs (right). Note that there is no Aurora C expression in blastocysts, nor in implanted embryos (E6.5-10.5) or in 3T3 cells.

embryos but not in later stages can be obtained from published expression profiles (Hamatani et al., 2004) (Figure 38c from GNF SymAtlas webpage http://biogps.gnf.org/).

4.4.2 Inhibition of Aurora B/C results in a severe arrest in early embryos

We then addressed whether Aurora C may complement Aurora B funcion during early embryonic development by using a small molecule inhibitor, ZM447439 (also known as ZM1), that is able to specifically inhibit both Aurora B and C kinases (IC50 Aurora B 50 nM ; IC50 Aurora C 250 nM ;

IC50 Aurora A 1000 nM ;(Girdler et al., 2006). Wild-type E2 (4-cell) embryos were treated with low dosis (2 μm) of ZM1 or carrier and analyzed 12 h after addition of the drug. As represented in Figure 39a, ZM1 treatment results in a severe arrest at the 4-cell stage in 80% of treated embryos, whereas most control embryos progress to the morula stage. Importantly, treatment with ZM1 results in a phenotype similar to that observed in Aurora B-deficient embryos by E7.5 (Figure 39), including prometaphase arrest, misaligned chromosomes and tetraploid or binucleated cells as previously reported for this drug (Figure 39b). (Girdler et al., 2006)

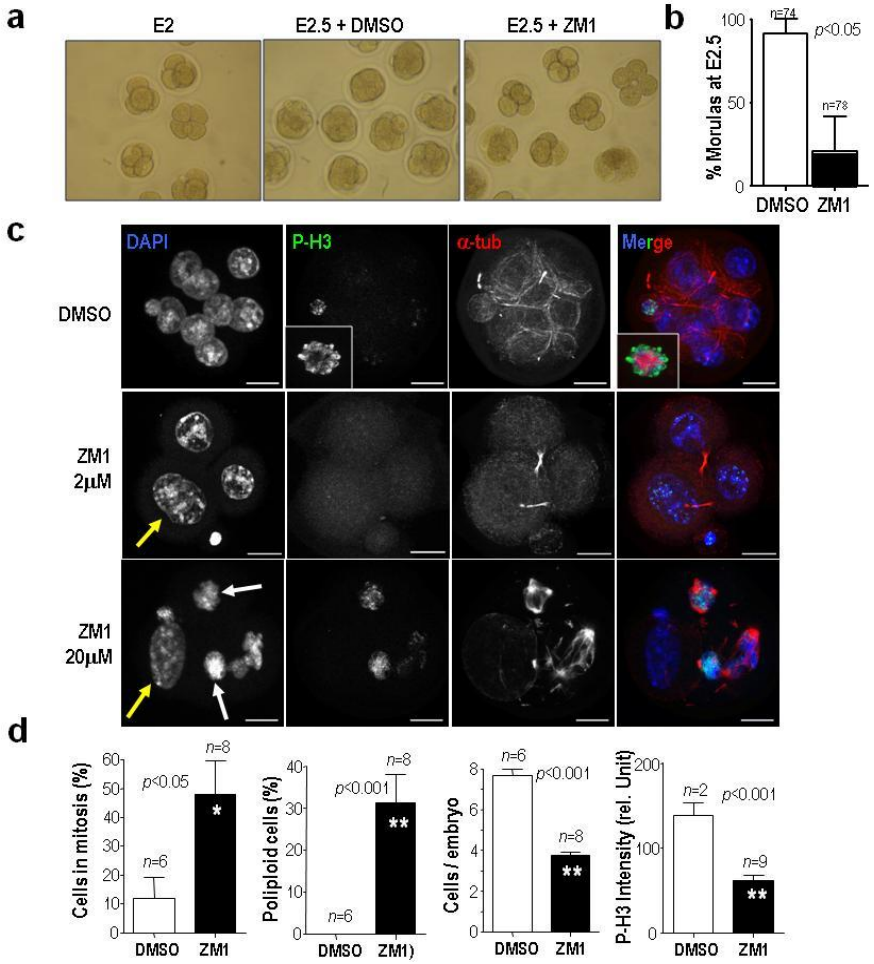

Figure 39. Early embryos arrest with mitotic defects after inhibition of Aurora B/C. **(a)** Sensitivity of early embryos at the 4-cell stage to ZM1, a small-molecule inhibitor of Aurora B and Aurora C. Treatment of these embryos with 2 μM ZM1 leads to arrest at the 4-cell stage, whereas a parallel treatment with DMSO results in the progression to the morula stage after 12 h. **(b)** Bar graph quantification of percentage of embryos that reach to morula state after 12h treatment with 2 μM ZM1. **(c)** Immunofluorescence analysis indicates a significant accumulation of cells in mitosis (white arrows) or poliploid cells (yellow arrows) that have underwent a failed cytokinesis. **(d)** The mitotic defects observed after Aurora B/C inhibition leads to accumulation of defective mitosis and subsequent poliploidy and to a reduction in the number of cells per embryo in ZM1 treated cells. To evaluate inhibition of Aurora B/C kinase acvity we confirmed that phosphorylation of histone H3 (P-H3) is significantly reduced in these ZM1-treated mitotic cells although some signal is still detected. α-tubulin (α-tub) staining is in red, phospho-histone H3 (P-H3) in green and DAPI (DNA) in blue. Scale bars, 20 μm.

4.4.3 Aurora C plays a crucial role in driving proper mitosis during early cell divisions

To further explore the possibility that Aurora C is responsible for supporting cell division during the morula and blastocyst stage, we microinjected in the pronucleus of fertilized embryos (E0.5) three different short hairpin interfering RNAs (shRNAs) specific for Aurora B or Aurora C kinases along with a reporter plasmid that expresses the green fluorescent protein fused to histone H2B (Figure 40a). One day after microinjection, most embryos were at the 2-cell stage and expressed the fusion protein GFP-H2B in the nucleus of each cell (Figure 40b). Efficient silencing was confirmed measuring transcripts levels three days after microinjection (Figure 40a). By E2.5, most embryos injected with a shRNA against luciferase (shluc) or Aurora B (shAurB) progressed normally forming morulas with 4-8 cells. However, most embryos injected with Aurora C shRNAs (shAurC) or a combination of Aurora B and Aurora C shRNAs were either arrested at the 2-cell stage (Figure 40b). These embryos, but not the embryos injected with shluc or shAurB constructs, displayed a high number of mitotic figures, mostly PM or M by E2.5 (Figure 40c) as previously described in the Aurora B-deficient inner cell mass. These abnormal divisions frequently result in chromosomal bridges and giant nuclei suggesting an ultimate defect in cytokinesis (Figure 40c) resulting in an arrest at the 2-4 cell stage (Figure 40d). All together, these results suggest that Aurora C, but not Aurora B, has a crucial role in driving proper mitosis during early embryonic development.

5. Essential functions of Aurora B in G1/S progression and mitosis

Loss-of-function studies of mammalian Aurora B have used RNA interference or chemical inhibitors of this kinase resulting in a clear characterization of its role in chromosome alignment and cytokinesys (Ruchaud et al., 2007) .However, these studies have the caveat that elimination of the protein is never complete and residual kinase activity may support certain activities. To analyze the cellular effects of the acute deletion of Aurora B in cultured cells we took advantage of the conditional *Aurkb*(lox) allele. Primary *Aurkb*(lox/lox) MEFs were isolated from E14.5 embryos and cultured in complete medium. Importantly, Aurora C is not expressed in MEFs as it is not expressed in mid-gestation embryos nor in immortal fibroblasts derived from them as depicted previously (Figure 38). Confluent MEFs were infected with adenoviruses expressing either GFP (AdGFP) or the Cre recombinase (AdCre) as indicated in Figure 41a. Expression of Cre, but not GFP, results in an almost complete deletion of exons 2-6 [*Aurkb*(Δ) allele; Figure 41b].

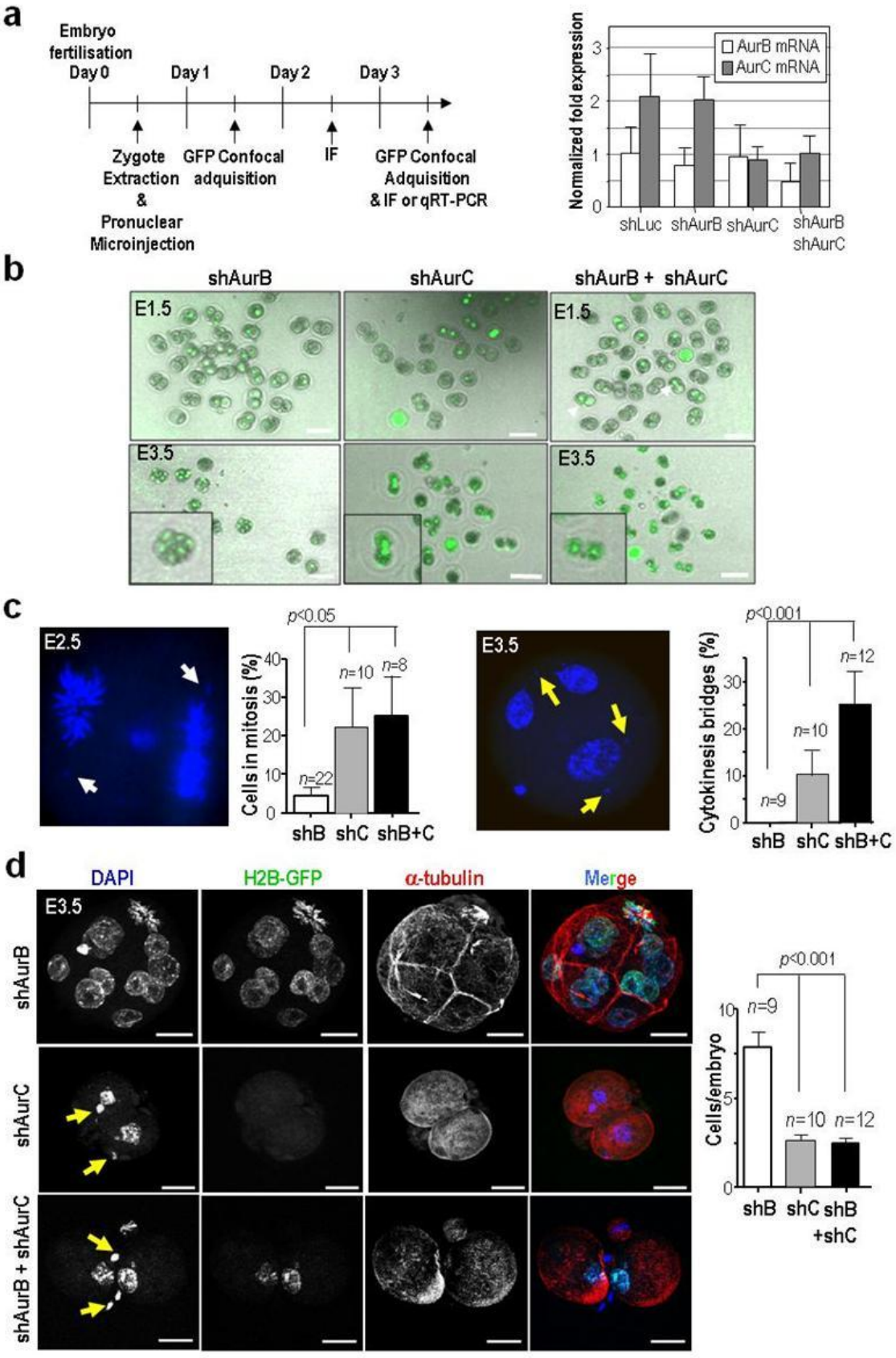
a
Embryo fertilisation
Day 0
Day 1
Day 2
Day 3
Zygote Extraction & Pronuclear Microinjection
GFP Confocal adquisition
IF
GFP Confocal Adquisition & IF or qRT-PCR
Normalized fold expression
AurB mRNA
AurC mRNA
shLuc
shAurB
shAurC
shAurB shAurC
b
shAurB
shAurC
shAurB + shAurC
E1.5
E3.5
c
E2.5
E3.5
p<0.05
Cells in mitosis (%)
n=22
n=10
n=8
shB
shC
shB+C
p<0.001
Cytokinesis bridges (%)
n=9
n=10
n=12
d
DAPI
H2B-GFP
α-tubulin
Merge
shAurB
shAurC
shAurB + shAurC
p<0.001
Cells/embryo
n=9
n=10
n=12
shB
shC
shB +shC

Figure 40 (previous page) Knock-down of Aurora C but not Aurora B results in cell cycle arrest in early embryonic development. **(a)** Schematic representation of the protocol followed for knock down of Aurora B and/or Aurora C in zygotes. Embryos were isolated at E0.5 and microinjected with vectors expressing shRNAs against luciferase (shLuc) and Aurora B (shAurB) and/or Aurora C (shAurC), as well as a plasmid expressing H2B-GFP. These embryos were analyzed at E1.5, E2.5 or E3.5 by fluorescent microscopy or quantitative (q)RT-PCR. qRT-PCR analysis shows a clear downregulation of Aurora C in these assays and a modest reduction of Aurora B. However, it is important to note that Aurora B mRNA levels are minimum at this stage and close to the background of mRNA detection in these assays. **(b)** Confocal microscopy in vivo images (combined bright field and green fluorescence) of embryos treated with these shRNAs indicating an arrest at the 2-4 cell stage in embryos treated with shAurC, shAurB-shAurC, but not shAurB or embryos treated with shRNAs against luciferase (not shown). Scale bars, 100 μm. **(c)** Knock down of Aurora C (shC) or Aurora B+Aurora C (shB+C) results in a significant increase in mitotic cells in most cases showing misaligned chromosomes (white arrows) by E2.5. By E3.5, most treated embryos display polyploid cells as well as cytokinesis bridges or micronuclei (arrows). These later abnormalities are not observed in shB cells or cells microinjected with shRNAs against luciferase (not shown). **(d)** Immunofluorescence analysis of these embryos by E3.5 shows mitotic aberrations and apoptotic figures after microinjection of shAurC or shAurB+AurC. These embryos arrested at the 2- or 4-cell stage whereas shAurB or shLuc embryos show an average of 8 cells per embryo. α-tubulin (α-tub) staining is in red, H2B-GFP signal in green and DAPI (DNA) in blue. Scale bars, 20 μm

5.1 Aurora B depletion in MEFs provokes a delay in the entry into S-phase

To analyze the initial phases of the cell cycle in *Aurkb*(lox/lox) MEFs, we first removed the serum during 2 days, re-plate the cells at low density and re-stimulate the cell cycle by adding 10%FBS (t=0). In primary MEFs, DNA replication starts at about 12 h with a peak in 18-20 h (Garcia-Higuera et al., 2008). Whereas infection of *Aurkb*(lox/lox) cells with AdGFP resulted in the normal pattern on DNA replication, AdCre-infected cells showed a dramatic delay (14% cells in S-phase versus 33% in AdGFP cells 18 h after serum stimulation) in the entry into S-phase (Figure 42a). This effect was also observed by analyzing DNA replication by a brief pulse (20 min) of BrdU. Six hours later, BrdU incorporation is reduced in AdGFP cells since these cells are exiting from S-phase. Expression of Cre however results in increased BrdU incorporation at 24 h (Figure 42b)

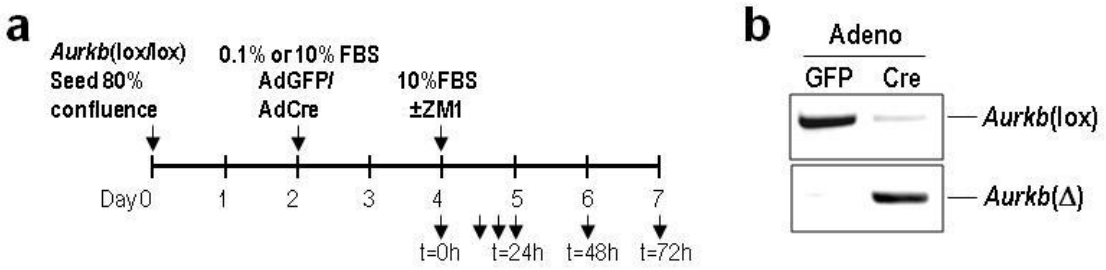

Figure 41. Acute deletion of Aurora B in MEFs. **(a)** Schematic representation of the protocol followed for acute deletion of Aurora B in MEFs. Primary (passage 2) *Aurkb*(lox/lox) MEFs were seeded at 80% confluence and allowed to form a completely confluent culture during 2 days. These cells were then cultured in 0.1% FBS (for G1/S assays) or 10% FBS (for analysis of mitosis) and infected with adenoviruses expressing GFP (AdGFP) or the Cre recombinase (AdCre). Two days after the infection, cells were seeded in new plates at low confluence in the presence of 10% FBS to induce entry into the cell cycle. The Aurora B/C inhibitor ZM1 was also added at this point to non-infected cells. **(b)** Expression of Cre, but not GFP, results in an efficient deletion of exons 2-6 (see Figure 18) as detected by PCR amplification of the *Aurkb*(lox) conditional allele or the resulting *Aurkb*(Δ) null allele.

suggesting that the absence of Aurora B provokes a delay in the entry into S-phase, rather than a complete impairment in DNA replication. Importantly, these phenotypes can be recapitulated by treating non-infected *Aurkb*(lox/lox) cells with the Aurora B/C inhibitor ZM1 at the time they are seeded at low density (t=0). ZM1-treated cells also display a significant delay in S-phase entry and BrdU incorporation similar to that observed in *Aurkb*(Δ/Δ) cells (Figure 42a,b).

5.2 Aurora B deficiency interfere with G1-S progression in vivo after partial hepatectomy

To test whether these defects in S-phase could also be observed in vivo, we induced cell cycle entry in adult *Aurkb*(+/–) mice by submitting *Aurkb*(+/+) and *Aurkb*(+/–) mice to hepatectomy assays, a model commonly used for synchronized G1/S progression in vivo. After excision of 2/3 of the liver, hepatocytes usually take 1.5-2 days to synthesize new DNA in a highly synchronized manner (Mitchell and Willenbring, 2008). We tested BrdU incorporation 4 h, 12 h, 48 h and 6 days after

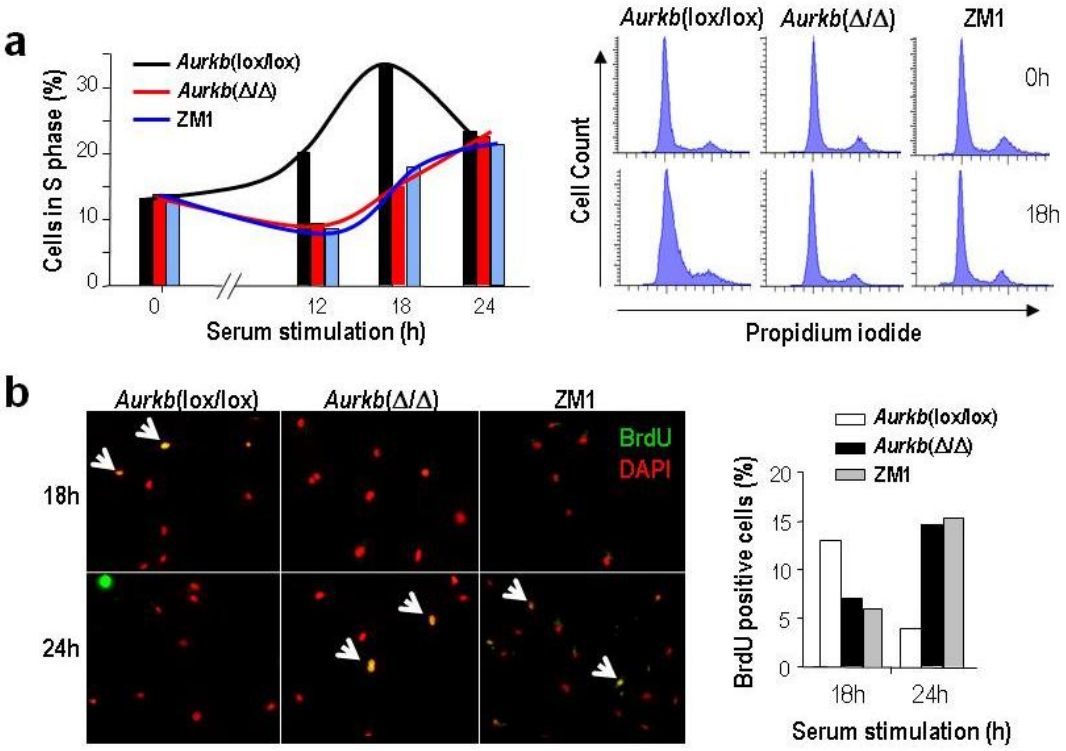

Figure 42. Aurora B is required for the G1/S transition in MEFs. **(a)** Progression into S-phase at different time points after addition of serum. Bar graph quantification of *Aurkb*(lox/lox) MEFs infected with AdGFP or AdCre or treated with ZM1 and analyzed by propidium iodide staining showing a dramatic delay in S-phase entry upon the genetic ablation or chemical inactivation of Aurora B. Representative FACS profiles of these samples at time serum was added (t=0) or 18 h after mitogenic stimulation. **(b)** Incorporation of BrdU was also tested by treating these cultures with a short (20 min) pulse of BrdU before harvesting the cells. BrdU incorporation was analyzed by immunofluorescence with specific antibodies (green). DAPI (DNA) is shown in red. Bar graph quantification of percentage of BrdU positive cells revealing a delay in entering into S phase in *Aurkb*(lox/lox) MEFs infected with AdCre or treated with ZM1 and not in control Ad-GFP infected cells.

partial hepatectomy. As depicted in Figure 43a, no BrdU incorporation is observed before 12 h. A clear peak in DNA synthesis (6.5% BrdU-positive cells) is observed in *Aurkb*(+/+) 48 h after partial hepatectomy. *Aurkb*(+/–) mice, however, do not enter S-phase during these first two days and only display a reduced (0.5%) number of BrdU-positive cells. Similar results are observed by quantifying Ki67 signal or mitotic figures in these samples (Figure 43b). During liver regeneration we observed a similar decrease in binucleated hepatocytes both in *Aurkb*(+/+) and *Aurkb*(+/–) mice indicating no further problems in cell division in these cells despite the initial problems in entering into S phase (Figure 43c). Indeed, heterozygous mice regenerate a significant percentage of dissected liver in 6 days although these mice frequently display abnormal tissue structure and necrotic areas suggesting an inefficient response to these stress conditions (Figure 43c,d).

5.3 Aurora B may regulate G1-S transition by modulation of the mTOR pathway or p21 levels

Although a role for Aurora B in G1/S progression has not been clearly established, some recent evidences suggest that Aurora B is able to modulate the mTOR pathway in T lymphocytes (Song et al., 2007) and may directly phosphorylate the retinoblastoma protein (pRb) at Ser780 (Nair et al., 2009). In addition, we found that Survivin deletion in cell lines provokes G1 arrest accompanied by induction of $p21^{Cip1}$, a p53 effector of cell cycle arrest (Yang et al., 2004). We therefore tested phosphorylation of the mTOR substrate p70S6 kinase (p70S6K) as well as phosphorylation of pRb and induction of $p21^{Cip1}$ either in Aurora B-depleted MEFs and in *Aurkb*(+/–) livers after hepatectomy.

5.3.1 In Aurora B-depleted MEFs

Despite the significant defects in the G1/S progression of Aurora B-null cells, we detected minor differences in the previous markers. Specifically, the p70S6K-T380 phospho signal is decreased in Aurora B deficient cells 10 h after entry into the cell cycle; and $p21^{Cip1}$ cell cycle inhibitor levels are slightly increased in the cell cycle, soon after cell cycle entry (Figure 44a).

5.3.2 In Aurkb(+/–) livers after hepatectomy

We also tested markers of the activation of the mTOR, pRb or p53 pathways at shorter times after hepatectomy. As represented in Figure 44b, phosphorylation of p70S6K is decreased in *Aurkb*(+/–) mice 4 h [a peak for this critical phosphorylation in this system; (Haga et al., 2009)] after partial hepatectomy. No clear differences in pRb phosphorylation are observed whereas $p21^{Cip1}$ is also

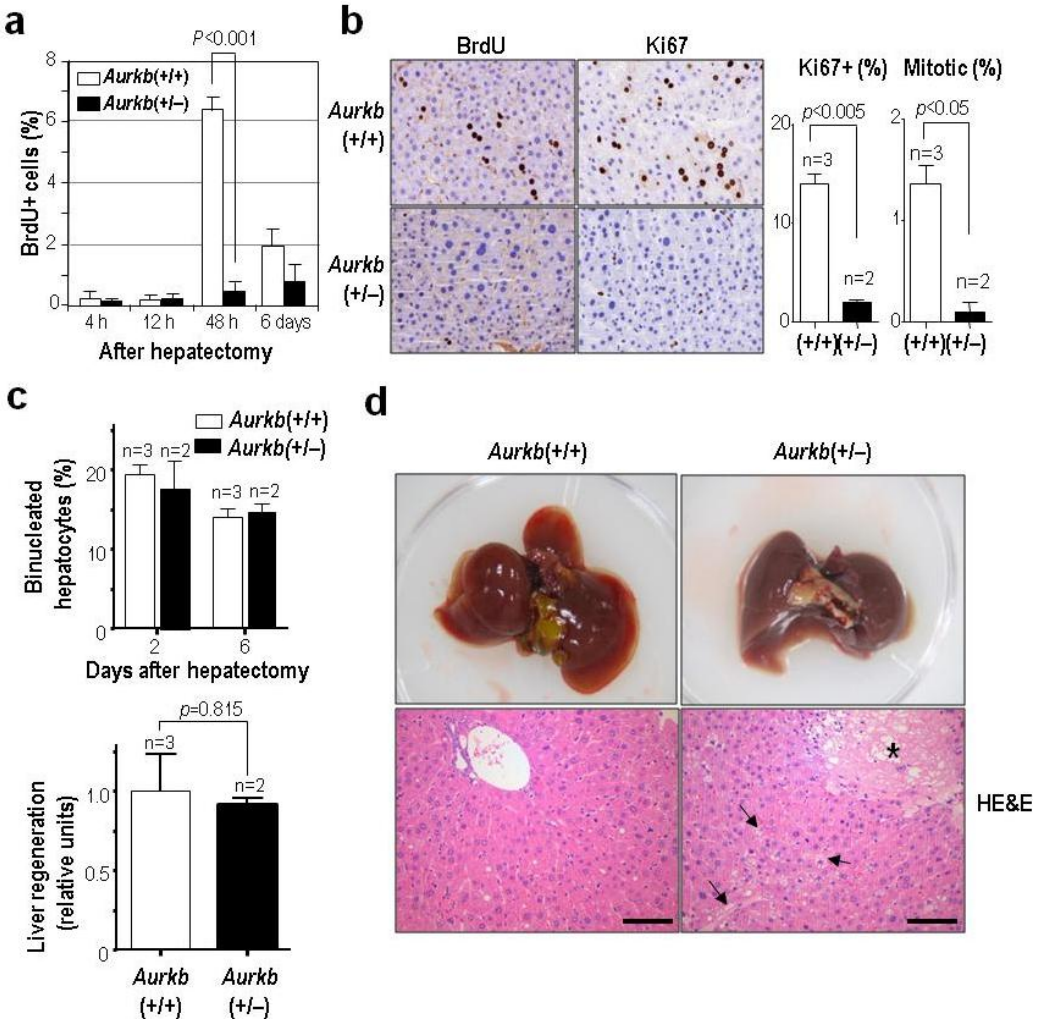

Figure 43. Aurora B is required for the G1/S transition in vivo after partial hepatectomy. **(a)** BrdU incorporation in vivo after 2/3 partial hepatectomy in *Aurkb*(+/+) n=3 and *Aurkb*(+/–) mice n=2. The percentage of BrdU-positive cells (as detected by immunohistochemistry) is shown 4, 12 and 48 h as well as 6 days after hepatectomy. Incorporation of BrdU is highly reduced by 48 h in Aurora B-mutant mice. **(b)** Representative images of proliferation markers (BrdU incorporation and Ki67 levels) 48 h after hepatectomy. Quantification of Ki67 or mitotic figures in these samples also indicates a significant reduction in cell cycle entry and progression in *Aurkb*(+/–) mice. (c,d) Normal recovery of liver mass after partial-hepatectomy in *Aurkb*(+/–) mice. **(c)** Bar graphs quantifications of percentage of binucleated hepatocytes 2 and 6 days after hepatectomy and final liver regeneration in *Aurkb*(+/+) and *Aurkb*(+/–) mice. Similar reduction is observed in binucleated hepatocytes from *Aurkb*(+/+) and *Aurkb*(+/–) mice and equivalent potential of the livers to recover its mass. **(d)** Gross appearance of regenerated livers 6 days after hepatectomy and HE&E stained liver sections revealing almost normal recovery of *Aurkb*(+/–) livers but suggesting inefficient responses to stress conditions due to the presence of necrotic areas (asterisk) and abnormal tissue structures (arrows) in *Aurkb*(+/–) livers. Scale bars, 100 μm

partially upregulated in *Aurkb*(+/–) livers. On the other hand, phosphorylation of p70S6K peaks at 12 h in these *Aurkb*(+/–) mice suggesting a delay in the activation of the mTOR pathway in these liver cells. All together, these results indicate that deficiency in Aurora B may interfere with G1/S progression at least partially by modulating the mTOR pathway or the levels of the p53 effector $p21^{Cip1}$ in different cell types.

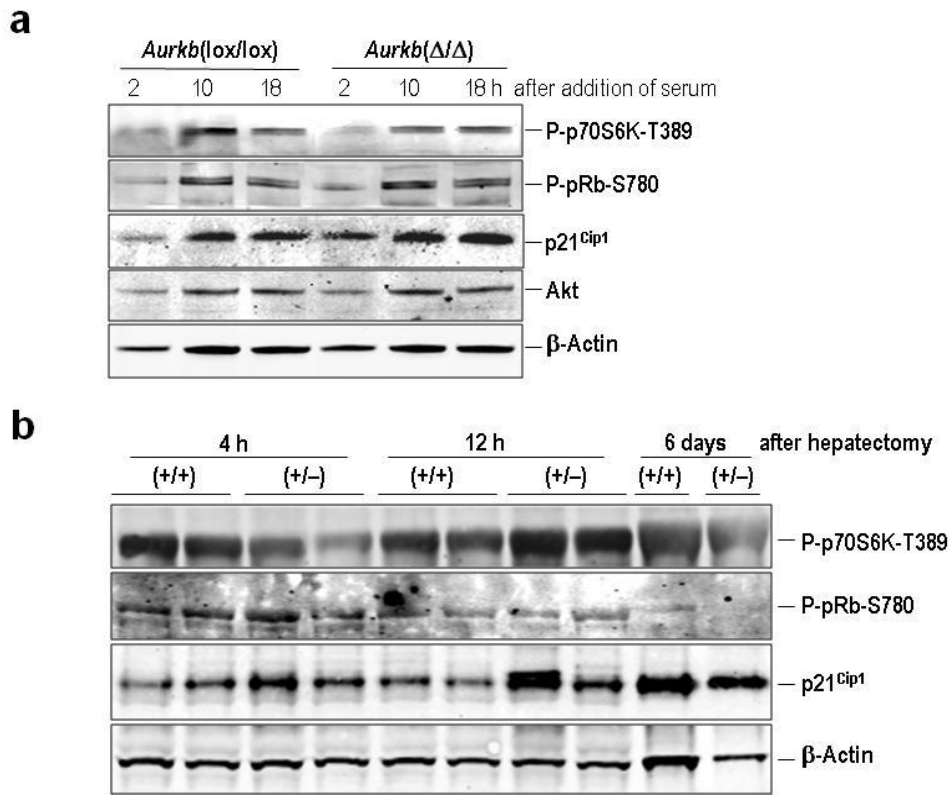

Figure 44. Aurora B may interfere with G1/S progression by modulating mTOR pathway or p21Cip1 levels. **(a)** Immunodetection of phospho-specific markers for the mTOR (phospho-p70S6K at Thr389) or pRB (phospo-pRb at Ser780) pathways 2, 10 or 18 h after stimulation with serum. The expression of the p53 effector p21Cip1 is slightly increased in *Aurkb*(Δ/Δ) cells. Immunodetection of Akt or β-actin was used as a loading control. **(b)** Immunodetection of phospho-p70S6K, phospo-pRb and p21Cip1 levels in *Aurkb*(+/+) and *Aurkb*(+/–) livers after different time points after partial hepatectomy. Immunodetection of β-actin was used as a loading control.

5.4 Depletion of Aurora B in MEFs results in multiple nuclei, micronuclei and apoptosis

In spite of the delay in S-phase entry, Aurora B-deficient MEFs continue cycling and are able to undergo mitosis. To explore new possible roles of Aurora B during the cell cycle, we performed acute deletion of Aurora B in *Aurkb*(lox/lox) cells, following the same protocol as before (Figure 41), and we analysed this cell population after two or three rounds of division (48 and 72h after infection). Note that doubling cycle is about 24h in MEFs. Seventy-two hours after expression of the Cre recombinase, Aurora B-deficient MEFs accumulate as 4N or >4N DNA content cells as depicted in Figure 45a. Examination of these cultures at 48 h by immunofluorescence indicates an efficient elimination of Aurora B at the protein level in Cre-infected cells (Figure 45b). After two rounds of division, lack of Aurora B is accompanied by a massive accumulation of abnormalities including multiple nuclei, as well as micronuclei and apoptotic figures (Figure 45c,d). About 40% of the culture accumulates as abnormal interphase cells including multinucleated cells, cells with micronuclei and apoptotic figures (versus 13% of AdGFP cells showing these phenotypes; Figure

45c). These defects are likely a consequence of abnormal cell divisions and, in fact, the few cytokinesis figures observed in AdCre-infected cells frequently display chromosomal bridges suggesting abnormal segregation of chromosomes during mitosis (Figure 45d).

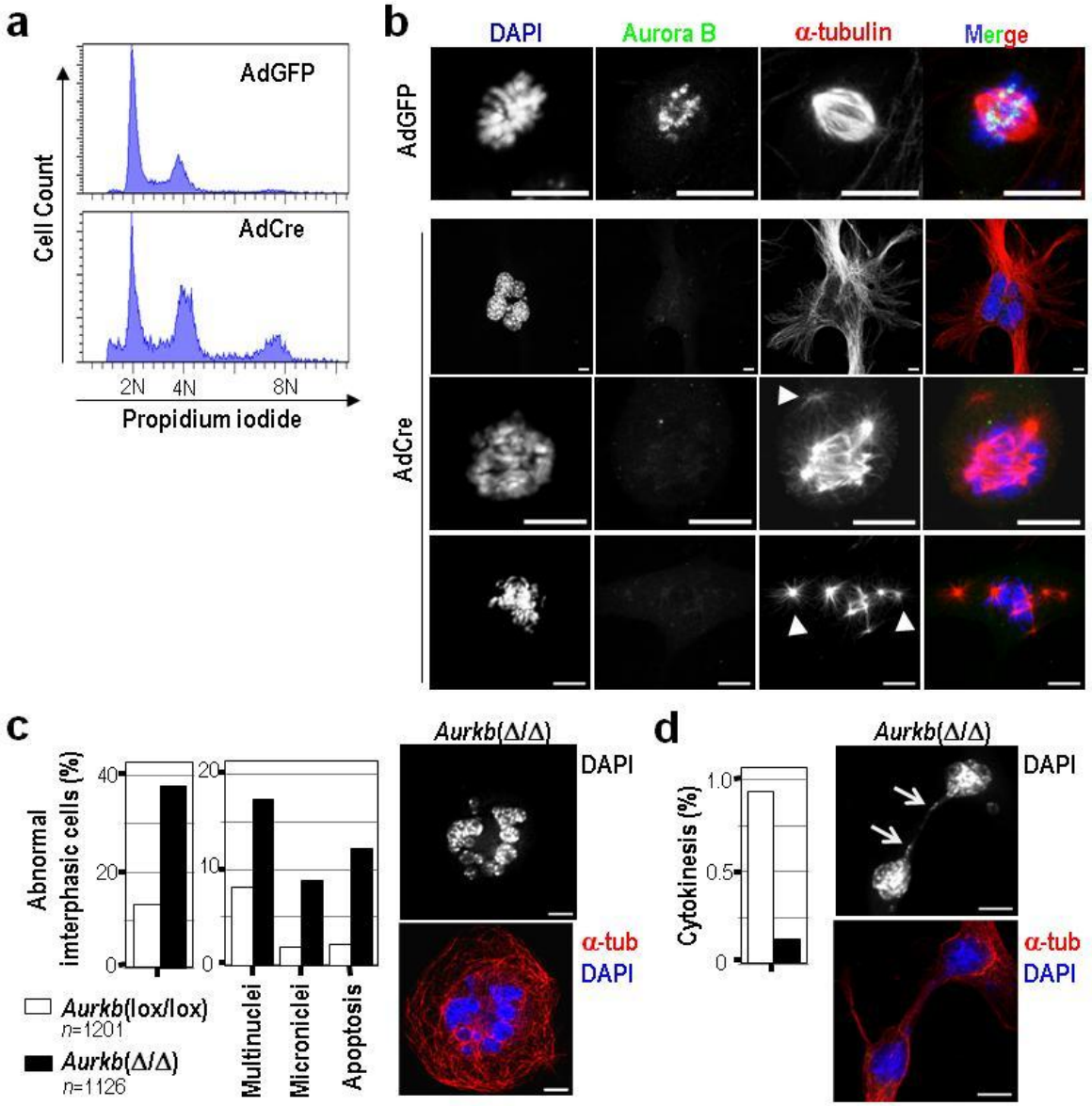

Figure 45. Acute deletion of Aurora B results in polyploidy and cell death. **(a)** Infection with AdCre in primary MEFs results in an accumulation of 4N and >4N cells 72 after the exit from quiescence as detected by flow cytometry. **(b)** Examination of these cultures by immunofluorescence at 48 h indicates efficient depletion of Aurora B (green signal) in AdCre-infected cells. These mutant cells display aberrant morphologies as indentified by staining with α-tubulin (α-tub) antibodies (red) and DAPI (DNA) staining (blue). **(c)** *Aurkb*(Δ/Δ) primary MEFs display an accumulation of abnormal interphase cells (bar graphs) including cells with several nuclei or micronucleai (see picture) and apoptotic cells. n indicates the number of cells counted for each genotype in (c) and (d). **(d)** In addition, there is a dramatic reduction in cytokinesis figures suggesting a defect in the later stages of cell division. The remaining cytokinesis figures in *Aurkb*(Δ/Δ) cells are usally abnormal with long chromosomal bridges (arrows) between the two daughter cells. Scale bars, 10 μm

5.5 Aurora B-deficient MEFs accumulate in prophase / prometaphase with misaligned chromosomes and spindle aberrations

Whereas most Aurora B-deficient cells accumulate in an abnormal 4N or >4N interphase stage with decondensed chromosomes, only 1.2% of these cells are in mitosis compared to 2.8% in control cultures (Figure 46a) suggesting a premature exit from mitosis in AdCre-infected cells. In fact, in contrast to normal mitotic distribution of control cells, Aurora B-deficient cells are characterized by an accumulation in P and PM with very few cells in metaphase or post-metaphase stages in agreement with the decreased cytokinesis observed in these cells (Figure 45d and 46a). Most of these mitotic figures are abnormal and present misaligned chromosomes and spindle aberrations. About 82% of mitotic figures display spindle aberrations in the absence of Aurora B (Figure 46b). These aberrations include monopolar (12% mitotic cells) and multipolar (50% mitotic cells) spindles in the majority of the cases accompanied by misaligned chromosomes. A detailed observation of the spindle structure detects additional abnormalities in microtubule behaviour in mitotic *Aurkb*(Δ/Δ) cells. About 25% of these Aurora B-deficient cells display a novel phenotype that consists on an accumulation of α-tubulin asters that are or are not connected to chromosomes ('multiaster' phenotype; see arrowheads in Figure 45b and 46b).

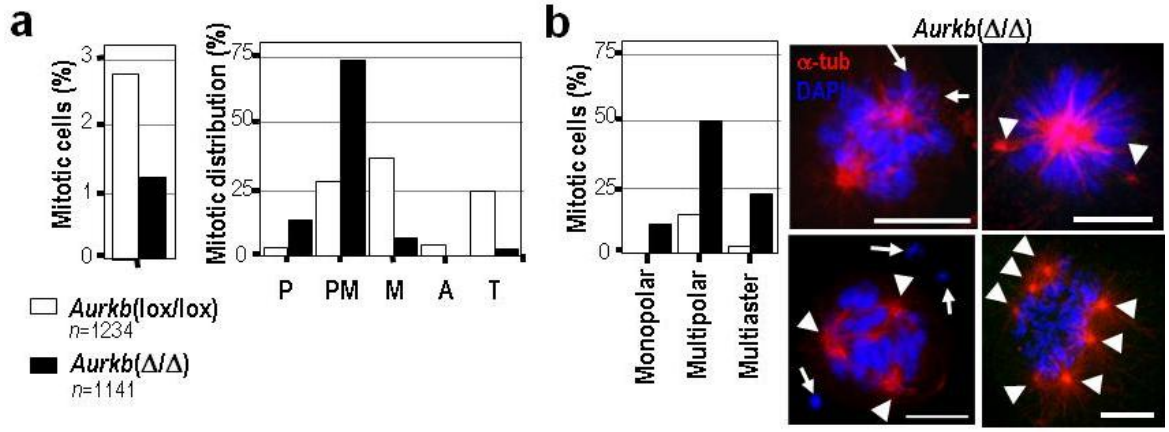

Figure 46. Aurora B-depleted MEFs accumulate in P/PM with chromosome misalignment and spindle aberrations. **(a)** Bar graphs quantification of mitotic index and mitotic distribution. Ablation of Aurora B results in a decrease in the total percentage of mitotic cells (condensed chromosomes) in these cultures. Most *Aurkb*(Δ/Δ) mitotic cells accumulate in prophase (P) or prometaphase (PM) with a dramatic reduction in metaphase (M), anaphase (A) or telophase (T) stages. **(b)** Immunoflorescence images showing that most P and PM are abnormal with abundant misaligned chromosomes (arrows). In addition, *Aurkb*(Δ/Δ) cells display severe spindle abnormalities as quantified in the bar graph. These cells show a dramatic increase of monopolar and multipolar spindles accompanied by isolated α-tubulin spots (multiaster phenotype; arrowheads) that in some cases display a robust nucleation of microtubules (see bottom-right panel). α-tubulin (α-tub) staining is in red and DAPI (DNA) in blue. Scale bars, 10 μm

5.6 Depletion of Aurora B in MEFs leads to accumulation of γ-tubulin asters and/or supernumerary MTOCs

The 'multiaster' phenotype is characterized by the presence of asters that contain an increase density of astral microtubules that are not observed in the spindle poles of Ad-GFP-infected cells. Whereas *Aurkb*(lox/lox) MEFs display two clear γ-tubulin-positive microtubule-organizing centers (MTOC) during mitosis, the number of γ-tubulin MTOCs can reach up to 12-13 in *Aurkb*(Δ/Δ) cells (Figure 47a). The multiple MTOCs may also explain monopolar spindles as these figures frequently contain multiple γ-tubulin spots grouped around the single pole (Figure 47b). In many cases, the supernumerary MTOCs are not connected to the chromosomes and, yet, they display a significant ability to nucleate microtubules. Since these MTOCs are observed 48 h after entry into the cell cycle, they are likely not a consequence of accumulating multiple cell divisions during this time. In fact, we counted chromosomes using ACA as a centromeric marker and all the analyzed cells with ≥12 MTOCs (n=6) were either 4N or 8N (Figure 47c), suggesting the presence of diploid or tetraploid cells but not a further increase in the ploidy of these cells.

5.7 Aurora B-deficient MEFs show a weak mitotic checkpoint that results defective after spindle partition

To explain whether the accelerated mitotic exit observed in *Aurkb*(Δ/Δ) cells is a consequence of having a deficient SAC, we checked Mad2 kinetochore localization 48h after expression of the Cre recombinase. Whereas Mad2 signal is clearly observed in PM figures of AdGFP-infected cells, we were not able to find detectable Mad2 signal in any of these abnormal PM in Aurora B-deficient cells (Figure 48a) thus suggesting that, despite these abnormalities, the SAC is inactive. We next tested whether spindle abnormalities were present in cyclin B1-positive or negative cells. Cyclin B1 shows a diffuse localization in mitotic *Aurkb*(lox/lox) cells before metaphase but it is degraded by the APC/C in the metaphase-to-anaphase transition, once the SAC is extinguished. As depicted in Figure 48b, cyclin B1 is also present in some PM *Aurkb*(Δ/Δ) cells. These cyclin B1-positive cells usually display a bipolar or pseudo-bipolar spindle with misaligned chromosomes. In some of these poles, γ-tubulin is normally concentrated. However, many other cyclin B1-positive cells display an unfocused distribution of γ-tubulin or fragmented poles with a few γ-tubulin spots near-by. Cyclin B1-negative cells on the other hand, display multiple γ-tubulin spots distributed all over the cell including distant areas from chromosomes (Figure 48b).

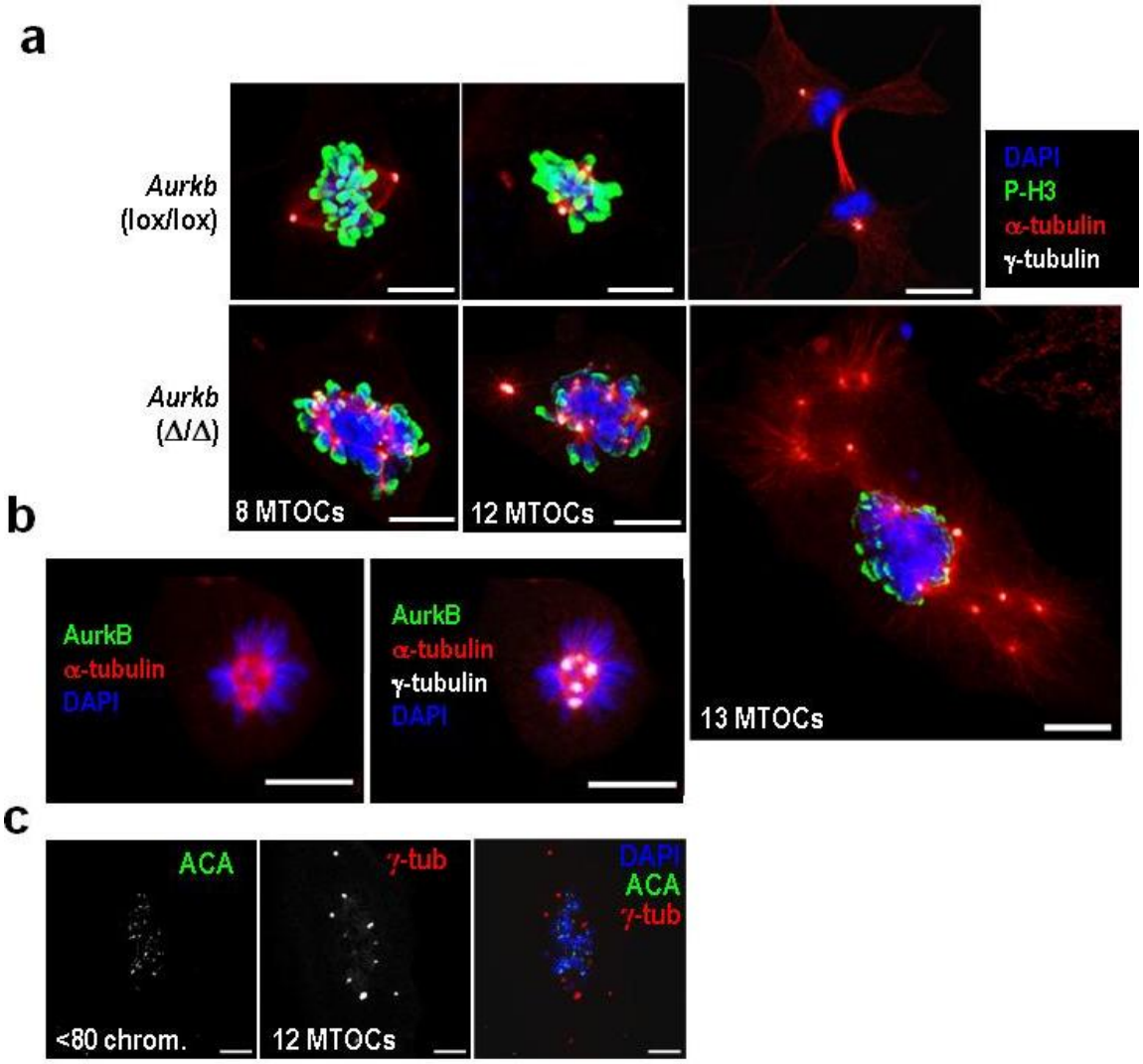

Figure 47. Ablation of Aurora B results in the formation of multiple γ-tubulin-positive microtubule organizing centers (MTOC) and aberrant astral microtubule nucleation. **(a)** Immunofluorescence detection of γ-tubulin (white) in *Aurkb*(Δ/Δ) cells indicates the presence of multiple γ-tubulin spots that are or are not part of the spindle structure. This γ-tubulin material is accompanied by dense microtubule asters and we refer to it as microtubule organizing center (MTOC). Phosphorylation of histone H3 (P-H3 in green) is reduced but not absent in Aurora B-deficient MEFs similar to that observed in ZM1-treated embryos (see Figure 30). **(b)** Monopolar spindles in Aurora B-deficient cells are usually formed by multiple γ-tubulin spots. Aurora B (*Aurkb*) staining is in green. **(c)** Parallel examination of the number of MTOCs using γ-tubulin (red) and the number of chromosomes using ACA (green) revealing a nearly tetraploid cell with 12 MTOCs. α-tubulin (α-tub) staining is in red and DAPI (DNA) in blue. Scale bars, 10 μm

Altogether, these results indicate that lack of Aurora B results in chromosome misalignment during a transient cyclin B1-positive PM and a concomitant fragmentation of spindle poles. After spindle partition, cyclin B1 dissapear and Mad2 is delocalized from the kinetochores, resulting in a defective SAC, and the multiple γ-tubulin-positive MTOCs continue to nucleate microtubules. These cells subsequently exit from mitosis directly from these aberrant PM to form cells with several nuclei or micronuclei.

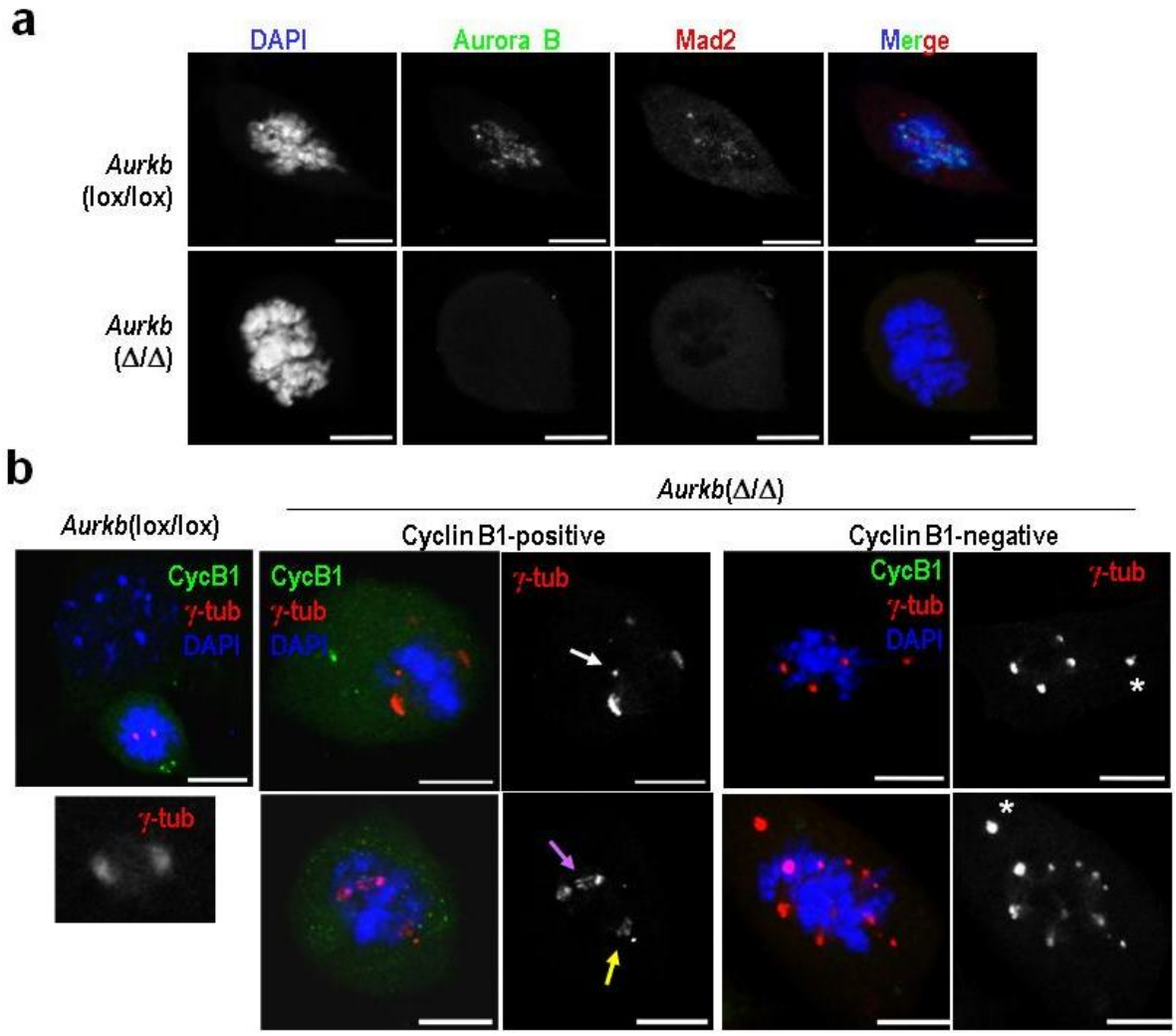

Figure 48. Fragmentation of spindle poles in Aurora B-deficient MEFs leads to disappearance of Cyclin B1 and to a defective SAC. Immunofluorescence detection of SAC markers Mad2 and Cyclin B1 (CycB1) in *Aurkb*(lox/lox) and *Aurkb*(Δ/Δ) MEFs. **(a)** Whereas control cells in PM display Mad2 (red) staining at the kinetochores, this SAC marker is not detected in PM figures deficient in Aurora B. **(b)** The number of γ-tubulin (red) spots increases from cyclin B1-positive (green) to cyclin B1-negative cells. *Aurkb*(lox/lox) cells display a clear bipolar spindle with γ-tubulin spots in the poles. Some *Aurkb*(Δ/Δ) cells are positive for Cyclin B1 staining. These cells usually display aberrant PM figures with bipolar spindles (Cyclin B1-positive; top panels) and two focused spots of γ-tubulin. Occasionally, additional small γ-tubulin spots is observed (white arrow). Other Cyclin B1-positive cells (bottom panels) display pseudo-bipolar spindles in which the γ-tubulin spots are fragmented (yellow arrow) or seem to disaggregate (pink arrow). In Cyclin B1-negative cells, multiple γ-tubulin spots are observed that are either forming part of a multipolar spindle or completely separated (asterisks) from the multipolar spindle. In the images, 5 (top panels) or 12 (bottom panels) MTOCs are observed in Cyclin B1-negative cells. DAPI (DNA) staining is in blue. Scale bars, 10 μm.

Discussion

1. Regulation of Aurora B by SUMOylation

In budding yeast, over 500 potential SUMOylation targets have been identified through systematic screens (Hannich et al., 2005; Panse et al., 2004; Wohlschlegel et al., 2004; Wykoff and O'Shea, 2005). Global mapping of the SUMO network by protein-protein interactions and genetic networks has linked SUMOylation to fifteen different broad biological processes. One of these processes is chromosome segregation and cell cycle (Makhnevych et al., 2009). In the last years, the SUMO pathway has been implicated in several aspects of mitosis, including chromosome structure, cell cycle progression, kinetochore function and cytokinesis (Dasso, 2008). Global inhibition of SUMOylation in mammalian cells has been reported to cause cells to arrest in mitosis (Zhang et al., 2008b) revealing the importance of this post-translational modification for mitotic progression. Indeed, the CPC has been intensively proposed to be regulated by SUMOylation. In this line, the CPC members Incenp and Survivin in yeast (Sli15 and Bir1, respectively) have been proposed to be modified by SUMO (Montpetit et al., 2006; Wohlschlegel et al., 2004). Similarly, Borealin has been shown to be modified by SUMO-2/-3 in human cells (Klein et al., 2009). However, the functional impact of SUMOylation on CPC activity remains to be elucidated.

In this work, we have identified and analyzed the consequences of SUMO modification of Aurora B, an essential regulator of mitosis. By the use of bioinformatics tools we found a consensus sequence for SUMO modification in Aurora B, which is highly conserved among species and in the other members of the Aurora family. Our data indicate that mouse Aurora B is susceptible to be SUMOylated *in vivo* by the three SUMO isoforms at lysine 207 (K207). Recent work has described that Aurora B was not significantly modified by SUMO-1 *in vitro* and that it is not able to interact with E2 SUMO-conjugating enzyme Ubc9 or SUMO isoforms in yeast two-hybrid assays (Klein et al., 2009). One explanation to these apparent contradictory results is that Aurora B conformation *in vivo* can be dramatically distinct than *in vitro*. Indeed, using our *in vivo* approach, Aurora B seems to be modified by SUMO when immunoprecipated from cell extracts where the CPC integrity is maintained. Moreover, crystalization of an active Aurora B protein was only successful in complex with IN-box segment of Incenp (Sessa, 2005). Using this crystal structure we have simulated the interaction between Aurora B and SUMO-2 in collaboration with Guillermo Montoya (CNIO) (Figure 49). The simulation showed that Aurora B SUMOylation is

possible and that Incenp may be necessary for it. Therefore the protein-protein interactions among the CPC members seem to be necessary to efficiently SUMOylate Aurora B.

An increasing number of works have associated SUMOylation and mitosis regulation. Borealin, a CPC member, is dynamically modified by SUMO-2/-3 in a conjugation-deconjugation cycle catalyze by the E3 SUMO-ligase RanBP2 and the SUMO-protease SENP3 (Klein et al., 2009). According to observations in *Xenopus* egg extracts and human cells, SUMO-2/-3 is found at centromeres and chromatin during prometaphase/metaphase, whereas SUMO-1 localizes to the mitotic spindle and the spindle midzone at same stages (Ayaydin and Dasso, 2004; Azuma and Dasso, 2002; Zhang et al., 2008b). These data suggest that centromeric proteins, such as Aurora B, would be preferentially modified by SUMO-2/-3. In addition, RanBP2 associates with Topoisomerase II, a known Aurora B substrate, and the CPC in mitosis and is essential for Borealin SUMOylation in vivo (Dawlaty et al., 2008; Klein et al., 2009). Thus, it is possible that RanBP2 may also serve as the E3 SUMO-ligase for Aurora B modification. Redarding SUMO deconjugation, there are three SUMO-proteases SENP-2, SENP-3 and SENP-5 that have been implicated in mitotic progression. Overexpression of SENP-2 results in global inhibition of SUMOylation during mitosis and persistent activation of the spindle checkpoint but does not affect the localization of Aurora B and other centromere-associated proteins (Zhang et al., 2008b). SENP-3 acts preferentially toward SUMO-2/-3 conjugates and catalyzes the removal of SUMO peptides from Borealin both *in vivo* and *in vitro* (Klein et al., 2009). However, its depletion does not interfere with CPC targeting or activity arguing against a deregulation of Aurora B. Finally, depletion of SENP-5 causes cytokinesis defects but does not disturb CPC localization or function (Di Bacco et al., 2006; Klein et al., 2009). Regarding Aurora B, further studies will be necessary to determine the SUMO isoform, ligase and protease that specifically participate in the control of Aurora B modification.

But, at the molecular level, how is modulating SUMO Aurora B function? SUMOylation alters protein surfaces and thereby positively or negatively influences interactions with other macromolecules (Geiss-Friedlander and Melchior, 2007). Thus, SUMOylation can interfere with or promote protein-protein interactions and provoke conformational changes in the modified target. The consequences of these molecular changes may influence *in vivo* any single aspect of a target protein, including *a*) localization, *b*) stability or *c*) activity. As shown in this work, SUMOylation of Aurora B seems to regulate the dynamics of Aurora B **localization** at the centromeres. Rescue experiments performed with a SUMO-deficient form (K207R) of Aurora B demonstrates that both Aurora B and Incenp fail to concentrate in inner centromeres during prometaphase/metaphase. This result suggests that lack of Aurora B SUMOylation affects the whole CPC localization. Indeed, the

CPC members are physically and functionally interpendent and perturbation of any member of the complex may delocalize the others (Gassmann et al., 2004; Jeyaprakash et al., 2007). Other examples of mitotic proteins whose localization at kinetochores/centromeres is regulated by SUMO are the kinesin CENP-E and the GTPase-activating protein RanGAP1 (Joseph et al., 2002; Zhang et al., 2008b).

Although we have not explored the hypothesis that SUMOylation of Aurora B might be able to regulate its **stability**, it is possible that this process take place through the recruitment of E3 ubiquitin-ligases (Geoffroy and Hay, 2009). Recent studies have shown that ubiquitination of Aurora B by the Cul3-Klhl9/Klhl13 E3 ligase complex during early mitosis might serve as a signal for its removal from chromosomes since in the absence of Cul3-Klhl9/Klhl13 activity, Aurora B is not ubiquitinated and accumulates on chromosomes (Sumara et al., 2007). Due to the similar phenotypes observed upon defective SUMOylation and failed Cul3-Klhl9/Klhl13 ubiquitination, one can think that both processes may be linked together. An attractive possibility is that CPC SUMOylation may act as a signal to recruit E3 ubiquitin-ligases directing the ubiquitination of the CPC members themselves and possibly other centromere proteins. Indeed, the fission yeast Aurora kinase (Ark1p) interacts with two RING-finger proteins that possess SUMO interacting motifs (SIMs), called Rfp1p and Rfp2p (Sun et al., 2007). These E3 ubiquitin-ligases recognize SUMOylated proteins and heterodimerize with Slx8, another RING-finger protein, to form a functional ubiquitin ligase (Sun et al., 2007; Uzunova et al., 2007). Therefore, it is possible that in mammals SUMOylation of Aurora B may facilitate the formation of a functional Cul3-Klhl9/Klhl13 ligase complex during mitosis. Indeed, we have found three predicted SIMs in each coadaptor, Klhl9 and Klhl13, and one additional SIM in the Cul3-ligase that are conserved in human and mouse in all cases (data not shown). Future experiments are necessary to test and validate this hypothesis.

SUMOylation of Aurora B may also modulate kinase **activity**. Surprinsingly, rescue experiments with a kinase-dead mutant D205A results in phenotypes that are similar to the ones obtained for the K207R Aurora B mutant. A detailed analysis of Aurora B crystal structure reveals that the mutated D205 residue is only two aminoacids upstream the SUMO-binding site (K207) and that both residues share the same structural loop (Figure 49b). It is, therefore, possible that D205A can behave as a kinase-dead mutant and additionally as a partial SUMO-dead mutant. It has been recently confirmed that Aurora B substrates phosphorylation depends on the distance of the substrate from the kinase at the inner centromere (Liu et al., 2009). This regulation, in turn, has probed to be an efficient way to correct improper microtubule-kinetochore attachments (Andrews, 2004; Knowlton et al., 2006). Here, we show that a SUMO-deficient Aurora B form is more active

than its wild-type counterpart *in vitro* but fails to phosphorylate CENP-A *in vivo*. This result can be explained by the fact that centromeric mislocalization of Aurora B can impede the encounter of the kinase with its substrates failing to phosphorylate them *in vivo* but obviously not *in vitro*. The *in vitro* kinase assay performed with immunoprecipated proteins is really interesting as it can explain many of the phenotypes observed with the different mutants. Based on our kinase assays, the SUMO-deficient form (K207R) is probably a hyperactive mutant. This result is certainly surprising given that, so far, no hyperactive mutants have been described for Aurora B, (T232E is not a hyperactive mutant, (Yasui, 2004). A detailed examination of the crystal structure reveals that SUMO binding may block the entrance of ATP to the kinase and/or the transference of phosphate groups to a given substrate (Figure 49a). Therefore, it is reasonable to think that lack of SUMOylation facilitates ATP binding and transfer. This increase in the kinase activity plus the delocalization of the kinase during early mitosis can account for the cellular defects and the impaired viability observed upon transient and stable expression of a SUMO-deficient form. On the other hand, both kinase-dead mutants (K111M and D205A) behave in distinct manner. This is probably due to the different grade of inhibition obtained with each mutation. Hence, K111M is a partial kinase-dead mutant and this residual activity does not compromise cell viability. However, D205A mutation renders almost complete inactivation of the kinase leading to high rates of polyploidy when overexpressed and compromising cell viability.

Importantly, Aurora B activity also correlates with its ability to promote tumorigenesis by enhancing oncogenic Ras transformation. Thus, our results show that an inactive Aurora B form (D205A) poorly cooperates with H-Ras as suggested previously (Kanda et al., 2005); whereas the possibly hyperactive Aurora B form (K207R) was able to increase H-Ras oncogenic potential significantly more than its wild-type counterpart. This link between SUMOylation and kinase activity may have relevant implications in tumorogenesis that deserve further research.

2. New models for studying Aurora B function and therapeutic value in vivo

Genetically modified mouse models are a highly valuable tool that permits a better understanding of the function of a particular gene in an organism. They constitute one of the best model systems for cancer investigations (Frese and Tuveson, 2007). Despite the diverse technical approaches used, genetically modified mouse models can be classified as either transgenic or endogenous. The first ones consist on mutant mice that express genes in a non-physiological manner owing to ectopic promoter and enhancer elements. In its original and simplest form, transgenic mice are generated by pronuclear injection of cDNA constructs that contain promoter elements designed to restrict

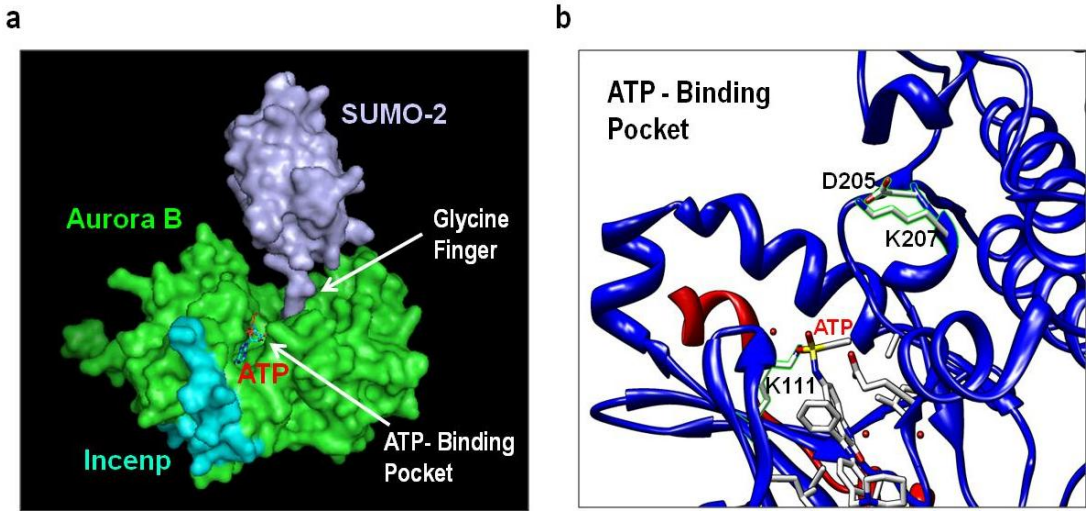

Figure 49. Modeling Aurora B-SUMO-2 covalent interaction. **(a)** Crystal structures of human SUMO-2 (Reverter and Lima, 2006; Sessa, 2005) and xenopus Aurora B in complex with IN-box segment of Incenp (Sessa, 2005) were used to simulate the interaction of both molecules. SUMO-2 covalently binds to mouse K207 residue (K218 in xenopus crystal structure) of Aurora B kinase domain through a finger composed by two glycine residues. By this interaction SUMOylation does not affect the binding of Aurora B partner and activator Incenp, but may disturb the transference of phosphate groups to its sustrates. **(b)** Detail of the ATP-binding pocket showing the localization of K111, D205 and K207 residues (K122, D216 and K218 in xenopus, respectively) used in this study. D205 and K207 share the same structural loop while K111 is far from this region interacting with ATP.

tissue tropism. However, owing to the random nature of transgene integration, chromosomal positional effects can result in variegation and incomplete penetrance, thus potentially confounding results. Therefore, a more controlled insertion of the transgene into a well-characterized euchromatic locus has overcome this limitation. An additional improvement of transgenic models came with the development of new systems in which it is possible to reversibly control target gene expression with exogenous ligands, such as doxycycline or interferon. Endogenous genetically modified mouse represent mutant mice that lose the expression of a given gene (knock-out) or express a mutant variant of it (knock-in) from their native promoters. Gene knock-out approaches entail the replacement of endogenous embryonic stem cell chromatin by a targeting vector that disrupts this allele, and were the first methods used to generate such mice. The biggest advantage of this approach is that, in contrast to other techniques, such as RNA interference or drug inhibition, targeting of a gene of interest can provoke the total elimination. Given the fact that germline biallelic disruptions of genes often cause embryonic lethality, the development of conditional knockout models has been a significant improvement of these models. Conditional mouse systems rely on the use of site-specific recombinases to control the spatiotemporal mutation of the genome. The most common conditional system uses the bacteriophage Cre-lox system in

which Cre recombinase recognizes a pair of inverted repeat DNA elements, or loxP sites, and catalyses recombination resulting in deletion or inversion of the intervening sequence.

In this project we have generated three different mouse models: a conditional knock-out model, a knock-in model in which Aurora B expression has been replaced by β-galactosidase and a tetracycline inducible model. The first two models have been used to perform the experiments described in this memory (see below), while the inducible model has been recently generated in collaboration with WC. Earnshaw's laboratory. This model allows the analysis of fine-tuning of Aurora B protein in vivo (work in progress).

Whereas complete inactivation of Aurora B, which was obtained with the *Aurkb*(–) and *Aurkb*(*Z*) alleles, leads to embryonic lethality at post implantation stages, its partial inactivation in heterozygous mice is associated with a slight increase in spontaneous tumours. The tumours formed in these mice occur late in life (>20 months old). The reason of the appearance of these tumors is not known. It might be possible that reduced expression of Aurora B could lead to accumulation of genomic instability that in turn, may facilitate tumor development in old mice. Indeed, chromosome missegregation, errors in spindle assembly and defects in cytokinesis are Aurora B loss-of-function phenotypes that have been associated with genomic instability and aneuploidy. Given that tumours are formed late in life, we can speculate that mice with reduced levels of Aurora B accumulate aneuploidy during life, increasing the probability of neoplastic transformation. Similar results have been obtained in mice with reduced expression of mitotic checkpoint components. Specifically, mice that are heterozygous for Mad1 and Mad2 develop benign lung tumours, whereas CenpE heterozygous animals show an increased incidence of benign lung tumours and splenic lymphomas (Iwanaga et al., 2007; Michel et al., 2001; Weaver et al., 2007). In the near future, we are planning to confirm by FISH technique whether there is an increase in genomic instability or aneuploidy in the tumours of Aurora B heterozygous mice.

Interestlingly, when we exposed Aurora B heterozygous mice to carcinogens or oncogene gain of function we did not observe an increase in tumour development but rather, a slight reduction in the formation of fibrosarcomas, papillomas and mammary tumors. One explanation for these observations is that tumour induction combined with the inherent aneuploidy of these mice may result in a rate of genetic instability above a threshold compatible with cell viability. Similar results were also observed in CenpE heterozygous mice after exposure to DMBA-TPA treatment (Weaver et al., 2007). Another explanation might be that reduced levels of Aurora B in mice compromise proliferation under stress conditions, as observed in the wound healing assay, being this impaired proliferation a possible cause of the reduction of induced tumours.

The conditional knock-out model generated in this work will allow the study of the effects of the conditional genetic ablation of Aurora B at the cellular and organism level. Knock down of Aurora B using RNA interference of partial inactivation using chemical inhibitors results in abnormal cell divisions due to defects in chromosome segregation, spindle checkpoint and cytokinesis (Ditchfield et al., 2003; Hauf et al., 2003; Ruchaud et al., 2007). However, these studies have the caveat that the elimination of this protein is never complete and residual kinase activity may support certain activities. In our system, complete ablation of Aurora B in primary MEFs has revealed not only the previously described roles for Aurora B but also, additional and novel critical role for this kinase in other cell cycle processes such as spindle dynamics and G1/S progression. The importance of these results will be discussed later in this section.

To understand the consequences of Aurora B ablation at the organism level, we are currently crossing the conditional mice with a knock-in strain that expresses the inducible Cre-ERT2 recombinase to deplete Aurora B in mice in a time-controlled manner. This system will allow us to analyze Aurora B requirement for embryo mid-gestation, adult life or even more important for tumour progression. For this last purpose we are setting up crosses with an inducible knock-in model in which KRasV12 oncogenic form leads to clinically relevant pancreatic and lung tumours (Guerra et al., 2003). These in vivo experiments will therefore, be crucial to validate Aurora B as a therapeutical cancer target.

The tetracycline inducible model is a very interesting tool that will permit us to upregulate or to inactivate Aurora B expression by the action of transcriptional activators (tTA or rtTA) which can be modulated by the addition of tetracycline. The key innovation of this promoter-hijack approach is that in the modified allele, Aurora B coding region remains intact with introns and the 3'UTR of the gene while its promoter is replaced with a minimal promoter responsive to transcriptional activators. So far, we have generated mice with the following genotype: *Aurkb*(+/tet) , *Rosa26*(+/rtTA), in which, after addition of tetracycline (or the derivative doxicycline) to the drinking water of the animals, Aurora B will be overexpressed in an ubiquitous manner in the mice. This approach is extremely useful as it will help us to know whether the upregulation of Aurora B observed in tumours is indeed causally related to tumourigenesis or a reflection of the high proliferative index of cancerous cells. Similar approaches have been used to upregulate mitotic genes such as the Aurora B substrate Hec1/Ndc80 and the mitotic checkpoint component Mad2 in the mice (Diaz-Rodriguez et al., 2008; Sotillo et al., 2007). Increased expression of Hec1 drives aneuploidy and an elevation on spontaneous lung and liver tumors in mice; whereas, conditional overexpression of Mad2 predisposes animals to a wide range of early

onset, lethal tumours. These results suggest that upregulation of mitotic regulators also leads to aneuploidy increasing the risk of neoplastic transformation.

3. Aurora B and Aurora C during early embryonic cell divisions

Whereas a single Aurora kinase (increase-in-ploidy 1; Ipl1) exists in yeasts, two Aurora-like genes (A and B) are found in nematodes, insects and cold-blood vertebrates. Mammalian Aurora B and Aurora C are two closely related paralogs that probably evolved from a duplication event involving the ancestral Aurora B found in cold-blood vertebrates (Brown et al., 2004). Aurora B is widely expressed in dividing cells. Aurora C, however, displays a very restricted expression pattern with a clear abundance during spermatogenesis and oocyte fertilization (Figure 38). Aurora C deficiency results in viable mice with subfertility defects such as heterogeneous chromatin condensation, loose acrosomes and blunted sperm heads (Kimmins et al., 2007). Interestingly, Aurora C displays frameshift mutations in infertile patients with abnormal spermatozoa characterized by large heads and increased chromosomal content (Dieterich et al., 2007), suggesting a critical role in mammalian spermatogenesis. Overexpression of wild-type Aurora C or loss-of-function mutants induces mitotic aberrations consistent with the hypothesis that this protein may act as a CPC component (Sasai et al., 2004; Slattery et al., 2008; Yan et al., 2005). Aurora C is highly expressed in oocytes and fertilized oocytes and its expression decreases during the first embryo divisions to reach a minimum expression during the blastocyst stage (Hamatani et al., 2004). However, its relevance in CPC function and mitosis in vivo has not been elucidated given the reduced endogenous expression levels in cultured cell lines.

The fact that Aurora B-null embryos survive up to post-implantation stages is certainly surprising given the earlier lethality of Incenp, Survivin or Borealin-deficient embryos (Cutts et al., 1999; Uren et al., 2000; Yamanaka et al., 2008) and the critical roles of the CPC in cell division. During pre-implantation, Incenp is properly located in the absence of Aurora B and the phenotypes expected from perturbed CPC function are not observed. However, these embryos are sensitive to Aurora B/C inhibitors such as ZM1 or to the concomitant interference with Aurora B and Aurora C expression using RNA interference approaches. In addition, we have observed that interference with Aurora C, but not Aurora B, expression at the 2-cell stage results in a significant number of abnormal mitosis and cell arrest. These data are in agreement with the fact that Aurora C expression is higher than that of Aurora B during these early stages (Figure 38a) and with the cell cycle arrest induced by long double-stranded RNAs against Aurora C in 2-cell mouse embryos (Lykke-Andersen et al., 2008). The fact that Aurora C-null embryos develop normally (Kimmins et

al., 2007) suggests that acute ablation of this protein may have stronger effects than germline deletion. Alternatively, Aurora B may compensate for Aurora C downregulation, at least partially. All together, these results suggest that Aurora B and Aurora C can compensate each other and that Aurora C is probably the major CPC kinase during these early cell divisions in vivo.

Despite the compensation by Aurora C in the early stages of embryonic development, Aurora B-null embryos die after implantation showing a dramatic increase in PM figures that finally lead to tetraploid or apoptotic figures both in vitro and in vivo. Incenp is not properly located in these cells suggesting a general defect in CPC function in these embryos. The massive arrest in PM in Aurora B-null embryos and the proper localization of Mad2 at the kinetochores suggests a robust, although transient, SAC in these developmental stages even in the absence of these CPC components. This contrast with the rapid exit from mitosis in primary Aurora B-null MEFs accompanied by lack of Mad2 at unattached kinetochores and degradation of cyclin B1 in these cells, and suggests differences in the strength of the SAC between these cell types.

Similar conclusions have been obtained using mouse models deficient in the other CPC components. Incenp-deficient embryos reveal a high mitotic index, absence of post-metaphase stages and formation of micronuclei and irregular macronuclei with large chromosome complements (Cutts et al., 1999). Similarly, Survivin- or Borealin-deficient embryos became polyploid, exhibit increased apoptosis and failed to survive beyond 4.5 days post coitum (Uren et al., 2000; Yamanaka et al., 2008).

4. Aurora B is a regulator of spindle dynamics and spindle pole integrity

Aurora B-depleted MEFs display a significant increase in the number of multipolar spindles. The formation of multipolar spindles has also been observed in cells in which Incenp (Cutts et al., 1999), Survivin (Yang et al., 2004) or Borealin (Gassmann et al., 2004) have been depleted by RNA interference or mouse knockouts.

In addition to the multipolar spindles, *Aurkb*(Δ/Δ) mitotic cells display a significant overgrowild-typeh of astral microtubules and fragmentation of γ-tubulin MTOCs (‘multiaster’ phenotype; Figure 47). Although a critical role for Aurora B in microtubule dynamics and the function of MTOCs has not previously demonstrated in mammals, there are some evidences from other CPC proteins or from depletion assays in *Xenopus*. Forced expression of Survivin influences microtubule dynamics reducing the pole-to-pole distance at metaphase and reduces microtubule nucleation from the centrosomes (Giodini et al., 2002; Rosa et al., 2006). On the other hand, suppression of Survivin by RNAi increased the number of microtubules nucleated by centrosomes

(Rosa et al., 2006). Whether the function of Survivin in microtubule dynamics is linked to its role as a CPC component remains controversial (Altieri, 2006; Lens et al., 2006). In fact, knock down or chemical inhibition of Aurora B in the same assays did not reveal any defect (Rosa et al., 2006), although this may be a consequence of residual Aurora B kinase activity. In the case of Borealin, the supernumerary poles observed in multipolar figures are proposed to be formed by abnormal partitioning of chromosomes during anaphase (Gassmann et al., 2004). On the other hand, inhibition of Aurora B by antibody injection in *Xenopus* cells also led to the overgrowild-typeh of astral microtubules (Kallio et al., 2002) although the effects on pole fragmentation were not reported. All together, these data suggest a model (Figure 50) in that Aurora B may modulate microtubule dynamics in the spindle poles by inhibiting the formation of excessive poles/MTOCs and its microtubule nucleation activity therefore resulting in bipolar spindles. This inhibitory function may be in agreement with the requirement for the yeast Aurora kinase in spindle disassembly following the completion of anaphase (Buvelot et al., 2003). Whether the role of Aurora B in preventing spindle pole fractionation and astral microtubule overgrowild-typeh is linked to its ability to regulate proper microtubule-kinetochore attachment is not known.

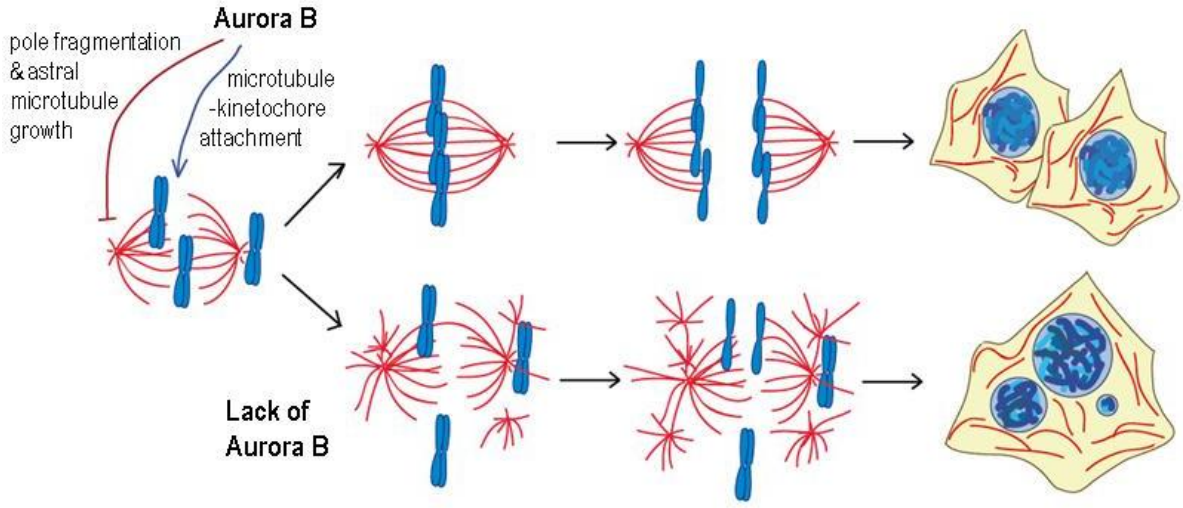

Figure 50. Roles of Aurora B in bipolar spindle assembly. Aurora B is essential for proper bipolar attachment between microtubules and kinetochores and its inhibition results in misaligned chromosomes. In addition, Aurora B is essential to prevent multiple MTOCs and growild-typeh of astral microtubules that are likely to result in multipolar (and in some cases monopolar by aggregation of MTOCs) spindles. Aurora B-null cells exit mitosis from these abnormal prometaphases resulting in nuclear fragmentation in the daughter cells.

5. Aurora B role in G1-S transition

Aurora B seems to have a relevant function in G1/S transition as revealed by acute elimination of this protein in G0 cells. *Aurkb*(Δ/Δ) cells display a significant delay (>6 h in MEFs and >1 day in liver cells) in the entry into S-phase after serum stimulation of quiescent cells. As a comparison, the defect in S-phase entry is significantly stronger than that observed in primary MEFs deficient in Cdk4, Cdk6 or both Cdk4/6 (Malumbres et al., 2004), two major kinases regulating G1/S transition in mammals. Similarly, S-phase entry in *Aurkb*(+/–) mice after partial hepatectomy is dramatically impaired whereas double Cdk4;Cdk2-null mice display a normal regeneration of the liver in vivo (Barriere et al., 2007). How Aurora B regulates S-phase entry is not clear. Aurora B and Survivin are known to participate in mTOR signalling in T lymphocytes by promoting the phosphorylation of mTOR targets such as p70S6K (Song et al., 2007). On the other hand, Survivin has been reported to bind directly to Cdk4 and to trigger phosphorylation of the retinoblastoma protein (pRb) (Suzuki et al., 2000). A recent analysis of the endoreduplication checkpoint suggests that Aurora B is able to directly phosphorylate pRb at Ser780 (Nair et al., 2009), a residue also phosphorylated by Cdk4. It is also known that deletion of Survivin provokes G1 arrest accompanied by induction of p53 function although these defects are not rescued by concomitant ablation of p53 (Okada et al., 2004; Yang et al., 2004). Our preliminary characterization of these pathways in Aurora B-deficient cells suggests a defect in p70S6K phosphorylation accompanied by induction of $p21^{Cip1}$, a p53 target involved in cell cycle arrest. Since genetic ablation of Aurora B is induced in quiescent/G0 cells, these defects are not a consequence of mitotic aberrations but a specific requirement for Aurora B during entry into the cell cycle from quiescence. Further work will be required for a detailed characterization of the role of Aurora B or Aurora B-Survivin complexes in G1 and possible interactions with the G1/S machinery.

6. Concluding remarks

Aurora kinases have recently received much attention due to their possible involvement in tumor development and their therapeutic value (Keen and Taylor, 2004; Perez de Castro et al., 2008). All three Aurora kinases are overexpressed in different types of cancers (Giet et al., 2005; Keen and Taylor, 2004). Whereas initial efforts were focused to Aurora A, recent data suggest that Aurora B is a relevant cancer target (Girdler et al., 2006; Girdler et al., 2008). Thus, the critical roles of this kinase in the regulation of G1/S during interphase or spindle organization and chromosome congression during mitosis may have relevant implications for cancer therapy. In addition, the ability of Aurora C to drive CPC function suggests the relevance of this protein in specific cell

types. Intriguingly, whereas no point mutations have been reported for Aurora B, four missense changes in Aurora C (G18E, G53A, E114Q and H210Q) have been found in lung adenocarcinomas (Davies et al., 2005; Forbes et al., 2008). Some of these changes affect the T-loop or activation segment of the kinase domain, a conserved and key functional region known to harbor activating somatic mutations in other kinases in cancer (Davies et al., 2005). Understanding the specific requirements for Aurora B/C in vivo in different tissues may therefore provide useful information in future therapeutic efforts.

Conclusions

1. Localization and kinase activity of Aurora B may be modulated by SUMO modification at a consensus site conserved in Aurora family members through evolution. This SUMOylation seems to favour proper localization of Aurora B at the centromeres during prometaphase and metaphase.

2. Partial genetic ablation of Aurora B does not result in major alterations during mouse development but slightly favors tumor progression in aged mice.

3. Aurora B is essential for mouse embryo development but dispensable during the early cell divisions due to the critical role of Aurora C during these first embryonic cycles.

4. Aurora B deficiency is lethal after embryo implantation due to mitotic defects and activation of p53-dependent apoptotic pathways in embryonic cells and degeneration of trophoblast giant cells.

5. Lack of Aurora B in advanced blastocysts arrests embryonic cells in prometaphase with misaligned chromosomes and spindle abnormalities, in the presence of a functional spindle assembly checkpoint.

6. Aurora B is essential to maintain the stability of the bipolar spindle in MEFs by promoting proper bipolar attachments between microtubules and kinetochores and by keeping the integrity of spindle poles and asters.

7. Aurora B regulates G1-S transition in vivo after partial hepatectomy and in primary MEFs, probably by modulating the mTOR pathway and/or the levels of the p53 effector $p21^{Cip1}$.

Conclusiones

1. La localización y actividad de Aurora B está regulada por la modificación por SUMO en un sitio consenso de la proteína conservado durante la evolución en los miembros de la familia de Aurora. Esta SUMOilación parece favorecer la correcta localización de Aurora B en el centrómero durante prometafase y metafase.

2. La eliminación genética parcial de Aurora B no da lugar a grandes problemas durante el desarrollo de la vida del ratón; pero sí incrementa la susceptibilidad a desarrollar tumores espontáneos en ratones de avanzada edad.

3. Aurora B es esencial durante el desarrollo embrionario del ratón, pero resulta dispensable durante las primeras divisiones celulares debido al efecto compensatorio que ejerce Aurora C en estos primeros ciclos embrionarios.

4. La deficiencia embrionaria de Aurora B es letal poco tiempo después de la implantación del embrión debido a defectos mitóticos y a la activación de rutas apoptóticas dependientes de p53 en las células embrionarias, y a la degeneración de las células gigantes del trofoblasto.

5. La ausencia de Aurora B en blastocistos avanzados produce un arresto celular en prometafase con cromosomas no alineados y abnormalidades en el huso mitótico, todo ello en presencia de un punto de control mitótico funcional.

6. Aurora B mantiene la estabilidad del huso mitótico bipolar en MEFs a través de promover el correcto anclaje entre los microtúbulos del huso y los cinétocoros, y de guardar la integridad de los polos y de los ásteres del huso.

7. Aurora B regula la transición G1/S en el hígado del ratón, después de realizar una hepatectomía parcial, y en fibroblastos en cultivo; seguramente mediante la regulación de la ruta de mTOR y/o de los niveles de $p21^{Cip}$, un conocido efector de p53.

References

Altieri, D.C. (2006). The case for survivin as a regulator of microtubule dynamics and cell-death decisions. Curr Opin Cell Biol *18*, 609-615.

Amabile, G., D'Alise, A.M., Iovino, M., Jones, P., Santaguida, S., Musacchio, A., Taylor, S., and Cortese, R. (2009). The Aurora B kinase activity is required for the maintenance of the differentiated state of murine myoblasts. Cell Death Differ *16*, 321-330.

Andrews, P.D. (2004). Aurora B regulates MCAK at the mitotic centromere. Dev Cell *6*, 253-268.

Ayaydin, F., and Dasso, M. (2004). Distinct in vivo dynamics of vertebrate SUMO paralogues. Mol Biol Cell *15*, 5208-5218.

Azuma, Y., and Dasso, M. (2002). A new clue at the nuclear pore: RanBP2 is an E3 enzyme for SUMO1. Dev Cell *2*, 130-131.

Barr, A.R., and Gergely, F. (2007). Aurora-A: the maker and breaker of spindle poles. J Cell Sci *120*, 2987-2996.

Barr, F.A., Sillje, H.H., and Nigg, E.A. (2004). Polo-like kinases and the orchestration of cell division. Nat Rev Mol Cell Biol *5*, 429-440.

Barriere, C., Santamaria, D., Cerqueira, A., Galan, J., Martin, A., Ortega, S., Malumbres, M., Dubus, P., and Barbacid, M. (2007). Mice thrive without Cdk4 and Cdk2. Mol Oncol *1*, 72-83.

Bartek, J., Lukas, C., and Lukas, J. (2004). Checking on DNA damage in S phase. Nat Rev Mol Cell Biol *5*, 792-804.

Bayliss, R., Sardon, T., Vernos, I., and Conti, E. (2003). Structural basis of Aurora-A activation by TPX2 at the mitotic spindle. Mol Cell *12*, 851-862.

Beard, C., Hochedlinger, K., Plath, K., Wutz, A., and Jaenisch, R. (2006). Efficient method to generate single-copy transgenic mice by site-specific integration in embryonic stem cells. Genesis *44*, 23-28.

Bischoff, J.R., Anderson, L., Zhu, Y., Mossie, K., Ng, L., Souza, B., Schryver, B., Flanagan, P., Clairvoyant, F., Ginther, C., *et al.* (1998). A homologue of Drosophila aurora kinase is oncogenic and amplified in human colorectal cancers. Embo J *17*, 3052-3065.

Bishop, J.D., and Schumacher, J.M. (2002). Phosphorylation of the carboxyl terminus of inner centromere protein (INCENP) by the Aurora B kinase stimulates Aurora B kinase activity. J Biol Chem *277*, 27577-27580.

Bolton, M.A. (2002). Aurora B kinase exists in a complex with survivin and INCENP and its kinase activity is stimulated by survivin binding and phosphorylation. Mol Biol Cell *13*, 3064-3077.

Brown, J.R., Koretke, K.K., Birkeland, M.L., Sanseau, P., and Patrick, D.R. (2004). Evolutionary relationships of Aurora kinases: implications for model organism studies and the development of anti-cancer drugs. BMC Evol Biol *4*, 39.

Buvelot, S., Tatsutani, S.Y., Vermaak, D., and Biggins, S. (2003). The budding yeast Ipl1/Aurora protein kinase regulates mitotic spindle disassembly. J Cell Biol *160*, 329-339.

Carmena, M., and Earnshaw, W.C. (2003). The cellular geography of aurora kinases. Nat Rev Mol Cell Biol *4*, 842-854.

Carter, S.L., Eklund, A.C., Kohane, I.S., Harris, L.N., and Szallasi, Z. (2006). A signature of chromosomal instability inferred from gene expression profiles predicts clinical outcome in multiple human cancers. Nat Genet *38*, 1043-1048.

Castro, A., Arlot-Bonnemains, Y., Vigneron, S., Labbe, J.C., Prigent, C., and Lorca, T. (2002). APC/Fizzy-Related targets Aurora-A kinase for proteolysis. EMBO Rep *3*, 457-462.

Clark, G.J., Cox, A.D., Graham, S.M., and Der, C.J. (1995). Biological assays for Ras transformation. Methods Enzymol *255*, 395-412.

Cowley, D.O., Rivera-Perez, J.A., Schliekelman, M., He, Y.J., Oliver, T.G., Lu, L., O'Quinn, R., Salmon, E.D., Magnuson, T., and Van Dyke, T. (2009). Aurora-A kinase is essential for bipolar spindle formation and early development. Mol Cell Biol *29*, 1059-1071.

Cutts, S.M., Fowler, K.J., Kile, B.T., Hii, L.L., O'Dowd, R.A., Hudson, D.F., Saffery, R., Kalitsis, P., Earle, E., and Choo, K.H. (1999). Defective chromosome segregation, microtubule bundling and nuclear bridging in inner centromere protein gene (Incenp)-disrupted mice. Hum Mol Genet *8*, 1145-1155.

Cheeseman, I.M., Anderson, S., Jwa, M., Green, E.M., Kang, J., Yates, J.R., 3rd, Chan, C.S., Drubin, D.G., and Barnes, G. (2002). Phospho-regulation of kinetochore-microtubule attachments by the Aurora kinase Ipl1p. Cell *111*, 163-172.

Cheeseman, I.M., and Desai, A. (2008). Molecular architecture of the kinetochore-microtubule interface. Nat Rev Mol Cell Biol *9*, 33-46.

Dasso, M. (2008). Emerging roles of the SUMO pathway in mitosis. Cell Div *3*, 5.

Davies, H., Hunter, C., Smith, R., Stephens, P., Greenman, C., Bignell, G., Teague, J., Butler, A., Edkins, S., Stevens, C., *et al.* (2005). Somatic mutations of the protein kinase gene family in human lung cancer. Cancer Res *65*, 7591-7595.

Dawlaty, M.M., Malureanu, L., Jeganathan, K.B., Kao, E., Sustmann, C., Tahk, S., Shuai, K., Grosschedl, R., and van Deursen, J.M. (2008). Resolution of sister centromeres requires RanBP2-mediated SUMOylation of topoisomerase IIalpha. Cell *133*, 103-115.

de Carcer, G., Perez de Castro, I., and Malumbres, M. (2007). Targeting cell cycle kinases for cancer therapy. Curr Med Chem *14*, 969-985.

Di Bacco, A., Ouyang, J., Lee, H.Y., Catic, A., Ploegh, H., and Gill, G. (2006). The SUMO-specific protease SENP5 is required for cell division. Mol Cell Biol *26*, 4489-4498.

Diaz-Rodriguez, E., Sotillo, R., Schvartzman, J.M., and Benezra, R. (2008). Hec1 overexpression hyperactivates the mitotic checkpoint and induces tumor formation in vivo. Proc Natl Acad Sci U S A *105*, 16719-16724.

Dieterich, K., Soto Rifo, R., Faure, A.K., Hennebicq, S., Ben Amar, B., Zahi, M., Perrin, J., Martinez, D., Sele, B., Jouk, P.S., *et al.* (2007). Homozygous mutation of AURKC yields large-headed polyploid spermatozoa and causes male infertility. Nat Genet *39*, 661-665.

Ditchfield, C. (2003). Aurora B couples chromosome alignment with anaphase by targeting bubR1, Mad2 and CENP-E to kinetochores. J Cell Biol *161*, 267-280.

Ditchfield, C., Johnson, V.L., Tighe, A., Ellston, R., Haworth, C., Johnson, T., Mortlock, A., Keen, N., and Taylor, S.S. (2003). Aurora B couples chromosome alignment with anaphase by targeting BubR1, Mad2, and Cenp-E to kinetochores. J Cell Biol *161*, 267-280.

Dutertre, S., Hamard-Peron, E., Cremet, J.Y., Thomas, Y., and Prigent, C. (2005). The absence of p53 aggravates polyploidy and centrosome number abnormality induced by Aurora-C overexpression. Cell Cycle *4*, 1783-1787.

Eckerdt, F., Yuan, J., and Strebhardt, K. (2005). Polo-like kinases and oncogenesis. *24*, 267-276.

Emanuele, M.J., Lan, W., Jwa, M., Miller, S.A., Chan, C.S., and Stukenberg, P.T. (2008). Aurora B kinase and protein phosphatase 1 have opposing roles in modulating kinetochore assembly. J Cell Biol *181*, 241-254.

Eyers, P.A., Erikson, E., Chen, L.G., and Maller, J.L. (2003). A novel mechanism for activation of the protein kinase Aurora A. Curr Biol *13*, 691-697.

Fang, G., Yu, H., and Kirschner, M.W. (1998). Direct binding of CDC20 protein family members activates the anaphase-promoting complex in mitosis and G1. Mol Cell *2*, 163-171.

Fisk, H.A., Mattison, C.P., and Winey, M. (2004). A field guide to the Mps1 family of protein kinases. Cell Cycle *3*, 439-442.

Floyd, S., Pines, J., and Lindon, C. (2008). APC/C Cdh1 targets aurora kinase to control reorganization of the mitotic spindle at anaphase. Curr Biol *18*, 1649-1658.

Forbes, S.A., Bhamra, G., Bamford, S., Dawson, E., Kok, C., Clements, J., Menzies, A., Teague, J.W., Futreal, P.A., and Stratton, M.R. (2008). The Catalogue of Somatic Mutations in Cancer (COSMIC). Curr Protoc Hum Genet *Chapter 10*, Unit 10 11.

Francisco, L., Wang, W., and Chan, C.S. (1994). Type 1 protein phosphatase acts in opposition to IpL1 protein kinase in regulating yeast chromosome segregation. Mol Cell Biol *14*, 4731-4740.

Frese, K.K., and Tuveson, D.A. (2007). Maximizing mouse cancer models. Nat Rev Cancer *7*, 645-658.

Garcia-Higuera, I., Manchado, E., Dubus, P., Canamero, M., Mendez, J., Moreno, S., and Malumbres, M. (2008). Genomic stability and tumour suppression by the APC/C cofactor Cdh1. Nat Cell Biol *10*, 802-811.

Gassmann, R., Carvalho, A., Henzing, A.J., Ruchaud, S., Hudson, D.F., Honda, R., Nigg, E.A., Gerloff, D.L., and Earnshaw, W.C. (2004). Borealin: a novel chromosomal passenger required for stability of the bipolar mitotic spindle. J Cell Biol *166*, 179-191.

Geiss-Friedlander, R., and Melchior, F. (2007). Concepts in sumoylation: a decade on. Nat Rev Mol Cell Biol *8*, 947-956.

Geoffroy, M.C., and Hay, R.T. (2009). An additional role for SUMO in ubiquitin-mediated proteolysis. Nat Rev Mol Cell Biol.

Giet, R., Petretti, C., and Prigent, C. (2005). Aurora kinases, aneuploidy and cancer, a coincidence or a real link? Trends Cell Biol *15*, 241-250.

Giodini, A., Kallio, M.J., Wall, N.R., Gorbsky, G.J., Tognin, S., Marchisio, P.C., Symons, M., and Altieri, D.C. (2002). Regulation of microtubule stability and mitotic progression by survivin. Cancer Res *62*, 2462-2467.

Girdler, F., Gascoigne, K.E., Eyers, P.A., Hartmuth, S., Crafter, C., Foote, K.M., Keen, N.J., and Taylor, S.S. (2006). Validating Aurora B as an anti-cancer drug target. J Cell Sci *119*, 3664-3675.

Girdler, F., Sessa, F., Patercoli, S., Villa, F., Musacchio, A., and Taylor, S. (2008). Molecular basis of drug resistance in aurora kinases. Chem Biol *15*, 552-562.

Glover, D.M., Leibowitz, M.H., McLean, D.A., and Parry, H. (1995). Mutations in aurora prevent centrosome separation leading to the formation of monopolar spindles. Cell *81*, 95-105.

Gritsko, T.M., Coppola, D., Paciga, J.E., Yang, L., Sun, M., Shelley, S.A., Fiorica, J.V., Nicosia, S.V., and Cheng, J.Q. (2003). Activation and overexpression of centrosome kinase BTAK/Aurora-A in human ovarian cancer. Clin Cancer Res *9*, 1420-1426.

Guerra, C., Mijimolle, N., Dhawahir, A., Dubus, P., Barradas, M., Serrano, M., Campuzano, V., and Barbacid, M. (2003). Tumor induction by an endogenous K-ras oncogene is highly dependent on cellular context. Cancer Cell *4*, 111-120.

Guse, A., Mishima, M., and Glotzer, M. (2005). Phosphorylation of ZEN-4/MKLP1 by aurora B regulates completion of cytokinesis. Curr Biol *15*, 778-786.

Haga, S., Ozaki, M., Inoue, H., Okamoto, Y., Ogawa, W., Takeda, K., Akira, S., and Todo, S. (2009). The survival pathways phosphatidylinositol-3 kinase (PI3-

K)/phosphoinositide-dependent protein kinase 1 (PDK1)/Akt modulate liver regeneration through hepatocyte size rather than proliferation. Hepatology *49*, 204-214.

Hamatani, T., Carter, M.G., Sharov, A.A., and Ko, M.S. (2004). Dynamics of global gene expression changes during mouse preimplantation development. Dev Cell *6*, 117-131.

Hanahan, D., and Weinberg, R.A. (2000). The Hallmarks of Cancer. Cell *100*, 57-70.

Hannich, J.T., Lewis, A., Kroetz, M.B., Li, S.J., Heide, H., Emili, A., and Hochstrasser, M. (2005). Defining the SUMO-modified proteome by multiple approaches in Saccharomyces cerevisiae. J Biol Chem *280*, 4102-4110.

Harrington, E.A., Bebbington, D., Moore, J., Rasmussen, R.K., Ajose-Adeogun, A.O., Nakayama, T., Graham, J.A., Demur, C., Hercend, T., Diu-Hercend, A., *et al.* (2004). VX-680, a potent and selective small-molecule inhibitor of the Aurora kinases, suppresses tumor growth in vivo. Nat Med *10*, 262-267.

Hauf, S., Cole, R.W., LaTerra, S., Zimmer, C., Schnapp, G., Walter, R., Heckel, A., van Meel, J., Rieder, C.L., and Peters, J.M. (2003). The small molecule Hesperadin reveals a role for Aurora B in correcting kinetochore-microtubule attachment and in maintaining the spindle assembly checkpoint. J Cell Biol *161*, 281-294.

Hay, R.T. (2005). SUMO: a history of modification. Mol Cell *18*, 1-12.

Hay, R.T. (2007). SUMO-specific proteases: a twist in the tail. Trends Cell Biol *17*, 370-376.

Hirota, T., Kunitoku, N., Sasayama, T., Marumoto, T., Zhang, D., Nitta, M., Hatakeyama, K., and Saya, H. (2003). Aurora-A and an interacting activator, the LIM protein Ajuba, are required for mitotic commitment in human cells. Cell *114*, 585-598.

Holland, A.J., and Cleveland, D.W. (2009). Boveri revisited: chromosomal instability, aneuploidy and tumorigenesis. Nat Rev Mol Cell Biol *10*, 478-487.

Honda, R., Korner, R., and Nigg, E.A. (2003). Exploring the functional interactions between Aurora B, INCENP, and survivin in mitosis. Mol Biol Cell *14*, 3325-3341.

Hsu, J.Y., Sun, Z.W., Li, X., Reuben, M., Tatchell, K., Bishop, D.K., Grushcow, J.M., Brame, C.J., Caldwell, J.A., Hunt, D.F., *et al.* (2000). Mitotic phosphorylation of histone H3 is governed by Ipl1/aurora kinase and Glc7/PP1 phosphatase in budding yeast and nematodes. Cell *102*, 279-291.

Hu, H.M., Chuang, C.K., Lee, M.J., Tseng, T.C., and Tang, T.K. (2000). Genomic organization, expression, and chromosome localization of a third aurora-related kinase gene, Aie1. DNA Cell Biol *19*, 679-688.

Iwanaga, Y., Chi, Y.H., Miyazato, A., Sheleg, S., Haller, K., Peloponese, J.M., Jr., Li, Y., Ward, J.M., Benezra, R., and Jeang, K.T. (2007). Heterozygous deletion of mitotic arrest-deficient protein 1 (MAD1) increases the incidence of tumors in mice. Cancer Res *67*, 160-166.

Jelluma, N., Brenkman, A.B., van den Broek, N.J., Cruijsen, C.W., van Osch, M.H., Lens, S.M., Medema, R.H., and Kops, G.J. (2008). Mps1 phosphorylates Borealin to control Aurora B activity and chromosome alignment. Cell *132*, 233-246.

Jeyaprakash, A.A., Klein, U.R., Lindner, D., Ebert, J., Nigg, E.A., and Conti, E. (2007). Structure of a Survivin-Borealin-INCENP core complex reveals how chromosomal passengers travel together. Cell *131*, 271-285.

Johansen, K.M., and Johansen, J. (2006). Regulation of chromatin structure by histone H3S10 phosphorylation. Chromosome Res *14*, 393-404.

Joseph, J., Tan, S.H., Karpova, T.S., McNally, J.G., and Dasso, M. (2002). SUMO-1 targets RanGAP1 to kinetochores and mitotic spindles. J Cell Biol *156*, 595-602.

Kallio, M.J., McCleland, M.L., Stukenberg, P.T., and Gorbsky, G.J. (2002). Inhibition of aurora B kinase blocks chromosome segregation, overrides the spindle checkpoint, and perturbs microtubule dynamics in mitosis. Curr Biol *12*, 900-905.

Kanda, A., Kawai, H., Suto, S., Kitajima, S., Sato, S., Takata, T., and Tatsuka, M. (2005). Aurora-B/AIM-1 kinase activity is involved in Ras-mediated cell transformation. Oncogene *24*, 7266-7272.

Kastan, M.B., and Bartek, J. (2004). Cell-cycle checkpoints and cancer. Nature *432*, 316-323.

Keen, N., and Taylor, S. (2004). Aurora-kinase inhibitors as anticancer agents. Nat Rev Cancer *4*, 927-936.

Keen, N., and Taylor, S. (2009). Mitotic drivers--inhibitors of the Aurora B Kinase. Cancer Metastasis Rev *28*, 185-195.

Kelly, A.E., and Funabiki, H. (2009). Correcting aberrant kinetochore microtubule attachments: an Aurora B-centric view. Curr Opin Cell Biol.

Kimmins, S., Crosio, C., Kotaja, N., Hirayama, J., Monaco, L., Hoog, C., van Duin, M., Gossen, J.A., and Sassone-Corsi, P. (2007). Differential functions of the Aurora-B and Aurora-C kinases in mammalian spermatogenesis. Mol Endocrinol *21*, 726-739.

Klein, U.R., Haindl, M., Nigg, E.A., and Muller, S. (2009). RanBP2 and SENP3 function in a mitotic SUMO2/3 conjugation-deconjugation cycle on Borealin. Mol Biol Cell *20*, 410-418.

Kleylein-Sohn, J., Westendorf, J., Le Clech, M., Habedanck, R., Stierhof, Y.D., and Nigg, E.A. (2007). Plk4-induced centriole biogenesis in human cells. Dev Cell *13*, 190-202.

Knowlton, A.L., Lan, W., and Stukenberg, P.T. (2006). Aurora B is enriched at merotelic attachment sites, where it regulates MCAK. Curr Biol *16*, 1705-1710.

Kufer, T.A., Sillje, H.H., Korner, R., Gruss, O.J., Meraldi, P., and Nigg, E.A. (2002). Human TPX2 is required for targeting Aurora-A kinase to the spindle. J Cell Biol *158*, 617-623.

Lens, S.M., Vader, G., and Medema, R.H. (2006). The case for Survivin as mitotic regulator. Curr Opin Cell Biol *18*, 616-622.

Li, C.C., Chu, H.Y., Yang, C.W., Chou, C.K., and Tsai, T.F. (2009). Aurora-A overexpression in mouse liver causes p53-dependent premitotic arrest during liver regeneration. Mol Cancer Res *7*, 678-688.

Li, D., Zhu, J., Firozi, P.F., Abbruzzese, J.L., Evans, D.B., Cleary, K., Friess, H., and Sen, S. (2003). Overexpression of oncogenic STK15/BTAK/Aurora A kinase in human pancreatic cancer. Clin Cancer Res *9*, 991-997.

Li, X., Sakashita, G., Matsuzaki, H., Sugimoto, K., Kimura, K., Hanaoka, F., Taniguchi, H., Furukawa, K., and Urano, T. (2004). Direct association with inner centromere protein (INCENP) activates the novel chromosomal passenger protein, Aurora-C. J Biol Chem *279*, 47201-47211.

Lin, Y.S., Su, L.J., Yu, C.T., Wong, F.H., Yeh, H.H., Chen, S.L., Wu, J.C., Lin, W.J., Shiue, Y.L., Liu, H.S., *et al.* (2006). Gene expression profiles of the aurora family kinases. Gene Expr *13*, 15-26.

Littlepage, L.E., and Ruderman, J.V. (2002). Identification of a new APC/C recognition domain, the A box, which is required for the Cdh1-dependent destruction of the kinase Aurora-A during mitotic exit. Genes Dev *16*, 2274-2285.

Liu, D., Vader, G., Vromans, M.J., Lampson, M.A., and Lens, S.M. (2009). Sensing chromosome bi-orientation by spatial separation of aurora B kinase from kinetochore substrates. Science *323*, 1350-1353.

Logarinho, E., and Bousbaa, H. (2008). Kinetochore-microtubule interactions "in check" by Bub1, Bub3 and BubR1: The dual task of attaching and signalling. Cell Cycle *7*, 1763-1768.

Lu, L.Y., Wood, J.L., Ye, L., Minter-Dykhouse, K., Saunders, T.L., Yu, X., and Chen, J. (2008). Aurora A is essential for early embryonic development and tumor suppression. J Biol Chem *283*, 31785-31790.

Lukas, J., Bohr, V.A., and Halazonetis, T.D. (2006). Cellular responses to DNA damage: current state of the field and review of the 52nd Benzon Symposium. DNA Repair (Amst) *5*, 591-601.

Lykke-Andersen, K., Gilchrist, M.J., Grabarek, J.B., Das, P., Miska, E., and Zernicka-Goetz, M. (2008). Maternal Argonaute 2 is essential for early mouse development at the maternal-zygotic transition. Mol Biol Cell *19*, 4383-4392.

Makhnevych, T., Sydorskyy, Y., Xin, X., Srikumar, T., Vizeacoumar, F.J., Jeram, S.M., Li, Z., Bahr, S., Andrews, B.J., Boone, C., *et al.* (2009). Global map of SUMO function revealed by protein-protein interaction and genetic networks. Mol Cell *33*, 124-135.

Malumbres, M., and Barbacid, M. (2001). To cycle or not to cycle: a critical decision in cancer. Nat Rev Cancer *1*, 222-231.

Malumbres, M., and Barbacid, M. (2005). Mammalian cyclin-dependent kinases. Trends Biochem Sci *30*, 630-641.

Malumbres, M., Sotillo, R., Santamaria, D., Galan, J., Cerezo, A., Ortega, S., Dubus, P., and Barbacid, M. (2004). Mammalian cells cycle without the D-type cyclin-dependent kinases Cdk4 and Cdk6. Cell *118*, 493-504.

Michel, L.S., Liberal, V., Chatterjee, A., Kirchwegger, R., Pasche, B., Gerald, W., Dobles, M., Sorger, P.K., Murty, V.V., and Benezra, R. (2001). MAD2 haplo-insufficiency causes premature anaphase and chromosome instability in mammalian cells. Nature *409*, 355-359.

Mitchell, C., and Willenbring, H. (2008). A reproducible and well-tolerated method for 2/3 partial hepatectomy in mice. Nat Protoc *3*, 1167-1170.

Miyoshi, Y., Iwao, K., Egawa, C., and Noguchi, S. (2001). Association of centrosomal kinase STK15/BTAK mRNA expression with chromosomal instability in human breast cancers. Int J Cancer *92*, 370-373.

Montpetit, B., Hazbun, T.R., Fields, S., and Hieter, P. (2006). Sumoylation of the budding yeast kinetochore protein Ndc10 is required for Ndc10 spindle localization and regulation of anaphase spindle elongation. J Cell Biol *174*, 653-663.

Moreno-Bueno, G., Sanchez-Estevez, C., Cassia, R., Rodriguez-Perales, S., Diaz-Uriarte, R., Dominguez, O., Hardisson, D., Andujar, M., Prat, J., Matias-Guiu, X., *et al.* (2003). Differential gene expression profile in endometrioid and nonendometrioid endometrial carcinoma: STK15 is frequently overexpressed and amplified in nonendometrioid carcinomas. Cancer Res *63*, 5697-5702.

Muller, W.J., Sinn, E., Pattengale, P.K., Wallace, R., and Leder, P. (1988). Single-step induction of mammary adenocarcinoma in transgenic mice bearing the activated c-neu oncogene. Cell *54*, 105-115.

Musacchio, A., and Salmon, E.D. (2007). The spindle-assembly checkpoint in space and time. Nature Rev Mol Cell Biol *8*, 379-393.

Nair, J.S., Ho, A.L., Tse, A.N., Coward, J., Cheema, H., Ambrosini, G., Keen, N., and Schwartz, G.K. (2009). Aurora B kinase regulates the postmitotic endoreduplication checkpoint via phosphorylation of the retinoblastoma protein at serine 780. Mol Biol Cell *20*, 2218-2228.

Nakayama, K.I., and Nakayama, K. (2006). Ubiquitin ligases: cell-cycle control and cancer. Nat Rev Cancer *6*, 369-381.

Nguyen, H.G., Chinnappan, D., Urano, T., and Ravid, K. (2005). Mechanism of Aurora-B degradation and its dependency on intact KEN and A-boxes: identification of an aneuploidy-promoting property. Mol Cell Biol *25*, 4977-4992.

Nigg, E.A. (2001). Mitotic kinases as regulators of cell division and its checkpoints. Nat Rev Mol Cell Biol *2*, 21-32.

Nowak, S.J., and Corces, V.G. (2004). Phosphorylation of histone H3: a balancing act between chromosome condensation and transcriptional activation. Trends Genet *20*, 214-220.

O'Connell, M.J., Krien, M.J., and Hunter, T. (2003). Never say never. The NIMA-related protein kinases in mitotic control. Trends Cell Biol *13*, 221-228.

Okada, H., Bakal, C., Shahinian, A., Elia, A., Wakeham, A., Suh, W.K., Duncan, G.S., Ciofani, M., Rottapel, R., Zuniga-Pflucker, J.C., *et al.* (2004). Survivin loss in thymocytes triggers p53-mediated growth arrest and p53-independent cell death. J Exp Med *199*, 399-410.

Ota, T., Suto, S., Katayama, H., Han, Z.B., Suzuki, F., Maeda, M., Tanino, M., Terada, Y., and Tatsuka, M. (2002). Increased mitotic phosphorylation of histone H3 attributable to AIM-1/Aurora-B overexpression contributes to chromosome number instability. Cancer Res *62*, 5168-5177.

Panse, V.G., Hardeland, U., Werner, T., Kuster, B., and Hurt, E. (2004). A proteome-wide approach identifies sumoylated substrate proteins in yeast. J Biol Chem *279*, 41346-41351.

Pardee, A.B. (1974). A restriction point for control of normal animal cell proliferation. Proc Natl Acad Sci U S A *71*, 1286-1290.

Pereira, G., and Schiebel, E. (2003). Separase regulates INCENP-Aurora B anaphase spindle function through Cdc14. Science *302*, 2120-2124.

Perez de Castro, I., de Carcer, G., and Malumbres, M. (2007). A census of mitotic cancer genes: new insights into tumor cell biology and cancer therapy. Carcinogenesis *28*, 899-912.

Perez de Castro, I., de Carcer, G., Montoya, G., and Malumbres, M. (2008). Emerging cancer therapeutic opportunities by inhibiting mitotic kinases. Curr Opin Pharmacol *8*, 375-383.

Peters, J.M. (2006). The anaphase promoting complex/cyclosome: a machine designed to destroy. Nat Rev Mol Cell Biol *7*, 644-656.

Pfleger, C.M., and Kirschner, M.W. (2000). The KEN box: an APC recognition signal distinct from the D box targeted by Cdh1. Genes Dev *14*, 655-665.

Price, D.M., Kanyo, R., Steinberg, N., Chik, C.L., and Ho, A.K. (2009). Nocturnal activation of aurora C in rat pineal gland: its role in the norepinephrine-induced phosphorylation of histone H3 and gene expression. Endocrinology *150*, 2334-2341.

Prigent, C., and Dimitrov, S. (2003). Phosphorylation of serine 10 in histone H3, what for? J Cell Sci *116*, 3677-3685.

Prudden, J., Pebernard, S., Raffa, G., Slavin, D.A., Perry, J.J., Tainer, J.A., McGowan, C.H., and Boddy, M.N. (2007). SUMO-targeted ubiquitin ligases in genome stability. EMBO J *26*, 4089-4101.

Reverter, D., and Lima, C.D. (2006). Structural basis for SENP2 protease interactions with SUMO precursors and conjugated substrates. Nat Struct Mol Biol *13*, 1060-1068.

Rodriguez, C.I., Buchholz, F., Galloway, J., Sequerra, R., Kasper, J., Ayala, R., Stewart, A.F., and Dymecki, S.M. (2000). High-efficiency deleter mice show that FLPe is an alternative to Cre-loxP. Nat Genet *25*, 139-140.

Rosa, J., Canovas, P., Islam, A., Altieri, D.C., and Doxsey, S.J. (2006). Survivin modulates microtubule dynamics and nucleation throughout the cell cycle. Mol Biol Cell *17*, 1483-1493.

Rosasco-Nitcher, S.E., Lan, W., Khorasanizadeh, S., and Stukenberg, P.T. (2008). Centromeric Aurora-B activation requires TD-60, microtubules, and substrate priming phosphorylation. Science *319*, 469-472.

Ruchaud, S., Carmena, M., and Earnshaw, W.C. (2007). Chromosomal passengers: conducting cell division. Nat Rev Mol Cell Biol *8*, 798-812.

Sabbattini, P., Canzonetta, C., Sjoberg, M., Nikic, S., Georgiou, A., Kemball-Cook, G., Auner, H.W., and Dillon, N. (2007). A novel role for the Aurora B kinase in epigenetic marking of silent chromatin in differentiated postmitotic cells. Embo J *26*, 4657-4669.

Sakakura, C., Hagiwara, A., Yasuoka, R., Fujita, Y., Nakanishi, M., Masuda, K., Shimomura, K., Nakamura, Y., Inazawa, J., Abe, T., *et al.* (2001). Tumour-amplified kinase BTAK is amplified and overexpressed in gastric cancers with possible involvement in aneuploid formation. Br J Cancer *84*, 824-831.

Samejima, K., Ogawa, H., Cooke, C.A., Hudson, D.F., Macisaac, F., Ribeiro, S.A., Vagnarelli, P., Cardinale, S., Kerr, A., Lai, F., *et al.* (2008). A promoter-hijack strategy for conditional shutdown of multiply spliced essential cell cycle genes. Proc Natl Acad Sci U S A *105*, 2457-2462.

Sasai, K. (2004). Aurora-C kinase is a novel chromosomal passenger protein that can complement Aurora-B kinase function in mitotic cells. Cell Motil Cytoskeleton *59*, 249-263.

Sasai, K., Katayama, H., Stenoien, D.L., Fujii, S., Honda, R., Kimura, M., Okano, Y., Tatsuka, M., Suzuki, F., Nigg, E.A., *et al.* (2004). Aurora-C kinase is a novel chromosomal passenger protein that can complement Aurora-B kinase function in mitotic cells. Cell Motil Cytoskeleton *59*, 249-263.

Sasai, K., Parant, J.M., Brandt, M.E., Carter, J., Adams, H.P., Stass, S.A., Killary, A.M., Katayama, H., and Sen, S. (2008). Targeted disruption of Aurora A causes abnormal mitotic spindle assembly, chromosome misalignment and embryonic lethality. Oncogene *27*, 4122-4127.

Schnutgen, F., Doerflinger, N., Calleja, C., Wendling, O., Chambon, P., and Ghyselinck, N.B. (2003). A directional strategy for monitoring Cre-mediated recombination at the cellular level in the mouse. Nat Biotechnol *21*, 562-565.

Schwenk, F., Baron, U., and Rajewsky, K. (1995). A cre-transgenic mouse strain for the ubiquitous deletion of loxP-flanked gene segments including deletion in germ cells. Nucleic Acids Res *23*, 5080-5081.

Sen, S., Zhou, H., and White, R.A. (1997). A putative serine/threonine kinase encoding gene BTAK on chromosome 20q13 is amplified and overexpressed in human breast cancer cell lines. Oncogene *14*, 2195-2200.

Sen, S., Zhou, H., Zhang, R.D., Yoon, D.S., Vakar-Lopez, F., Ito, S., Jiang, F., Johnston, D., Grossman, H.B., Ruifrok, A.C., *et al.* (2002). Amplification/overexpression of a mitotic kinase gene in human bladder cancer. J Natl Cancer Inst *94*, 1320-1329.

Sessa, F. (2005). Mechanism of Aurora B activation by INCENP and inhibition by hesperadin. Mol Cell *18*, 379-391.

Shih, I.M., Zhou, W., Goodman, S.N., Lengauer, C., Kinzler, K.W., and Vogelstein, B. (2001). Evidence that genetic instability occurs at an early stage of colorectal tumorigenesis. Cancer Res *61*, 818-822.

Slattery, S.D., Mancini, M.A., Brinkley, B.R., and Hall, R.M. (2009). Aurora-C kinase supports mitotic progression in the absence of Aurora-B. Cell Cycle *8*.

Slattery, S.D., Moore, R.V., Brinkley, B.R., and Hall, R.M. (2008). Aurora-C and Aurora-B share phosphorylation and regulation of CENP-A and Borealin during mitosis. Cell Cycle *7*, 787-795.

Song, J., Durrin, L.K., Wilkinson, T.A., Krontiris, T.G., and Chen, Y. (2004). Identification of a SUMO-binding motif that recognizes SUMO-modified proteins. Proc Natl Acad Sci U S A *101*, 14373-14378.

Song, J., Salek-Ardakani, S., So, T., and Croft, M. (2007). The kinases aurora B and mTOR regulate the G1-S cell cycle progression of T lymphocytes. Nat Immunol *8*, 64-73.

Sotillo, R., Hernando, E., Diaz-Rodriguez, E., Teruya-Feldstein, J., Cordon-Cardo, C., Lowe, S.W., and Benezra, R. (2007). Mad2 overexpression promotes aneuploidy and tumorigenesis in mice. Cancer Cell *11*, 9-23.

Steigemann, P., Wurzenberger, C., Schmitz, M.H., Held, M., Guizetti, J., Maar, S., and Gerlich, D.W. (2009). Aurora B-mediated abscission checkpoint protects against tetraploidization. Cell *136*, 473-484.

Sumara, I., Quadroni, M., Frei, C., Olma, M.H., Sumara, G., Ricci, R., and Peter, M. (2007). A Cul3-based E3 ligase removes Aurora B from mitotic chromosomes, regulating mitotic progression and completion of cytokinesis in human cells. Dev Cell *12*, 887-900.

Sun, H., Leverson, J.D., and Hunter, T. (2007). Conserved function of RNF4 family proteins in eukaryotes: targeting a ubiquitin ligase to SUMOylated proteins. EMBO J *26*, 4102-4112.

Suzuki, A., Ito, T., Kawano, H., Hayashida, M., Hayasaki, Y., Tsutomi, Y., Akahane, K., Nakano, T., Miura, M., and Shiraki, K. (2000). Survivin initiates procaspase 3/p21 complex formation as a result of interaction with Cdk4 to resist Fas-mediated cell death. Oncogene *19*, 1346-1353.

Tang, C.J., Lin, C.Y., and Tang, T.K. (2006). Dynamic localization and functional implications of Aurora-C kinase during male mouse meiosis. Dev Biol *290*, 398-410.

Tatsuka, M. (1998). Multinuclearity and increased ploidy caused by overexpression of the aurora- and Ipl1-like midbody-associated protein mitotic kinase in human cancer cells. Cancer Res *58*, 4811-4816.

Taylor, S., and Peters, J.M. (2008). Polo and Aurora kinases: lessons derived from chemical biology. Curr Opin Cell Biol *20*, 77-84.

Terada, Y. (1998). AIM-1: a mammalian midbody-associated protein required for cytokinesis. EMBO J *17*, 667-676.

Thornton, B.R., and Toczyski, D.P. (2006). Precise destruction: an emerging picture of the APC. Genes Dev *20*, 3069-3078.

Trinkle-Mulcahy, L., Andersen, J., Lam, Y.W., Moorhead, G., Mann, M., and Lamond, A.I. (2006). Repo-Man recruits PP1 gamma to chromatin and is essential for cell viability. J Cell Biol *172*, 679-692.

Tybulewicz, V.L., Crawford, C.E., Jackson, P.K., Bronson, R.T., and Mulligan, R.C. (1991). Neonatal lethality and lymphopenia in mice with a homozygous disruption of the c-abl proto-oncogene. Cell *65*, 1153-1163.

Ulisse, S., Delcros, J.G., Baldini, E., Toller, M., Curcio, F., Giacomelli, L., Prigent, C., Ambesi-Impiombato, F.S., D'Armiento, M., and Arlot-Bonnemains, Y. (2006). Expression of Aurora kinases in human thyroid carcinoma cell lines and tissues. Int J Cancer *119*, 275-282.

Ulrich, H.D. (2008). The fast-growing business of SUMO chains. Mol Cell *32*, 301-305.

Uren, A.G., Wong, L., Pakusch, M., Fowler, K.J., Burrows, F.J., Vaux, D.L., and Choo, K.H. (2000). Survivin and the inner centromere protein INCENP show similar cell-cycle localization and gene knockout phenotype. Curr Biol *10*, 1319-1328.

Uzunova, K., Gottsche, K., Miteva, M., Weisshaar, S.R., Glanemann, C., Schnellhardt, M., Niessen, M., Scheel, H., Hofmann, K., Johnson, E.S., *et al.* (2007). Ubiquitin-dependent proteolytic control of SUMO conjugates. J Biol Chem *282*, 34167-34175.

Walter, A.O., Seghezzi, W., Korver, W., Sheung, J., and Lees, E. (2000). The mitotic serine/threonine kinase Aurora2/AIK is regulated by phosphorylation and degradation. Oncogene *19*, 4906-4916.

Wang, X., Zhou, Y.X., Qiao, W., Tominaga, Y., Ouchi, M., Ouchi, T., and Deng, C.X. (2006). Overexpression of aurora kinase A in mouse mammary epithelium induces genetic instability preceding mammary tumor formation. Oncogene *25*, 7148-7158.

Watts, F.Z. (2007). The role of SUMO in chromosome segregation. Chromosoma *116*, 15-20.

Weaver, B.A., Silk, A.D., Montagna, C., Verdier-Pinard, P., and Cleveland, D.W. (2007). Aneuploidy acts both oncogenically and as a tumor suppressor. Cancer Cell *11*, 25-36.

Wohlschlegel, J.A., Johnson, E.S., Reed, S.I., and Yates, J.R., 3rd (2004). Global analysis of protein sumoylation in Saccharomyces cerevisiae. J Biol Chem *279*, 45662-45668.

Wykoff, D.D., and O'Shea, E.K. (2005). Identification of sumoylated proteins by systematic immunoprecipitation of the budding yeast proteome. Mol Cell Proteomics *4*, 73-83.

Yamanaka, Y., Heike, T., Kumada, T., Shibata, M., Takaoka, Y., Kitano, A., Shiraishi, K., Kato, T., Nagato, M., Okawa, K., *et al.* (2008). Loss of Borealin/DasraB leads to defective cell proliferation, p53 accumulation and early embryonic lethality. Mech Dev *125*, 441-450.

Yan, X., Cao, L., Li, Q., Wu, Y., Zhang, H., Saiyin, H., Liu, X., Zhang, X., Shi, Q., and Yu, L. (2005). Aurora C is directly associated with Survivin and required for cytokinesis. Genes Cells *10*, 617-626.

Yang, D., Welm, A., and Bishop, J.M. (2004). Cell division and cell survival in the absence of survivin. Proc Natl Acad Sci U S A *101*, 15100-15105.

Yasui, Y. (2004). Autophosphorylation of a newly identified site of Aurora-B is indispensable for cytokinesis. J Biol Chem *279*, 12997-13003.

Zhang, D., Shimizu, T., Araki, N., Hirota, T., Yoshie, M., Ogawa, K., Nakagata, N., Takeya, M., and Saya, H. (2008a). Aurora A overexpression induces cellular senescence in mammary gland hyperplastic tumors developed in p53-deficient mice. Oncogene *27*, 4305-4314.

Zhang, X.D., Goeres, J., Zhang, H., Yen, T.J., Porter, A.C., and Matunis, M.J. (2008b). SUMO-2/3 modification and binding regulate the association of CENP-E with kinetochores and progression through mitosis. Mol Cell *29*, 729-741.

Appendix

The following manuscripts have been generated as a result of the work reported in this memory and other collaborations not described in the main text.

Gonzalo Fernández-Miranda, Ignacio Pérez de Castro, Javier Martín, Norbert B. Ghyselinck, Sagrario Ortega, Christopher Heeschen, Marta Cañamero and Marcos Malumbres. *Cellular Requirements for Mammalian Aurora B in G1/S Progression, Chromosome Alignment and Spindle Pole Integrity*. Submitted.

Paulina Wachowicz, Guillermo de Cárcer, Eva Porlan, **Gonzalo Fernández-Miranda**, Mireia Moreno, Eusebio Manchado, Beatriz Escobar, Marta Cañamero Isabel Fariñas and Marcos Malumbres. *Plk1 haploinsufficiency causes hypertrophic cardiomyopathy, altered neuroblast asymmetric cell divisions and cognitive dysfunction*. Submitted.

Beatriz Escobar, Guillermo de Cárcer, Caterina Alfano, **Gonzalo Fernández-Miranda**, José J. Bravo-Cordero, María C. Montoya, Mercedes Robledo, Marta Cañamero, Francisco J. Blanco and Marcos Malumbres. *Brick1 ablation impairs embryonic development and protects cells from malignant transformation*. Submitted.

Silvana Mourón, Guillermo de Cárcer, Esther Seco, **Gonzalo Fernández-Miranda**, Marcos Malumbres and Angel R. Nebreda. *RINGO/Speedy C is required to sustain the spindle assembly checkpoint*. Submitted.